Faculty of Science and Technology

MASTER'S THESIS

Study Program/Specialization

Petroleum Geosciences & Engineering

Spring Semester, 2021
Open Access

Writer
Shujah Nasir

Faculty Supervisor
Professor Udo Zimmerman

Thesis Title

Effectiveness of Frantz Machine for Separation of Heavy Minerals

Keywords
Frantz Magnetic Separation
Heavy Minerals
Provenance
Scanning Electron Microscope

Effectiveness of Frantz Machine for Separation of Heavy Minerals

By

Shujah Nasir

MSc Thesis

Petroleum Geosciences Engineering

Presented to the Faculty of Science and Technology

University of Stavanger

Norway

University of Stavanger

July 2021

ACKNOWLEDGEMENT

Firstly, I would like to express my sincerest gratitude to my supervisor, Dr. Udo Zimmermann, for the opportunity to conduct and complete this thesis. Your continuous guidance, engagement, and encouragement have been very much appreciated. Your dedication to geology has deeply inspired me. Thank you for sharing your knowledge!

I would also like to acknowledge everyone at UiS who has been a part of my life during this master's degree. I want to express my appreciation to Lab Engineer Mona Wetrhus Minde for assistance with the FE-SEM. Thank you for sharing your enthusiasm for working in the laboratory and for providing sound guidance and support. I want to thank Andreas for help with BSE-images of mineral grains and Caroline Ruud for assistance and guidance with mounting and other sample preparations.

Lastly, I want to thank you, family and friends, especially my Mother, for

always being there for extra encouragement, and my friend Zohyab Afzal for his support.

ABSTRACT

This project research the provenance of Precambrian formations: Vredefontein Formation, Grootderm Formation, and Derburg Formation from Namibia. The aim is to enhance provenance understanding after the separation of minerals with the Frantz Magnetic Separator. The results obtained from the magnetic separator were also matched with Scanning Electron Microscope and X-Ray Diffraction (XRD).

The rock samples were mainly lavas and gabbro. So, we had both types of rocks (Plutonic and Volcanic). Gabbro is observed mainly with pyroxenes, amphiboles, and plagioclase. The Vredenfontein Formation contains mostly albites, hematite, microcline, and sanidine. Important minerals include apatite and zircons in Vredefontein Formation. Major minerals in the Grootderm Formation are epidotes, chlorites, and lawsonites.

Samples were sieved into fractions of different sizes and then those fractions were analyzed through Frantz Separator. Mounts were prepared and epoxied. The EDS spectra were obtained from SEM and are then identified for the minerals and are matched with XRD spectrums. The XRD graphs were obtained on low intensity but showed major minerals in rock samples. Minerals were separated in Frantz according to their magnetic susceptibilities which can be further used in hydrocarbon industry and mineral industry.

TABLE OF CONTENTS

LIST OF FIGURES

TABLE OF FIGURES

CHAPTER 01

INTRODUCTION

The need for magnetic separation of minerals varies with the purpose of the required research. There are different goals that can be achieved by applying different techniques to acquire the specified result. In this thesis, the technique of magnetic separation has been applied to focus the heavy minerals in three different meta-igneous samples from Namibia. These samples belong to the Neoproterozoic era.

Order to identify the dawn of succession by analyzing the meta-igneous rock samples is frequently considered difficult to study due to the existence of a variety of minerals in the rock. The identification of specific heavy minerals is much more effective than petrography which is also an important method.

Magnetic separation

The technique of magnetic separation is basically dependent on the susceptibility of the magnetic properties of minerals. It takes the benefits of differences in their magnetic properties. The minerals are divisible into three categories on the basis of magnetic properties.

- Ferromagnetic
- Paramagnetic
- Diamagnetic

Ferromagnetic (magnetite and pyrrhotite) minerals are mostly composed of iron constituents, and they are easily separable from other minerals with the help of a magnet. Paramagnetic and diamagnetic minerals are basically not magnetic in nature; however, they can be separable on the basis of their interaction with a magnetic field. The former is fragilely attracted to a magnetic field, and the latter are fragilely repelled by a magnetic field.

Frantz Isodynamic Magnetic separator

It is a convenient device that is used for the magnetic separation of minerals. It incorporates a large electromagnet. The mixture of minerals, such as a mixture of paramagnetic and diamagnetic minerals, is passed on a trough made of metal through the electromagnet. There they will be dragged into the field if they are paramagnetic, and in other cases if they are diamagnetic in nature,

they will be repelled. The metal trough, near the exit end, is divided and used to the minerals that vary the strength of the magnetic field and the separation of the slope.

1.1. Objectives of the study

In this thesis, one of the main objectives is to discern the mineral abundances and quantify different mineral species, if feasible. Later on, this will aid in developing the paleographic model when merged with other suitable required data (this is not the aim of this project).

The other objectives of this study are to then correlate the samples, derived from Namibia and which have been deposited in different levels of the stratigraphy and in different areas of the geographic context, even partly on defined different terranes (Frimmel et al., 2011), on the basis of magnetic properties of minerals. After that we deduced the provenance of these rock samples from the available data.

1.2. Tools used in this study

The main tool that is used in this project/study is:

- Frantz Magnetic Separator.

It includes in one of the recently developed high gradient magnetic separation devices. It is efficient in the application of magnetic separation to very weakly magnetic minerals of small size particles and it was helpful for the objective of the study.

Following are the other techniques/tools that have also been used to accomplish the objective.

- XRD
- SEM
- Google earth.

1.3. Physiography of the study area

The study area is mainly consisting of three sites with three coordinates which are as follows.

- S27-54-55.7/E15-41-6.2
- S28-30-26.8/E16-42-39.9
- S28-48-59.9/E17-13-8

The google earth image of these coordinates (Fig, 1.1) shows that it encompasses Namibia and South Africa as study area of this work.

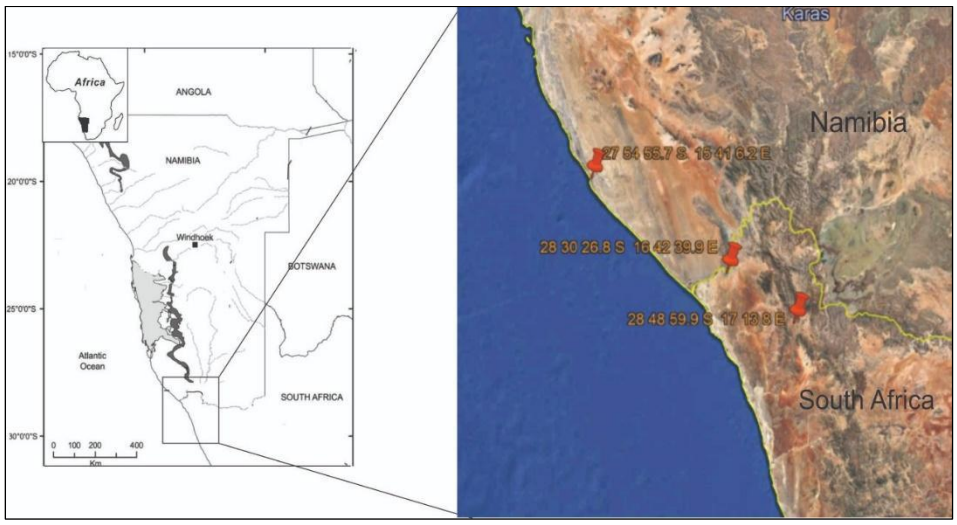

Figure 1.1 Shows the Google earth image of the study area.

Three different samples have been collected from these given coordinates which belongs to three different formations.

- Dernburg Formation
- Grootderm Formation
- Vredefontein Formation, respectively.

1.4. Regional geology of the study area

The study area is basically situated on two different localities the one is situated in Port Nolloth Zone (PNZ) at western part of south Africa and other two are situated in Marmora Terrane at the southwestern margin of Namibia. The regional geology of both these localities are basically part of Gariep belt. The Gariep belt is a part of western Gondwana orogenic belts that belongs to Neoproterozoic to Cambrian age (Zimmermann et al., 2011).

Schakalsberge fault thrust is one of the main lithological & structural discontinuity that separates Port Nolloth Zone (para-authochthonous) from Marmora terrane (allochthonous) (MT;

Hartnady and von Veh, 1990).

1.5. Stratigraphy of the study area

The formations include as a sample in this work are as follows.

- **Grootderm Formation**. Its age is Neoproterozoic. It is located in Marmora terrane and placed under the Schakalsberge sub-terrane.
- **Dernburg Formation**. It belongs to Neoproterozoic era. It is located in Marmora terrane and placed under Chameis group of Chameis sub-terrane.
- **Vredefontein Formation**. Its age is also Neoproterozoic. It is situated in Port Nolloth Zone and placed under the Stinkfontein sub-group. It overlies the Lekkersing Formation.

CHAPTER 02

REGIONAL GEOLOGY

2.1. Introduction

A supercontinent is assembly of all continental blocks which are accreted together to form single large landmass. During Proterozoic era, supercontinent existed twice and the oldest supercontinent that is known to be existed was Columbia about 2-1.8 Ga ago. The next supercontinent formed was Rodinia as result of disintegration of previous Columbia, and when it assembled to a new supercontinent (Fig. 2.1) around ~1 Ga ago (Zhao et al., 2006).

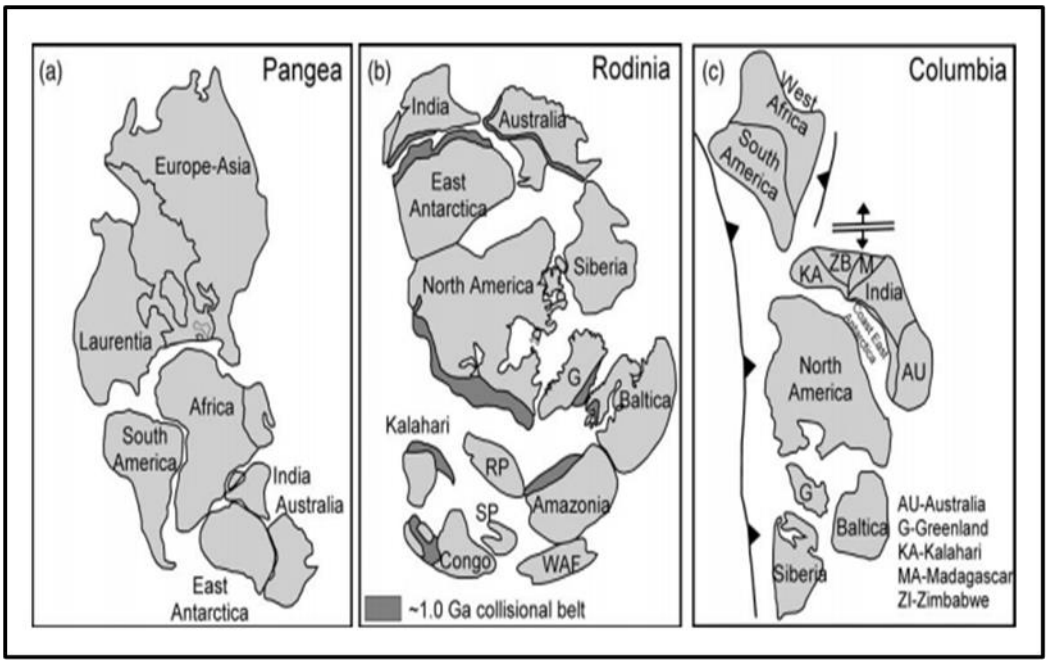

Figure 2.1The three supercontinents that existed in earth's record were: (c) Columbia that formed 1.8 billion years ago; (b) Rodinia that formed 1.0 billion years ago and (a) Pangaea that is younger, formed around 300-250 million years ago (Zhao et al., 2006). Acronyms: WAF: West Africa; G: Greenland; SF: Sao Francisco; RP: Rio de la Plata.

At the beginning of Neoproterozoic era, Rodinia existed which consist of all landmasses, at that time and lasted 1.1 Ga until 750 million years ago. Rodinia was formed between 1300 Ma and 900 Ma as result of global orogenic episodes. The assembly as well as breakup of Rodinia is considered diachronous, as breakup of Rodinia initiated around 850-750 Ma, as result of rifting along with

plume episodes about 825-740 Ma (LiZ.V. et al., 2008). Rodinia was disintegrated in Cambrian that followed by events like Pan African orogeny and opening of Iapetus Ocean. After disintegration it is believed that two glacial activities preceded and followed by reconfiguration of cratons that made up Gondwanaland (Zimmermann et al., 2011).

A siliciclastic Rocha group linked to the Mesoproterozoic basement of Neoproterozoic stratigraphic unit. That Rocha group found in Dom Feliciano Belt (Punta del Este Terrane) in South America has an equivalent lithological related unit in Gariep belt (Marmora Terrane) in southwestern Namibia and western South Africa (Basei et al., 2005). This also explains the coalescence of south America and south Africa (in the course of congregation of Gondwanaland).

The formation of various orogenic belt during the era of late Proterozoic to early Paleozoic marks the geographically tectonic features of the western Gondwanaland (Frimmel et al., 1996). Around 780 million years ago, the process of rifting starts between Kalahari in southern Africa and Rio de la Plata in south America, which remained in action for about 35-45 million years, which lead to opening of Adamastor Ocean (Frimmel et al., 1996, Frimmel and Frank., 1998). However, the extensional regime was then followed by the compressional regime which leads to the closure of Adamastor Ocean (Gilchrist et al., 1994).

During late Proterozoic, as a result of rifting, the Gariep & Kaoko belts developed as a suture between South American and South African cratons. The Damara belt, at south-western part of Africa separate the Congo Craton from Kalahari Craton, however the northward part of south Africa is occupied by the Kaoko Belt which extends southward at the coastal margin of Southern Africa to Gariep Belt (Fig 2.2).

2.2. Geologic Setting of Gariep Belt

A Gariep belt is basically a part of Pan African/Brasiliano orogenic belt, is north-south trending an arcuate shaped tectonic feature. It is exposed on the western South Africa and on the margin of Kalahari Craton of South-western Namibia (Macdonald et al., 2010). The Gariep Belt links to the Damara Belt in north and on south it shrinks out to the ocean. It runs along the coast of Lüderitz in Namibia (Northward) and Kleinzee in South Africa (southwards).

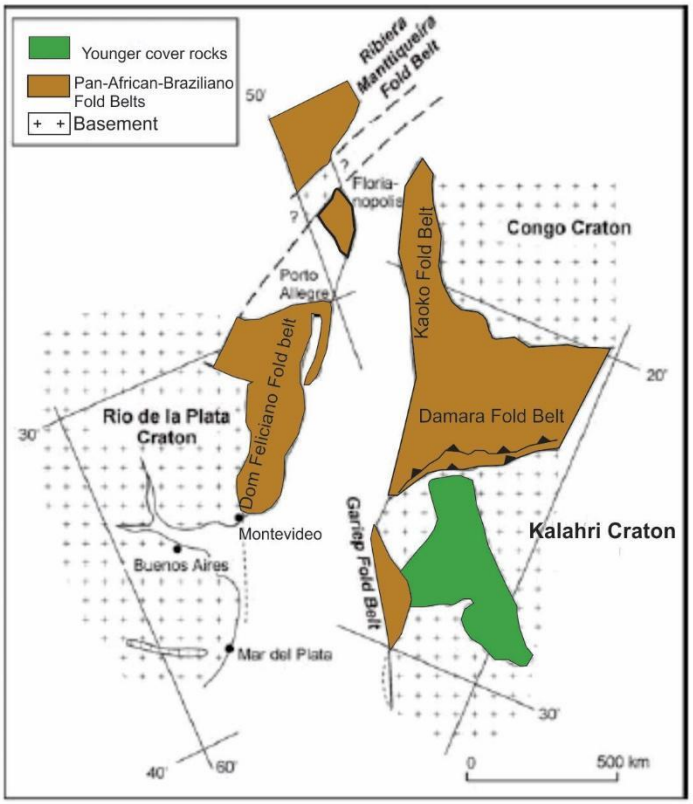

Figure 2.2 Shows the regional location of Gariep Belt of Neoproterozoic in South western Africa, explained with the network of Pan African Orogeny Brasiliano Fold Belts.

The Gariep Belt's succession is anticipated to deposit first during the opening of Adamastor Ocean and then during the closure of the ocean is divided into different terranes (Hartnady et al. 1985; Stanistreet et al. 1991; Frimmel et al. 1996; Frimmel and Frank 1998). The Gariep belt is also often anticipated as retro arc type basin (Basei et al., 2005,2008).

It is divided into two terranes the first is known as Port Nolloth Zone (PNZ) which is para-autochthonous (continental) in the east and the other is allochthonous Marmora Terrane (oceanic) in the northwest (Zimmermann et al., 2011). Schakalsberge thrust is one of main lithological discontinuity which separated the Port Nolloth Zone in the east form the Marmora Terrane in south east (Fig 2.3). The Marmora Terrane is basically thrust up on the crest of PNZ in southeast direction (Basei et al., 2005).

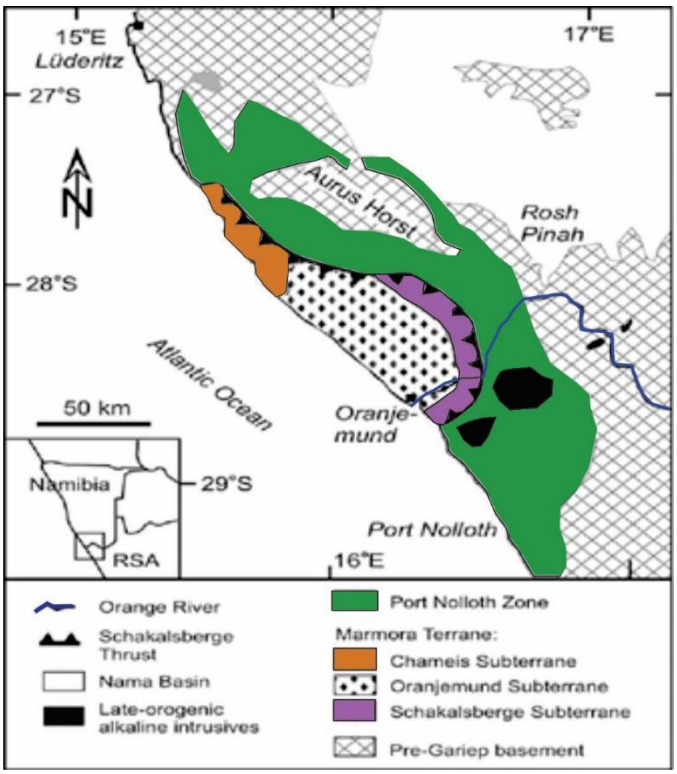

Figure 2.3 Shows different tectonostratigraphic units of Gariep Belt and the Schakalsberge thrust which divides the PNZ from Marmora Terrane.

2.2.1. Port Nolloth Zone (PNZ)

The port Nolloth zone marks the eastern side of the Gariep belt. This was deposited during the rifting of the cratons (opens the Adamastor ocean), drifting and the formation of passive margins all these events were believed to lasted around 200 million years, and that forms the depositional cycle of this zone with approximate thickness of about 3.2 km (Zimmerman et al., 2011).

It is further sub-divided into different formations which are then placed under three mega-sequences (Fig 2.4) (Frimmel et al., 2002) which represent the tectonic phases pf their basin development, named as follows.

- Stinkfontein sub-group (continental rift deposits)
- Hilda sub-group (passive margin deposits)
- Holgat Formation (syn-orogenic foredeep deposits)

The native basement rock composed of sections of Eburnean younger crust, which is approximately 1.8-2.1 Ga years old along with the 1.2-1.0 Ga old high grade metamorphic rocks

that belongs to Namaqualand Metamorphic complex is overlying by the strongly deformed Port Nolloth Zone. Therefore, it is considered as para-autochthonous as they majorly consist of sediments deposit of continental origin. The Nama Group then succeeded the rocks succession of Port Nolloth Zone and Gariep belt. Nama Group holds the fauna of Ediacara (well renowned), it dates the rock into Late Ediacaran which are approximately 550-1 Ma old (Zimmermann et al., 2018).

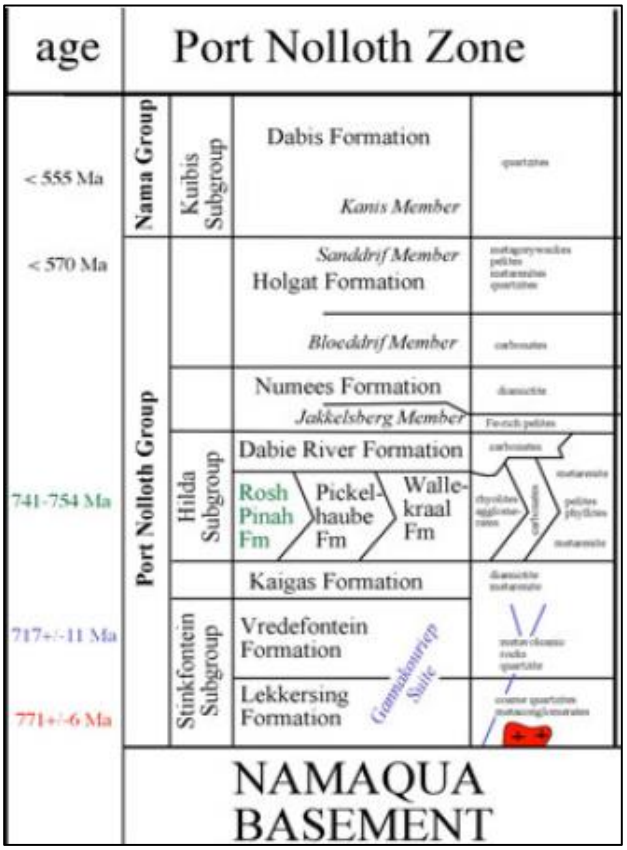

Figure 2.4 Shows the table of subdivided formations of Port Nolloth Zone under different subgroups, overlying by the Nama Group of late Ediacaran.

2.2.2. Marmora Terrane

The Marmora terrane is one of the two tectonic units of Gariep Belt. As Marmora terrane does not relying on any basement rock, like PNZ, hence it is considered as completely allochthonous. However, the contact between these two tectonic units of Gariep Belt is distinguished by the Schakalsberge Thrust along which the Marmora Terrane lies over the top of Port Nolloth Zone.

The Marmora terrane is believed to be devised in contiguous environment, nonetheless the oceanic crust of Marmora terrane on the basis of geochronological evidences, lithostratigraphic and chemo stratigraphic correlation is believed to be 600 Ma old and the formation of succeeding basin inversion is about 580-600 Ma. On the basis of distinct differences, relative amount of certain rock types and its distribution, the Marmora terrane is sub divided into three different tectonostratigraphic units which are also termed as sub-terranes (Fig 2.5).

- Chameis sub-terrane
- Oranjemund sub-terrane
- Schakalsberge sub-terrane

The sequence of these sub-terranes is that the Schakalsberge sub-terrane is the lowest tectonostratigraphic unit which is then succeeded by the Oranjemund sub-terrane and then Chameis sub-terrane (Basei et al., 2005).

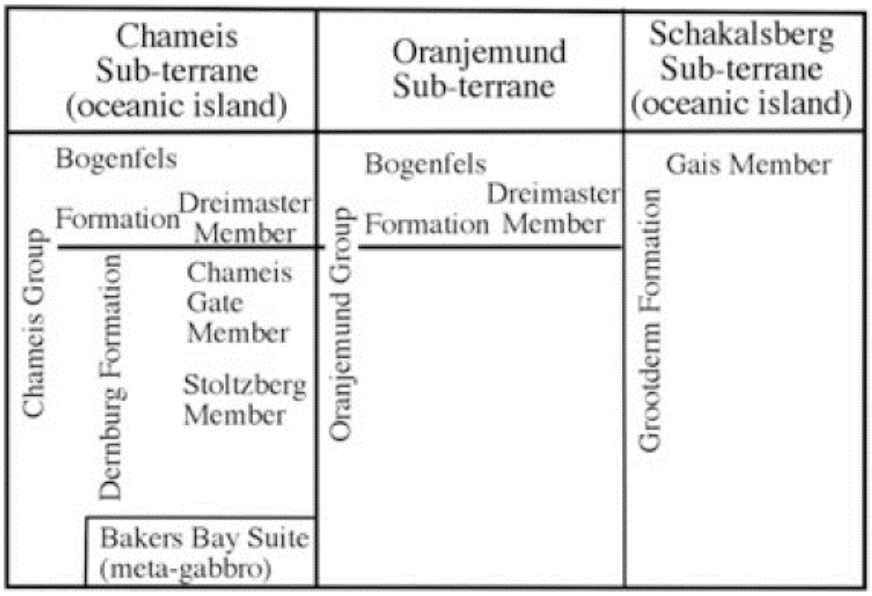

Figure 2.5 Shows the three tectonostratigraphic sub-terranes of Marmora Terrane, comprising of different formations.

2.3. Stratigraphy of concerned formations

The study area involves three different formations from three localities. One sample belongs to the Vredefontein Formation of Stinkfontein sub-group of Port Nolloth Zone (Eastern tectonic unit of

Gariep Belt) in South Africa. Whereas, the other two belongs to Marmora Terrane (western tectonic unit of Gariep Belt) in south-western Namibia. The two samples are Dernburg Formation and Grootderm Formation, belongs to Chameis and Schakalsberge sub-terranes respectively. The detailed description of these formations is given below.

2.3.1. Vredefontein Formation (lava agglomerate)

The deposition of Port Nolloth Group in southern Africa of Gariep Belt, imitate with the assembly of volcanic rocks (bimodal) and siliciclastic rocks of coarse grained that range in thickness of about eighty meters (Von Veh, 1993). This stratum is placed under the sub-group of Stinkfontein of Port Nolloth Zone, in this group the target formation i.e., Vredefontein Formation is overlying the Lekkersing Formation. Whereas, the strata of Stinkfontein sub-group overlie by the Hilda Group (Mcdonald et al., 2010). The formation contains various sedimentary structures i.e., crossbedding, ripple marks that points out the direction of paleocurrents, along with other sedimentary features, which are thoroughly preserved in medium bedding which is composed of felspathic arenite. The thickness of the formation is about 300 meters. As we move towards the top bed of the formation, we encountered sand to gritty breccia along with the pieces of angular-sub rounded quartz vein, volcanic rocks (felsic), gneiss, calcareous grit, granitoid, ortho-quartzite and microgranites embedded in the grit groundmass of fuzzy feldspathic cross bedding. The formation is dominant by the abundant accumulation of across laminations in internal sedimentary structures. The top portion of the formation also contains intercalated volcanic rocks of minor felsic, intermediate and mafic in nature (Middlemost 1963).

2.3.2. Dernburg Formation (gabbro)

The Dernburg Formation is exposed in Chameis sub-terrane, of Marmora Terrane, underlain by the Bogenfels Formation. The north-western surround of Marmora Terrane is inhabited by the tapered Chameis sub-terrane on the coastal strip. The wide volcanic-sedimentary sequence could be created as the intense folding of the sub-terrane is uncertain about the prime lithostratigraphic distributions/sub-divisions over there. Mafic hyaloclastites, intercalated metapelite, alkali basaltic lava flows which are metamorphosed, serpentinized picrite along with the mass of slenderly laminated greenschists that indicates the initial beds of tuff, constitutes to form the lithological characteristics of Dernburg Formation (Basei et al., 2005). It is mainly composed of volcanic rocks of mafic composition. The matrix of mafic volcaniclastic constitutes the diamictites having exotic

drop stones impart the verification of transport from continental margin to an oceanic environment by ice. The Bakers Bay Suite involves the bodies of tectonically displaced metagabbro (intrusive), found more often in this formation. The top bed of the Dernburg Formation has thin chert band. At various localities the limestones and drop stones of gneiss, quartzite, dolomite and granite occur within the slenderly laminated greenschists & metapelites, that is about 1.5 meter in diameter constitutes the Chameis Gate Member.

2.3.3. Grootderm Formation (lava agglomerate)

The Grootderm formation belongs to the lowest tectonic sub-division unit of Marmora terrane which is Schakalsberge sub-terrane which majorly constitutes the volcanic rocks of mafic composition, that is the predominant lithology of Grootderm Formation, which are capped by the dolomite, which is the predominant lithology of Gas member. The Gas member is compared to the underlying Grootderm formation is less intense & deformed regions in which the presence of stromatolites is merely identifiable, along with the localized oolites (Basei et al., 2005). Both formations are distinguished from each other by a band of iron formation which is approximately one meter thick. The overall thickness of Grootderm Formation is about 4-5km, due to intense folding and thrust imbrication it is impossible to estimate the true thickness of the formation. the formation is mainly composed of metabasalt (aphyric, porphyric & amygdaloidal) of alkaline composition. The base of the formation has invasions of serpentinized picrite & alkali metagabbro. The formation also has horizons of tuff, younger fragments of metabasalt and agglomerates along with the dolomite. The evidence of fairly sub-aqueous volcanic eruption is the presence of structures of pillow lava and copious number of hyaloclastites (Frimmel et al., 1996). The lack of terrigenous siliciclastic sediments represents aseismic ridge instead of near continental or intra-continental margin.

CHAPTER 03

THEORY

3.1. Introduction

Magnetic separation is a technique that has been used in olden days either for the removal of iron minerals or for the aggregation of ores of iron. The separation of magnetic minerals is basically dependent on the susceptibility of magnetic properties of minerals. It is a property (useful for its division) of a mineral contain material and how it will react and controls their response in a magnetic field. It takes the benefits of difference in their magnetic properties. The minerals are divisible in three categories on the basis of magnetic properties.

- Ferromagnetic (magnetite and pyrrhotite etc.)
- Paramagnetic (monazite, ilmenite, hematite etc.)
- Diamagnetic (plagioclase, zircon, calcite etc.)

Ferromagnetic (magnetite and pyrrhotite) minerals mostly composed of iron constituents, and they are easily separable from other minerals with the help of a magnet. Whereas, paramagnetic and diamagnetic minerals are basically not magnetic in nature however they can be separable on the basis of their interaction with a magnetic field. The former is fragilely attracted in a magnetic field and latter are fragilely repelled by a magnetic field.

The ferromagnetic minerals are the easiest to separate, as they are themselves magnetic in nature. For example, magnetite, pyrrhotite. Therefore, they can separate by using a strong magnet having two magnetic poles, by wrapping a pole with a paper and drag the magnet onto the sample containing ferromagnetic minerals. Then remove the paper having attracted minerals from the magnet. However, the other two types are not magnetic in nature, but they do respond differently when placed into a magnetic field. Therefore, a mixture of diamagnetic and paramagnetic minerals is then isolated with the help of a magnetic separator that is able to induce a magnetic field and monitor their responses individual and then separate it.

The device that is used in this study to separate the minerals on the basis of their magnetic properties is Frantz Magnetic Separator.

3.2. Frantz Magnetic Separator

The Frantz magnetic separator is an isodynamic separator. Samuel G. Frantz collected his copyright for his invention (isodynamic separator) in 1936 and then around 1971 the Frantz magnetic separator was using globally. This device is calibrated with known magnetic susceptibilities of various substances, which aids in the deduction of magnetic susceptibilities of other substances as well (Murty, 1963)

This device is of great importance in the concentration processes of minerals, as it concentrates and separate minerals from the mixture of dry grains material on the basis of their paramagnetic nature. In order to understand the paramagnetic behavior of minerals we need to revisit the basic chemistry of atoms that makes up an element and minerals. In an atom the shells which are also known as orbits are present in an elliptical order around the nucleus containing protons and electrons. Each atom is distinguished on different number of electrons that resides in orbit around the nucleus. The successive order of orbits is termed as K-shell, L-shell, M-shell depending on the maximum number of electrons that can reside in a specific shell. For example, K-shell can reside maximum 2 electrons whereas, L-shell 8 electrons (every shell have even numbers of electrons). The electrons always configured in pair, where they can spin in pairs, the opposite spin imparts balancing effect which make the substance non-magnetic in nature however, when the pair lacks one electron or single electron spins without any alignment it will spin in an aimless direction (Fig 3.1), this basically causes magnetic susceptibility.

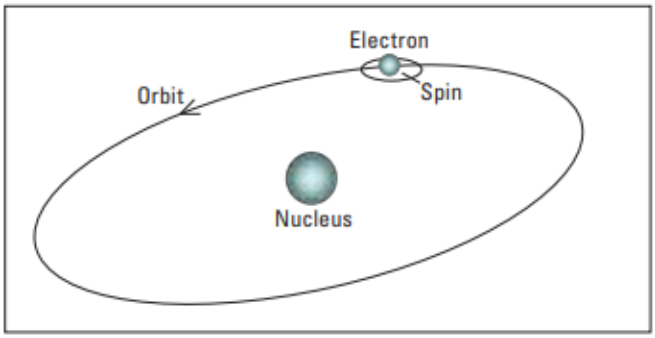

Figure 3.1 Showing a spin of a single pair electron of an atom.

This atom when subjected to an induced magnetic field, provided by the Frantz Magnetic separator, it will align its spin with magnetic field and make itself magnetic in nature as soon as

the magnetic field is removed it goes back to its random spin making it non-magnetic in nature. Hence, that temporary change in magnetic change is termed as paramagnetic.

3.2.1. Constituents of Frantz Magnetic Separator

Following are the constituents of Frantz Magnetic Separator, that are arranged in such a way to separate the magnetic minerals from the rest of dry mixture.

- External magnet
- Two-channeled aluminum tray
- Two bin containers
- Hopper (thistle funnel)
- Vibration's controller

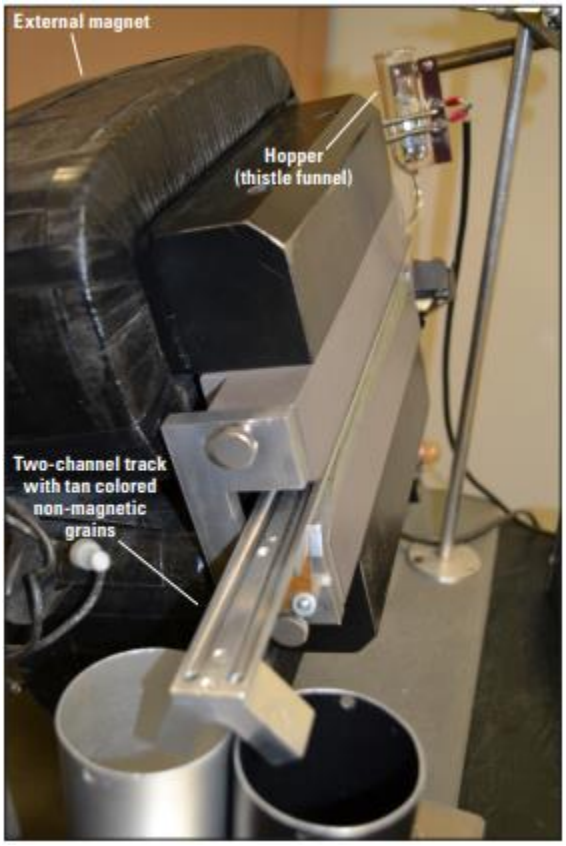

Figure 3.2 Showing the photograph of Frantz Magnetic separator with its different components.

3.2.2. Working Principle

The two-channeled aluminum tray is placed an angle to make a slope easier for the feed to pass slide over it. A magnet is placed above and parallel to the tray. The tray is constituted in such a way that it receives the feed of dry material from the hopper without any disturbance. The sample drives over the channel in downward direction under the influence of magnet by the means of vibration. The generated vibration can be adjusted to overcome or control both the rate of the introduced feed into the separator and the movement of grains in the material. Just like with the vibrations the intensity of the magnetic field generated can be controlled and adjusted in order to separate the magnetic susceptible of desired intensity (Strong and Driscoll., 2016). For example, the strength of the magnetic field can be generated at minimum intensity such as 0.01 A to separate the minerals of high magnetic susceptibility from the sample of granules and the field can also be adjusted at maximum such as 1.70 A to separate the minerals of lower magnetic susceptibility. The minerals passing through the two channeled aluminum trays under the magnets are then separated on these two channels, minerals with paramagnetic in nature are pass onto left channel whereas, the minerals that are non-magnetic in nature are pass onto the right channel. Two bins type containers are placed at the end of both the tray chutes to collect the arriving mineral samples (Fig. 3.2).

3.3. X-Ray Diffraction

X-Ray diffraction technique is basically an analytical technique. It is most preferably useful in the identification of phases as well as the characterization of the crystalline structure in different minerals that are extensively accessible in the geological samples of rocks. For the determination of dimensions of unit cell, the information resulting from this technique is extremely useful. The type of the material that is used is generally described as amorphous or crystalline. The sample first ground finely and homogenized and then the average bulk composition of the sample is determined in order to carry out the analysis. Moreover, sometimes the variety of different samples of rocks contains number of mineral phases which leads to number of peaks emerging in the diffractogram which can overlap and gives us fallacious interpretations.

After the analysis of the fractions acquired in magnetic separation are then subjected to XRD for further analysis. Sample comprising of low silica content is capable of introducing lesser number of peaks along with the peaks having higher relative intensities which aids in the characterization

of its mineralogy. Whereas, the sample with high silica content, epidote the identified accessory mineral was acquired as a fraction which was then was not identified in diffractogram in total sample. The results proved that the magnetic separation of minerals by Frantz isodynamic magnetic separator provides extensive aid in the analysis by XRD, by identifying the accessory minerals and characterization of various samples having multiple possible mineral phases.

Therefore, in this study, first we performed the magnetic separation of the minerals with the help of Frantz isodynamic magnetic separator, from the rock samples and then we performed XRD in order to enable the identification of minerals of the study.

3.3.1. Working Principle

The technique of X-Ray Diffraction is basically based on Bragg's law, which states that the relation between the spacing of atomic planes in crystals lattice & the angle of incident wave, at this angle these planes generate reflection of electromagnetic radiations (Fig 3.3). The equation of Bragg's law is given as

$$n\lambda = 2d\sin\theta$$

here,

d=spacing between the atomic planes of crystal
n= is an integer
θ= angle of incidence
λ= beam wavelength

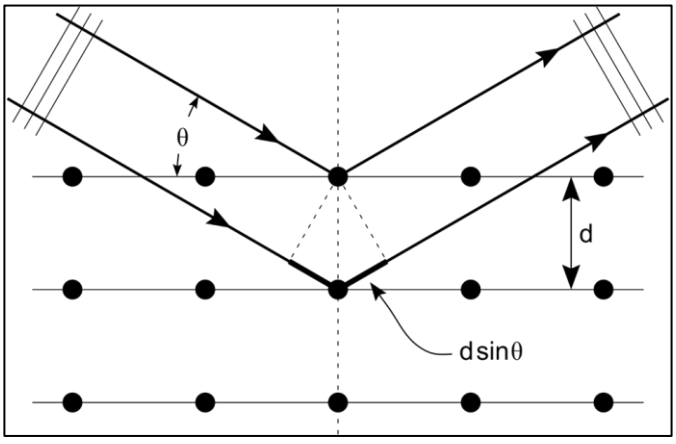

Figure 3.3 Shows schematic diagram of working Bragg's Law.

The crystalline material act as three-dimensional grating as well as the spacing between atomic planes of crystal lattice, when subjected to X-ray wavelengths. The x-rays were basically generated from the cathode ray tube, the monochromatic beam of x-rays is then collectively bombarded on the sample specimen. As long as Bragg's law satisfied by the planes of crystal lattice of the sample, the constructive interference is fabricated. The law is generally related to the wavelength of incident electromagnetic radiation and the diffraction angle of the reflected waves because of the spacings in the crystal lattice. After that, we examine the angle from different angles, about twenty different angles in order to acquire the possible diffractions of the crystal lattice (Fig. 3.4). Due to the random orientations of the material sample in powdered from to identify, process and count the X-rays.

The identification of specific minerals is basically done on the basis of difference in peaks generated due to different plane spacings in crystal lattice of every mineral, which is achieved by collaborating the peaks of different spacings with the standard reference pattern.

3.3.2. Instrumentation

The instruments of XRD include following main parts (Connolly., 2007).

- X-Ray tube
- A sample holder
- X-Ray detector

As we all know that, X-rays are the fast-moving beam of charged electrons. A cathode ray tube is used to generate that beam by heating the filament by applying a voltage. The beam of charged electrons are then focused on the target sample. The generated wavelengths are basically the distinctive of the sample. The spectra of X-ray produced, when the incoming beam of electrons have adequate amount of energy to remove the valence electrons of target sample atoms (Bunaciu et al., 2015). The generated spectra comprise of different components which are distinguished on basis of length of the wavelengths. For example, $K_{\alpha 1}$ has shorter wavelength and low intensity as compared to the $K_{\alpha 2}$ of K_{α} components which is the common in spectra along with the K_{β}. The count and intensity of the incident X-Rays can be adjusted and controlled according to the need.

The potency of the X-rays that are reflected off the sample are then recorded by rotating the sample. The peaks in intensity will appear on the graph as long as the incident rays descend on the sample fulfilled the Bragg's law to generate constructive interference.

The geometric orientation of XRD allows the sample to rotate at an angle of 20, from where it is subjected under the X-Ray detector to collect the beam of X-rays. Goniometer in basically an arm in XRD, upon which X-Ray detector is situated, help in sustaining the angle of the sample on rotation (Fig. 3.4).

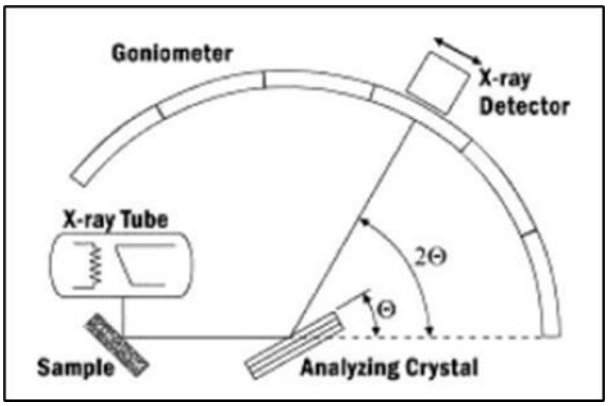

Figure 3.4 Showing the schematic diagram of Xray diffraction.

3.3.3. Applications

The X-Ray Diffractometer tool is a most useful technique in various manners suited for the identification of different internal chemical structures of substances along with the recognition of fine structures of substances and mineral identification. Furthermore, it allows us to determine the following parameters.

- Recognition of crystalline phases and orientation
- Governing of structural properties:
    - Lattice parameters
    - Strain
    - Grain size
    - Epitaxy
    - Phase composition
    - Preferred orientation
- Estimation of thickness of thin films and multi-layers

- Investigation of atomic arrangement

XRD is also useful in various industries and disciplines as well, such as glass industry, pharmaceutical industry, microelectronics industry, forensic science, corrosion analysis (Guma et al., 2012) and geological applications.

3.4. Scanning Electron Microscope

The scanning electron microscope, also abbreviated as SEM, is used to provide the additional data set about the texture, composition and all the other external attributes of the sample that is placed under examination (Fig 3.5).

The scanning electron microscope tool uses a distinct beam of electrons having high energy or highly charged onto a sample that will create various signals on the interaction of electron-sample surface. These signals are then processed to give the detailed image about the outer surface morphology also termed as texture, the chemical composition of the surface, orientations of crystal, internal morphology of the sample crystal lattice. Most of the samples that have been thoroughly examined under scanning electron microscope are of solid subjects.

Figure 3.5 showing the SEM image of asbestos mineral form.

The data also collected from different selected spots over the same sample in order to get qualitative results. The area of the sample that has been examined under the SEM can range from

1 cm to 5 microns in width by using conventional SEM techniques of varying resolutions and magnifications depending upon the requirement of the acquiring data set.

3.4.1. Working Principle

As SEM uses the distinct beam of highly energized electrons, therefore these electrons are rich in kinetic energy which dissipates on the interaction of these electrons with the surface of the target sample and get deaccelerated on collision and generate various signals to give a fine high-resolution image. These signals include different parts on dissipation, each part has significant input in the collective result of the resulting image (Smith and Oatley., 2004). These parts (signals) include secondary electrons and back scattered electrons that both put their inputs in the formation of the surface SEM images whereas the diffracted back scattered electrons put its input in the determination of the structure of the crystal along with the orientation of the minerals that makes up the whole sample under examination. On the dissipation of highly charged electrons on the surface of the sample also generates photon or characteristic X-Rays during deacceleration or the returning of the excited electron to the states of low energy (Swapp., 2014). The SEM is considered as non-destructive form of analysis because the generation of characteristic X-rays for each element in a mineral is due to the excited state of the electron beam.

3.4.2. Instrumentation

The instrumentation of scanning electron microscope tool is comprised of different components. The list of these components and its purpose is briefed below (Fig. 3.6).

- Electron Source/Gun

  It is used to generate the focused beam of electrons targeted onto the sample.
- Electron lenses
- Sample stage

  The stage is required and used to put the solid sample onto and subjected to beam of highly charged electron coming from electron gun.
- Detectors

SEM include generally one detector and sometimes multiple or additional detector which aids in defined the capabilities of certain instrument which critically dependent on information of the detectors.

- Data output devices

  These devices displayed the resulting image of the sample.

- The requirements of infrastructures include
  - Power supply
  - System of vacuum
  - System of cooling
  - Free floor
  - For required magnetic and electric field room free

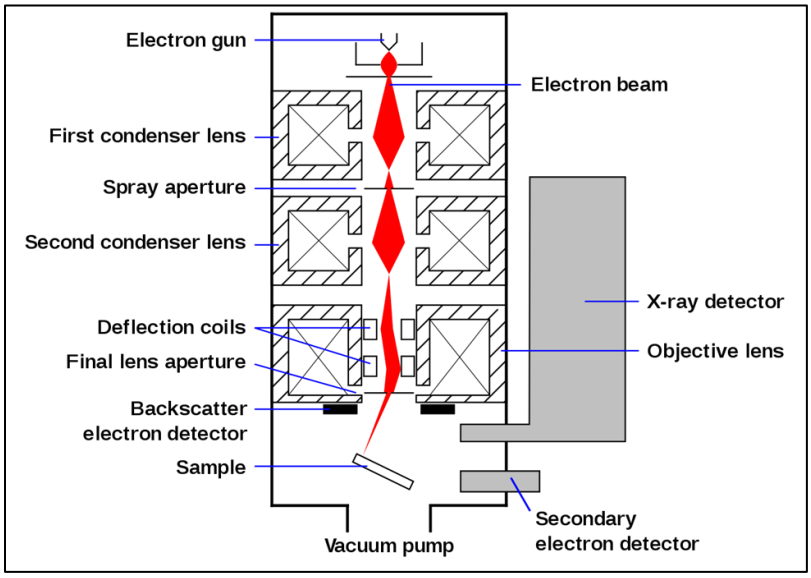

Figure 3.6 Shows the schematic illustration of typical SEM apparatus.

The above diagram shows several different components Scanning Electron Microscope (SEM). All these components come under the umbrella of seven operational systems which are as follows.

- Vacuum system
- Electron beam generation system
- Electron beam manipulation system

- Beam specimen interaction system
- Detection system
- Signal processing system
- Display and recoding systems

All these above-mentioned systems of SEM linked with different sets of its components. These systems are interlinked to one another and operate together, however the any change in the operation of the system leads to a different set of results. Therefore, the operator is able to make changes in system in order to obtain a certain desired result (Dunlap & Adaskaveg., 1997). The operation of these systems briefly described below.

3.4.2.1. The Vacuum system

This system plays an important role in maintaining the vacuum pressure inside the column of SEM, because without the required amount of vacuum the electron beam cannot be generated and cannot be monitored or controlled. We require an atmospheric pressure of about 10^{-6} torr at this pressure the vacuum is higher which results in greater efficiency in microscope function. In order to obtain this pressure, we need different sets of vacuum pumps (higher and lower) which are named differently and all are designed to create the vacuum or prevent it from back streaming as well by opening and closing of required adjacent valves. In some microscopes these valves are automatically controlled while some are manually when changing the sample (Fig 3.7).

According to the figure there are three main valves i.e., roughing valve backing valve and main valve. At first, when we change the sample from the stage, all the valves are closed. After changing the sample, open the roughing valve between the mechanical pump and chamber to pre pump it at 10^{-3} torr so that high vacuum pump can begin pumping. Now closed the roughing valve to prevent backing of mechanical pump and open the backing valve and let the chamber attains its required atmospheric pressure and can back the high pump. After that open the main valve and wait for the chamber to the point where it actually attains the operating pressure.

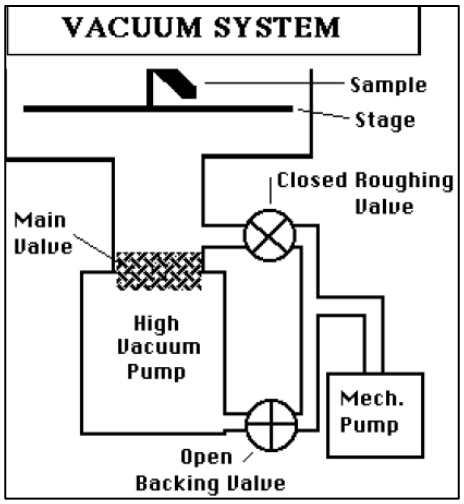

Figure 3.7 Showing the schematic diagram of one of the seven operations systems of SEM i.e., The Vacuum system.

3.4.2.2. Electron Beam generation

The electron beam generation is a system for electron gun of an electron microscope. Filament, grid cap and anode plate, which is positively charged to attract the negatively charged electrons of the beam and accelerates them in the descending column of the microscope, are the three main components of electron gun.

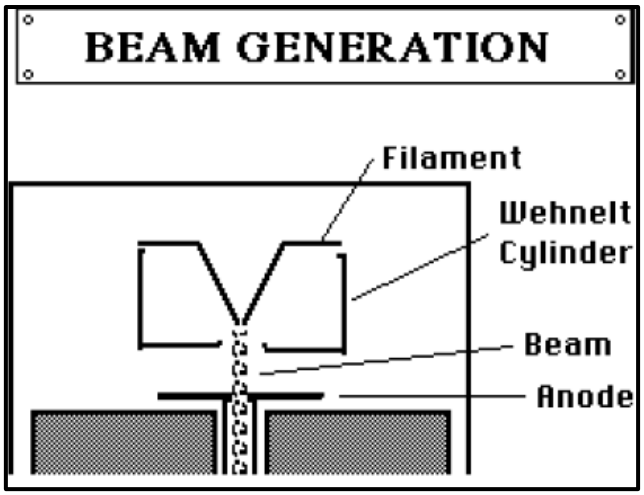

Figure 3.8 Showing the schematic illustration electron gun in beam generation.

The filament is made up of tungsten wire, it a basically a cathode. The wide range of voltages are usually generated in SEM. The range of voltages that have been used is from 0.1 volts to 40 kilo volts. The strength of voltage varies from specimen to specimen such as normally 10 kilo volts are

good enough for biological specimens. The main switch is used as power on and off button that supplied voltages to the filament. The filament power supply aids in adjusting the voltage that heat the filament knob known as filament current control knob which plays an important role in the discharge of balanced flow of electrons by thermal emission. The filaments are made up of different types of materials as well such as tungsten, Lanthanum Hexaboride crystal and Cerium Hexaboride etc.

A Wehnelt cylinder which is basically a grid cap. The purpose of the grid cap is to adjust the course of accelerating electrons. The final part of electron beam generation is an anode which is a positively charged plate that collect the electrons by attracting them and focused them down the column to the specimen.

3.4.2.3. Electron Beam Manipulation

The flow electrons are principally controlled by two main fields which are magnetic field and electrostatic field. The magnetic field is only used in the column of SEM excluding the beam generation part. The magnetic fields play an important role in the formation of electromagnetic lensed with the passing of electron current through a wire that is made up of copper.

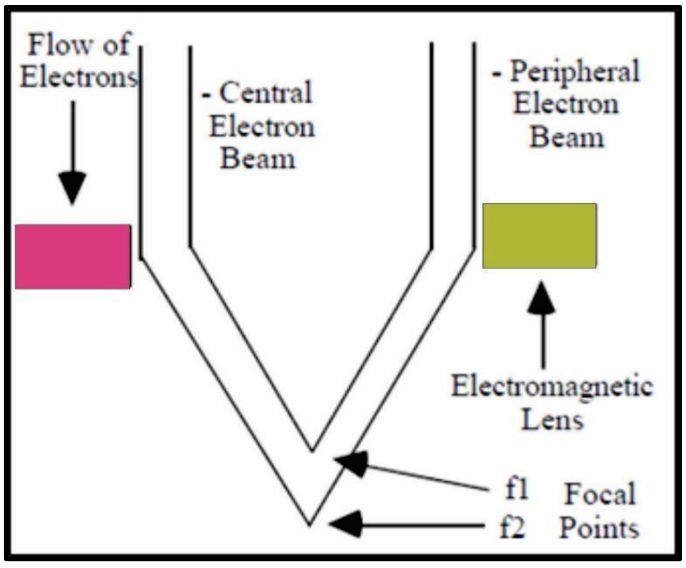

Figure 3.9 Shows the schematic position and working of electrostatic and electromagnetic lenses.

The negative part and positive part in the electron gun which are cathode and anode. When both these parts are near to each other they formed an electrostatic lenses or electrostatic field which controlled the generation as well as the flow of the electrons.

The electrostatic lenses and electromagnetic lenses (Fig 3.9) vary in Scanning Electron Microscope depending upon the type of specimen being examined. The magnification of SEM is mainly dependent upon the ratio of different areas of specimen being examined thoroughly to the dimensions of Cathode Ray Tube. The smaller the area of the specimen being examined the larger and clearer would be the magnification results.

There are commonly two main ways to adjust the magnification of SEM. The first one is to adjust the magnification control to rotate the area of specimen being scanned. The second way is to adjust or collaborate the beam focal point and the working distance which is a z-axis until the desired magnification of the results received.

3.4.2.4. Beam Specimen Interacting System

The interaction of beam with specimen involves scattering. The events of scattering are the most interesting at it contributes to the resulting resolution of the image from SEM. The detection of a signal starts when the beam of primary electrons hits the specimens and travels a certain distance before hitting a particle or an electron in the specimen. When the beam of electrons hits a particle or an atom of a specimen the process of scattering starts which involves back-scattered electrons, x-rays, transmitted electrons, secondary electrons and visible light. All these scattered events take place in a reaction vessel of a specimen (Fig 3.10). A reaction vessel is a part of a specimen that has been interacted with the beam of primary electrons.

The backscattered electrons are basically those primary electrons which does not interact with the specimen which means that they have the same energy as the incident beam of primary electrons.

The secondary electrons are the electrons that are emitted from the specimen electrons that have been dislodged by primary electrons. Secondary electrons can also dislodge the secondary electrons thus their energy level is low as compared to primary electrons and have very minute volts in the reaction vessel.

X-rays are generated when the beam of primary electrons dislodged the electrons from the orbit of the specific atom. The x-rays have characteristic properties such as wavelength and energy which can be detected and measured but the problem comes when then hit other atoms on their

way and lose their characteristic energy to a great extent on multiple encounters then they are termed as background X-rays.

Transmitted electrons are the primary electrons that pass through the specimen without being hit or encountered as the thickness of the specimen is thin. They somewhat provided the density information or the atomic density information about the specimen.

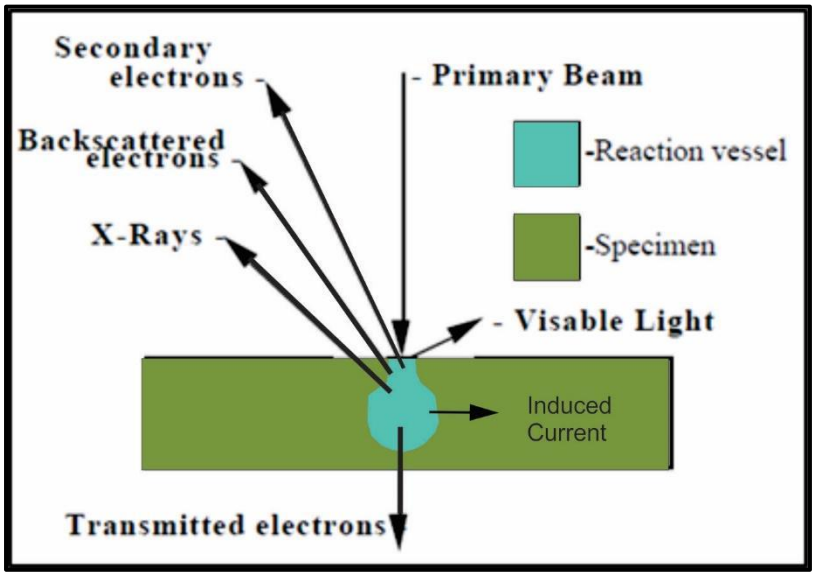

Figure 3.10 Shows a schematic illustration of beam interaction with the specimen.

The small reaction vessel that has been formed after the encounter of beam of primary electrons with the specimen provides greater resolution if the vessel is small in size however, the large reaction vessel, on contrary, provides greater signal.

3.4.2.5. Signal Detection

The signal detection is done by the emission and detection of secondary electrons that have been emitted when the beam of primary electrons hit the specimen. The secondary electron detector has various parts and attracts magnetically the secondary electrons by a voltage of 200 plus potential applied by a faraday cup (Fig 3.11). These electrons then pass through a photomultiplier tube where it increases and amplify the incoming signal. The signal strength that has been amplified was measured and controlled by PM which is dependent on the number of secondary electrons that has been emitted during the interaction of primary electron with the

specimen particle or atom in a reaction vessel. These signals are then detected and displayed over the signal detector.

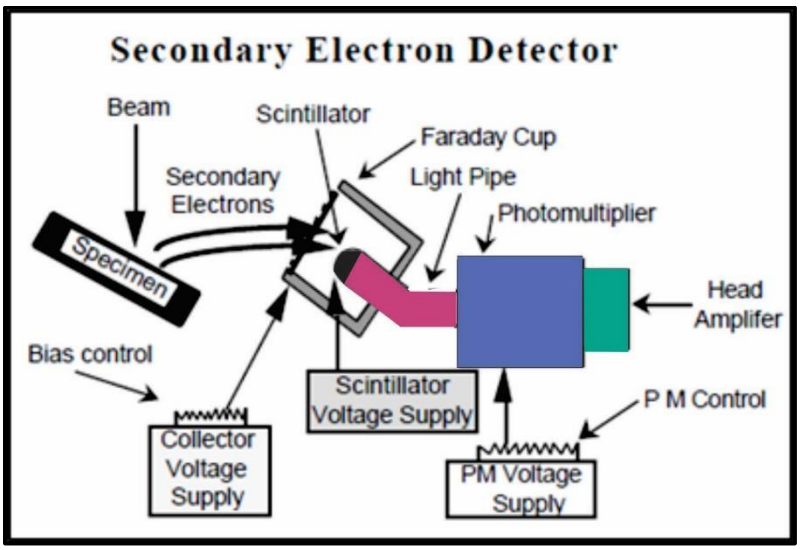

Figure 3.11 Illustrates the schematic diagram of Secondary Electron Detector or Signal Detector.

3.4.2.6. Signal Manipulation

The manipulation of signal basically starts form the amplification of a signal from signal detector to the view of the signal image on the screen in the end. The signal manipulation system also adjust, manipulates and controls the contrast, brightness and other attributes of the displaying image. In SEM the image is converted in cathode ray tube after the signal have been received, the cathode ray tube consists of numbers of pixels. Different values are assigned to multiple pixels in order to generate the list of numbers that form or represent a resulting image.

3.4.2.7. Display and Record System

The display and record system controls the visualization of an image by adjusting its various attributes that determines the quality of a micrographic image. These attributes include, noise, brightness, contrast, depth of field, composition magnification and resolution.

3.4.3. Applications

The applications of SEM lie over a broad range of discipline and studies. As this tool is used to produced high-resolution images of a solid surface of at least 5 microns in a detailed manner by achieving the elemental aps of the study sample. It is also use to give information about the spatial variations of chemical compositions of the solid sample as well by generating the compositional maps of the study sample. Also provides aid in the determination of phase changes, crystal structure and crystal lattice of different minerals by giving the qualitative information. It is used in various biological studies, physics, mineral identification, chemical structures and chemical composition of various substances etc.

CHAPTER 04

METHODOLOGY

4.1. Introduction

This chapter includes the explanation of all the methods that are involved in order to acquire the desired results for magnetic separation of mineral by Frantz Isodynamic Magnetic Separator. The steps involving in the process of methodology are explained in order of application in laboratory.

The samples of three formation are involved in this study. Among which one sample belongs to Dernburg formation of Marmora-Chameis sub-terrane (CR 06) which is a gabbro. The next sample belongs to Grootderm formation of Marmora-Chameis sub-terrane (R 125) which is a lava agglomerate. The final sample belongs to Vredefontein formation of Port Nolloth Group (PNG) (R 16) which is also a lava agglomerate. All the rock samples belong to same age group of Neoproterozoic age.

All three samples are then processed further step by step. The first step is sieving, after sieving every formation's sample would have three fractions. The first fraction is the original size, the second fraction is of less than 150 microns size and the third fraction is of less than 250 microns size. Therefore, each formation has one sample and each sample would further have three fractions of sizes.

4.2. Sieving

The first step of this work is the sieve analysis or sieving of the samples. The two samples of each formation were marked and organized in a way that it would not get mixed. Then we took the section of each sample one by one and separate each section in four different mounds of equal proportions with the help of a blade. The four mounds of same proportion of every sample were prepared (Fig 4.1). The purpose of making four different mounds of section of a sample is to equally distribute the grains of various sizes such as fine grained and coarse-grained particles and different minerals, all this material is equally distributed in four parts. Out of parts of each sample section one was further processed for mounting and Frantz analysis, whereas the rest of the three mounds were saved for later.

The one part was then undergone through sieving by using two different sieve sizes. The sieve sheet is basically a sheet of net with different sizes such as 150, 250 microns (Fig 4.2) etc. These sheets are used to separate the certain size of grains from the rest of the granular material in order to acquire the constant size in sieve analysis.

Figure 4.1 Shows the distribution of section of a sample in four different mounds of equal proportions with the help of a blade.

In this study we have used two sheet sizes of less than 150 microns and less than 250 microns to separate the grains of certain size from the rest of the sample part.

Figure 4.2 Shows sieve sheets pf different sizes.

In order to separate the grains of less than 150 microns and 250 microns we had arranged the apparatus. We took a holder and a sieve sheet of 150 microns and 250 microns. Then we cut the two pieces of those sheet sizes respectively and glued the sheet at the bottom of the holder (Fig 4.3).

Figure 4.3 Shows the picture of two holders with sieve and without sieve.

The two holders with two different sizes of sieve glued at the bottom of the holder are then placed separately over a funnel on which filter paper is folded in a shape of the cone and is fixed inside along the sides of the funnel. The funnel is then placed inside a flask (Fig 4.4).

Firstly, all the sections from three samples of study were placed inside the holder one by one, which had piece of sieve of size 150 microns at its bottom. It allows the grains of 150 microns in size to pass through the sieve and collected on filter paper and the rest of the residue that are larger than 150 microns in size remains inside the holder. After that, we used distilled water as well in the end to facilitate the remaining residue to cross the sieve sheet. At the end of the sieving the desired size of the sample will collect on the filter paper which was then extracted. Whereas, the residue that was left inside the holder was then removed, cleaned and then used for further sieving of other fractions. This procedure was repeated for each sample for 150 microns and then the same procedure repeated again but this time for 250-micron size. In total, we get 6 sample from three formation, two samples (one of 150 micron and one of 250 micron) for each formation.

Figure 4.4 Shows the holder placed over funnel that is aligned with filter paper and placed over a flask used for sieving.

4.3. Frantz Isodynamic Magnetic Separator

The next step involved the magnetic separation of minerals. The magnetic separation of the mineral is initially done by using the hand magnet which is an oldest known method for magnetic separation. The purpose of doing the magnetic separation of ferromagnetic minerals before further placing the sample into Frantz apparatus is to avoid clogging of grains from the sample. Initially, the sample contains both ferromagnetic, paramagnetic and non-magnetic minerals. The ferromagnetic minerals are those which can be extracted from the sample simply by using a hand magnet, this is usually done because ferromagnetic minerals are more and easily attracted to magnet as compared to others that is why if we extract them earlier before feeding it into Frantz where it can attract to magnetic poles of the instrument and disturb the whole process in progress.

First, we took the three fractions of the sample, placed it or evenly spread it on A4 page. Then grabbed a magnet placed it inside a plastic bag and then we hold the magnet over a sample sheet at a short distance and run the magnet slowly on the top of it over a whole range of spread sample. The ferromagnetic minerals inside a sample fraction got attached to the magnet above it and then we turned the plastic bag over a magnet, inside out and collect the ferromagnetic minerals. The

process was repeated at least 3 to 4 times to remove the possible ferromagnetic minerals from the different fractions of sample (Fig 4.5).

Figure 4.5 Shows the separation of ferromagnetic minerals by a magnet by hand or manually.

Now there were three fractions of each sample belongs to three formations of study area were ferromagnetic minerals free. All these fractions were then further moved towards Frantz Isodynamic Magnetic Separator to separate the paramagnetic minerals from non-magnetic minerals at different amperes. First, the fraction of mixed grains size was separated, then the fraction of less than 150 microns and in the last the fractions of less than 250 microns were separated at different amperes by adjusting it from the control system.

The Frantz Isodynamic Magnetic Separator was first thoroughly cleaned parts by parts such as chute, bolts, aluminum trays, feed, collecting tins etc. All these parts were then carefully attached back to its place without leaving any dirt stain or grease of our hands that was capable of contaminating the sample. First of all, the butcher sheet was placed beneath the apparatus and then parts were attached. Firstly, the aluminum ramp was attached back under the magnetic poles carefully with the help of a brass bolts. The bolt on the top of the ramp was fixed properly or tight enough to prevent it collapsing from the continuous shaking of the instrument which can last from hours to all day long at maximum in the process of separation. When we were installing the brass chute or ramp back, after cleaning the parts, we made sure that we did not touch the inside of the ramp, where the sample would be travelling, that could leave the grease stains out of hands. As the

grease will not only contaminate the sample but also acts as barrier on the floor of the ramp which would make difficult for the sample to move down the ramp for separation.

The angle of the ramp can be adjusted or its tilt angle can be selected from the scale that is present at the top the forward scale and at the side the tilted scale (Fig 4.6). The forward scale is commonly adjusted between 21-22 and the tilted scale was adjusted depending upon the sample capacity of falling fast or stickiness to the ramp or slow on the slope. For example, if your sample is super magnetic and nothing will fall out, we need to make the angle steeper.

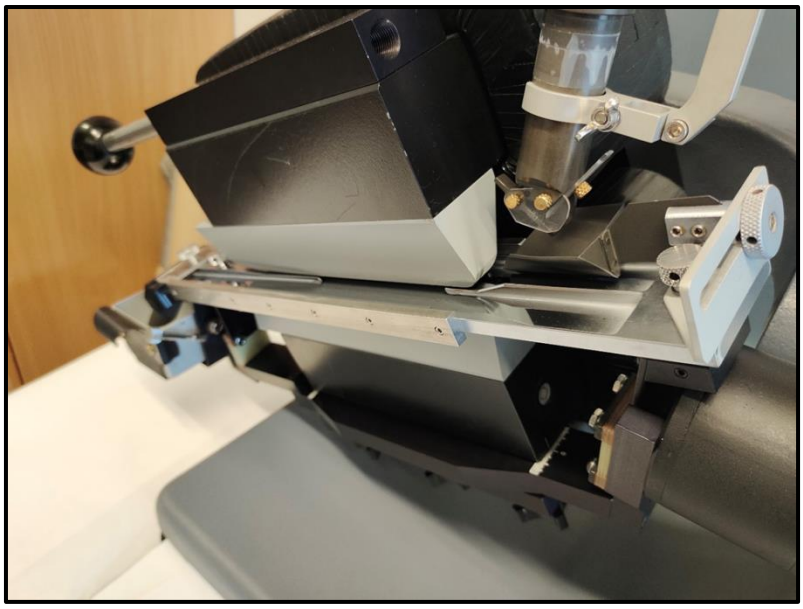

Figure 4.6 Shows the tilted angle of chute which has been adjusted by using a scale.

In the next step we took the fork chute and aluminum shield that went over the top of the chute in a way that both the parts can slid over the bottom part of the ramp in such a way that, with the help of an aluminum bolt both parts can be attached (Fig 4.7). The aluminum bolt was not overtightened as it was a plastic chute.

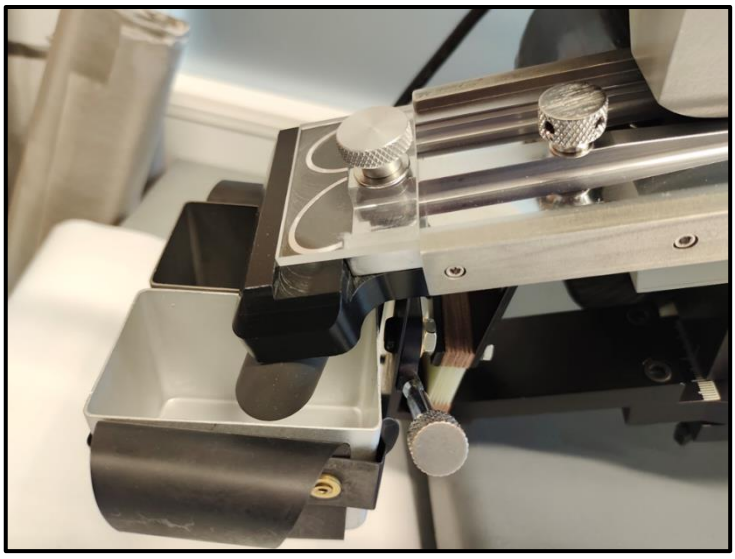

Figure 4.7 Shows the aluminum bolt to fix the fork chute along with the distribution bins at the bottom end of the ramp.

The following step was to install a two collecting bins with two different colors. The dark colored that goes towards left was for collecting magnetic grains and the light-colored bin that goes right was for collecting the non-magnetic minerals. Both the bins were fixed at the bottom of the fork chute. The springs on either end were grabbed and slide for a bit until the bins fixed into place where we heard a clipping sound that indicates the proper fixation of the bins (Fig 4.8).

Figure 4.8 Shows two separation bins attached at the end of the chute to separate non-magnetic grains and magnetic grains.

After that we moved towards the feed of the instrument. The parts of the feeds were adjusted by bolts in a way to adjust the entry of the feed from the holder to the ramp tight enough so that certain size of the grains can pass through and the angle of mini hopper parts were adjusted in such a way to avoid the collapsing of magnetic minerals coming from the feed towards the magnetic poles over the ramp (Fig 4.9). In order to avoid the collapsing and scattering of the feed is to adjust the angle of opening below the magnet and towards the ramp so that if any magnetite that was still present in the feed would not disturb the process by directly sticking to the magnet in front and scattered the feed everywhere, also make sure that the instrument is turned off before adjustment. The funnel and plunger were then adjusted above it in sequence respectively and attached perfectly still with the help of a bolt. After that the funnel and the top of the mini hopper had a minimum gap which can be diminish by putting a tap along the boundary of both parts.

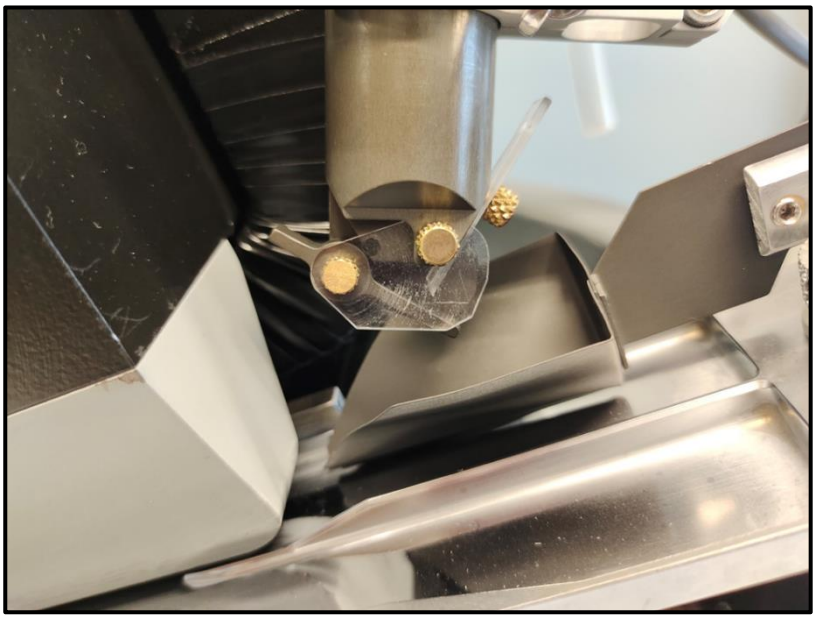

Figure 4.9 Shows the tilted angle of mini hopper that allows the sample grains to travel from the sample feed to the chute without collapsing with the frontal magnetic poles.

After that we took out our sample and pour it inside the sample holder or sample feed. In order to start the process, make sure that all the voltages are turned to zero before switching on the instrument to avoid the fluctuations and surges of voltages. The strength of voltage can be adjusted and changes from the controller provided (Fig 4.10). Then turned on the machine and adjust the voltages according to the requirements or need. The voltages can start at all levels such as 0.1, 0.2 or 0.3 etc.

Figure 4.10 Shows the voltage controller that aids in adjusting the voltage provide to the Frantz Instrument according to requirement.

The same precautions go for the 'Chute' and 'Feed' of the vibrator controller (Fig 4.11). Both the chute and feed first dialed down to zero and then switched on. The chute and feed both can be adjusted according to the needs while pouring the sample to prevent any spills out and also the chute to stop the fall out of sample grains whole travelling through the chute to prevent the loss of magnetic or non-magnetic grains.

Figure 4.11 Shows the chute and feed controller to adjust the speed of feed and the vibration of the chute.

The rate of feed and chute depends upon the amount of non-magnetic and magnetic grains so the controls were adjusted according to it. The knobs, bolts and controls were checked thoroughly for safety purposes.

The fractions of samples were then separated in Frantz in a sequence to acquire the desired magnetic separation on different voltages.

4.4. Mounting

The next step in this study is termed as mounting. Mounting is a specific method in which the fractions of the sample after sieving of certain size are then individually placed or mount on a glass slide. The sample after being analyzed by Frantz magnetic separator at different amperes i.e., 0.1 A, 0.2 A, 0.3 A, 0.4 A, 0.8A depending upon the strength or properties of the grains being analyzed under Frantz Magnetic Separator including non-magnetic grains and ferromagnetic grains.

The three study samples i.e., CR 06, R 125 and R 16 have three fractions of sizes each i.e., original fraction size, less than 150 microns and less than 250 microns. The total 12 slides of mounting had been prepared after analyzing all the fractions at different amperes until not enough sample left for further separation. In case of R 16 sample the grains have been separated at the strength of 0.8 - 1.0 A.

For the preparation of the mounting slides. First, we took a glass slide and with the help of a black marker we drew too circles in order to make mounting maps (Fig 4.12).

Figure 4.12 Shows a glass side on which two circles drew with a black marker

After that we grabbed a double-sided tape and paste it over the slide in a way that circles, we drew were still visible enough to place the grains inside the circles and also the grains can be able to stick on the tape as well. We placed the grains on Whatman paper.

The next step is to mount sample grains being separated on different amperes with the help of a needle which was attached with a pen to ease the process of picking grains and placing them on the glass slide in a line of certain ampere one by one (Fig 4.13).

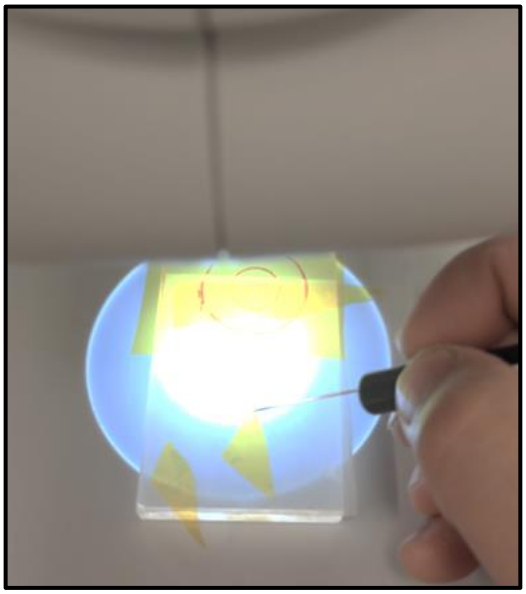

Figure 4.13 Illustrates the process of mounting under Microscope with the help of a needle being attached to a pen.

This process took a while in order to make 12 glass slides with varying amperes lines and in the end the line of non-magnetic grains and ferromagnetic grains. All this was done under binocular microscope (Fig 4.14) as it requires minute observation and working on grains in microns size. Approximately around 100-400 grains were placed in a single line of a certain ampere.

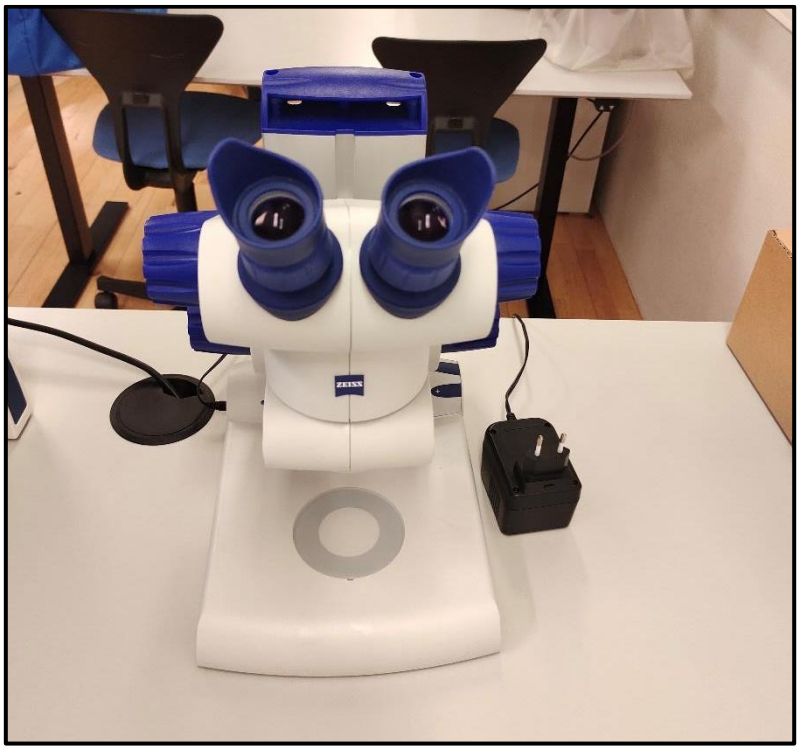

Figure 4.14 Shows a picture of a Binocular Microscope used for mounting.

Now after preparing the slides under microscope, we are then directed to prepared mounting maps of each sample formation having further fractions of sizes each. The mounting maps are prepared on paper sheets that helps us in understanding the slide easily about the lines of grains being separated at which amperes and the separation of non-magnetic minerals and ferromagnetic minerals. The sample of mounting maps are explained in the figure below (Fig 4.15). The mounting maps are usually the representative of the mounting slides in order to ease the understanding of the slides and the grains magnetic separations.

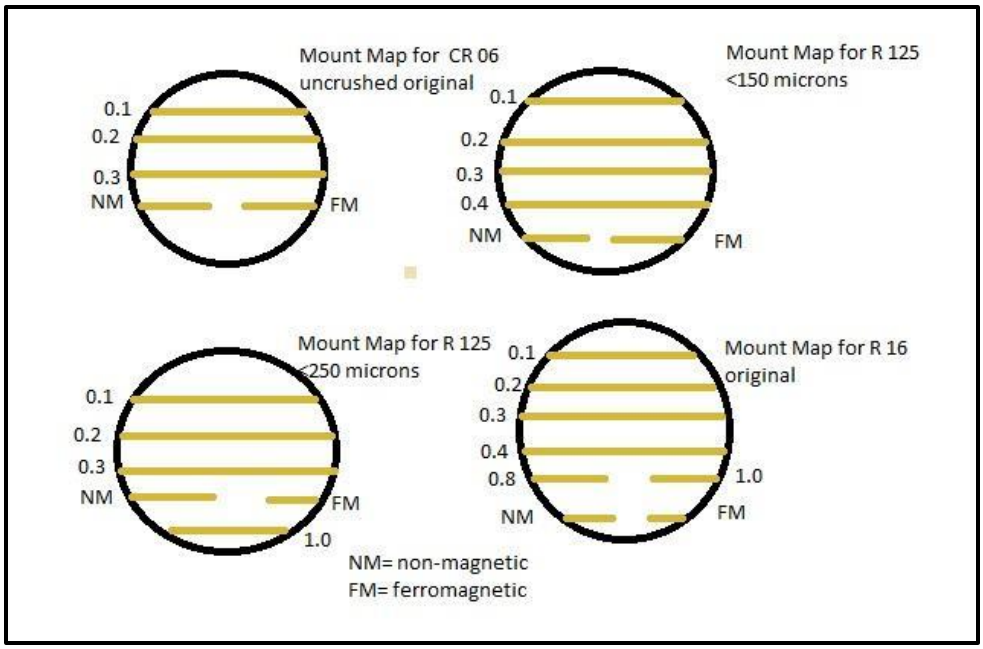

Figure 4.15 Represents Mounting maps of each fraction size of sample formations in order to understand the mounting slides.

The proportion of grains for each fraction of a sample formation was being separated on different amperes in Frantz. All the grains of one proportion that was being separated on let's say 0.1 A are then aligned in one line of mounting slide or mounting map, one by one with the help of needle that was being attached to the pen. The similar process was repeated for every ampere of each proportion of fractions until there was no magnetic grain left for separation. Then the rest of the grains were then aligned on a non-magnetic (NM) line. Whereas, the ferromagnetic grains (FM) that were previously separated by hand magnet were arranged in ferromagnetic line one by one on mounting slide.

4.5. Epoxy

Epoxy is a final step in the study. In order to prepare a suitable epoxy for the sample we used two chemicals named as Epofix resin and Epofix hardener are poured into a jar or a plastic cup in a specific proportion. The ratio of resin and epoxy varies and quantifies in grams. Add 3g and 25g epoxy, 6g resin and 50 gm epoxy, 1.5g resin and 12.5g epoxy respectively. Then we sterilize tit and mixed thoroughly until all the bubbles are gone. The cup was now put on weighing machine in order to weight the amount of liquids being added to attain a required proportion for the making of epoxy. The liquids are mixed with the help of a glass pellet (Fig 4.16). The glass pellet aids like

a spoon and helps in mixing the liquids with efficiency, the liquids were mixed thoroughly and slowly until there were no bubbles left.

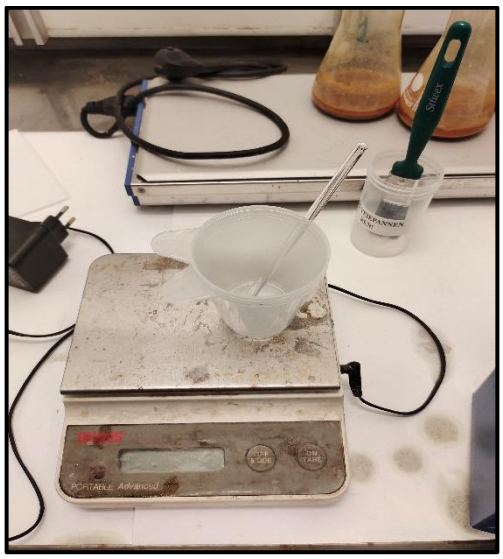

Figure 4.16 Shows the picture of a plastic cup with a glass pellet on a weighting machine, used for the mixing of equal proportions of chemicals to form an epoxy.

After that we placed the plastic jar with epoxy in it into an oven where it was heat at optimum temperature for almost 8 to 10 minutes at the temperature of 55 degree Celsius. After that we took a glass slides and holders for each slide. The bottom of the holders was usually uneven, so we have to even the bottom surface of the holder so that the holder can easily place over a mounted glass slide (Fig 4.17) and when we pour epoxy inside it, the epoxy would not make its way out of the minute gaps between holder and the slide. The holder was rubbed on Rhaco grit paper of 220 (coarse), 320 and 500 (fine). The holders were then cleaned with ethanol before being used.

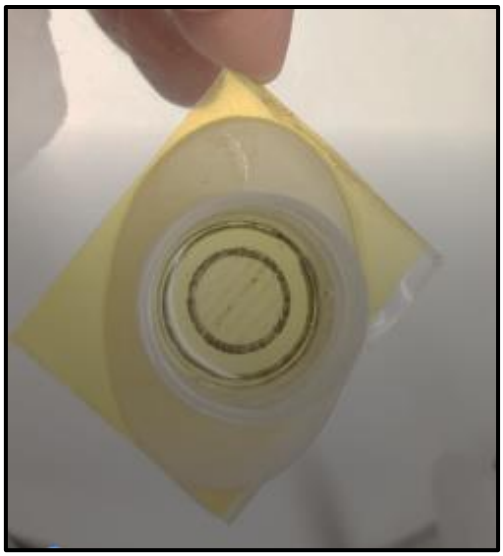

Figure 4.17 Shows an already prepared mounted glass slide with a holder placed over it in such a way to accommodate epoxy inside it.

The bottom surface of the holders is generally polished with the help of Rhaco Grit paper. The Rhaco grit paper comes in different sizes i.e., 220, 320, 500 and 100. We had used the Rhaco grit paper of three different sizes which are P220, P320 and P500 (Fig 4.18). All these three sizes were used in a sequence to polish or even the bottom surface of the holder.

Figure 4.18 Shows the box of Rhaco Grit paper of different sizes.

Now after making the glass slide ready for epoxying by gluing the polished holder over the mounted glass slide. The glass slide was then placed inside the mounting press machine by Struers (Fig 4.19).

Figure 4.19 Shows the mounting press machine used.

The machine was then turned on, when we pressed the switched-on button the glass lid over the container, that contains sample slide, covered the container and pressed downward to start the process of vacuum inside the container to avoid contaminations and prevent the formation of bubbles inside the epoxy (Fig 4.20). The percentage of the epoxy start to shows over the screen, wait till the percentage of vacuum reaches 100 percent.

Figure 4.20 Shows the glass slide placed inside a vacuum container with a closed glass lid and epoxy flows through a pipe opening inside the vacuum.

Then, remove the plastic cup filled with epoxy from the oven and placed it besides the mounting press machine. There is a pipe that passes through a valve and reaches inside of the vacuum

container. The other end of the pipe was then dipped inside the plastic cup of epoxy which transfers the epoxy from the cup via pipe all the way to the vacuum container. The flow of the epoxy though pipe form cup to the slide was controlled through a valve between it. The vacuum that has been created first inside the closed container was to avoid the formation of bubbles inside the epoxy filling. The epoxy was not filled up to the mark of the holder in fact it was filled at median level of the holder to cover the exposed surface of mounted glass slide with epoxy.

After the filling of epoxy, the vacuum was removed and then we took the glass slide out of the container and placed it outside. Weight was applied or placed on the top of the holder of mounted glass slide and let it sit there for approximately 18 hours.

4.6. Polishing

The next step is to polish the mounted slide with epoxy. The purpose of the polishing is to remove the excess epoxy which was hiding the grains. For this purpose, we used the glass slide on which the mounted slide had been polished (Fig 4.21) along with the mixture of tap water and Silicon Carbide Powder of #1000 (the chemical used for lapping mineralogical and ceramic samples) size. The glass slides of various sizes were available such as 220, 320, 600 and 1000.

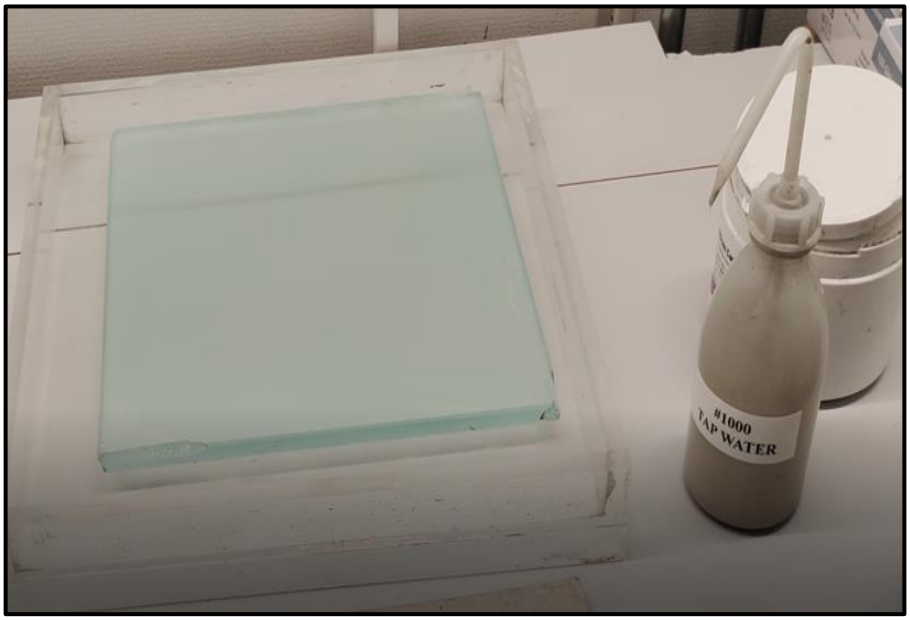

Figure 4.21 Shows the glass slide and bottle of tap water and Silicon Carbide Powder (#1000) for polishing.

Then we took a glass slide and polished its front side in episodes by frequently adding tap water mixture from the bottle when needed. The process took almost 20-25 minutes until the grains in the epoxy were at the surface enough to shine and examined easily but not too much exposed to get damaged or lost. After polishing the front side of the mound, we then moved to the machine of polisher and grinder (Fig 4.22) where we used the Rhaco grit paper placed on the machine plate and with the help of a tap above it the water was sprinkled when needed. The plate rotated at a speed to polish the bottom side of the mound slide. The front side was polished by hand and the back side was polished by the polisher-grinder machine to even the surface.

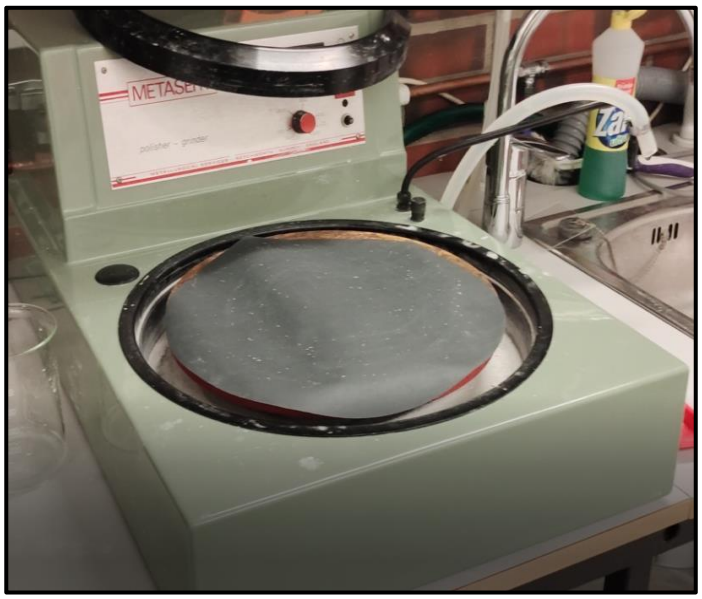

Figure 4.22 Shows the Polisher-Grinder Machine to polish the back side of the slide.

After that we moved forward to the next instrument which is a 'Struers Rotopol-35'. This instrument is specifically designed for polishing and griding and for the fast preparation of the sample slides (Fig 4.23). In this we put on the blue plate (3µm) DAC. Wet with 3µm DAC liquid + blue liquid. Polish the backside for 5 minutes on 10 Newton force. Then turn the mount, polish front side for 5 minutes with 5 Newton force. If needed then make it more 5 minutes.

Figure 4.23 Shows Struers Rotopol-35 instrument used specifically for polishing and grinding.

Now the mount slides are completely polished from both sides. In order to remove the remaining or extra dust particles that were somehow got captured in slides during polishing were then removed by the Ultrasonic water tank (Fig 4.24). We took our samples and placed it in a beaker along with the and placed the beaker inside the Ultrasonic water tank and turn on the machine for like 3-5 minutes. The machine created a sound resonance which then helped to remove the remaining dust particles.

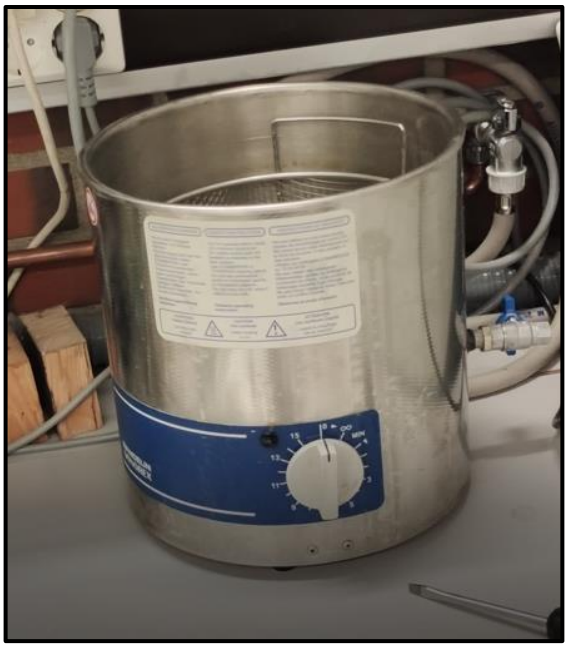

Figure 4.24 Shows the Ultrasonic water tank used to remove the dust particles from the sample after polishing.

4.7. Carbon Coating

The carbon coating is the final stage in the preparation of the mound/samples. The purpose of carbon coating is to remove any surface charging that can be created when analyzing the mound/samples in SEM. In this step the mounds are coated with an electrically conductive material (i.e., carbon) that would allow the steady flow of electron flux. The carbon coating of the mounds is important before their analysis in SEM otherwise due to the generation of surface charging the image deduced from SEM will have image distortions.

The instrument used in this step is known as Emitech K250 Sputter Coater (Fig 4. 25). The sample slides or mounds were first placed inside a glass chamber and covered with a lid having two carbon electrodes that are exposed insider the chamber. The carbon thread was placed in between these two electrodes by loosening the screws of the electrodes and then tightened them. After that the machine was switched on and then turned on the pump to create the vacuum of about 1×10^{-1} mbar pressure. Once the vacuum was achieved, we turned on the outgas switch for about 60 seconds that burned the carbon thread inside the vacuum chamber for 60 seconds after that we stopped outgas and turned on the vacuum again which now then achieved the pressure of 7×10^{-2}. Once this

vacuum is again created inside the vacuum chamber, we turned on the evaporate switch which caused the sprinkles of recently burnt carbon onto the mounds/slides we placed inside the chamber.

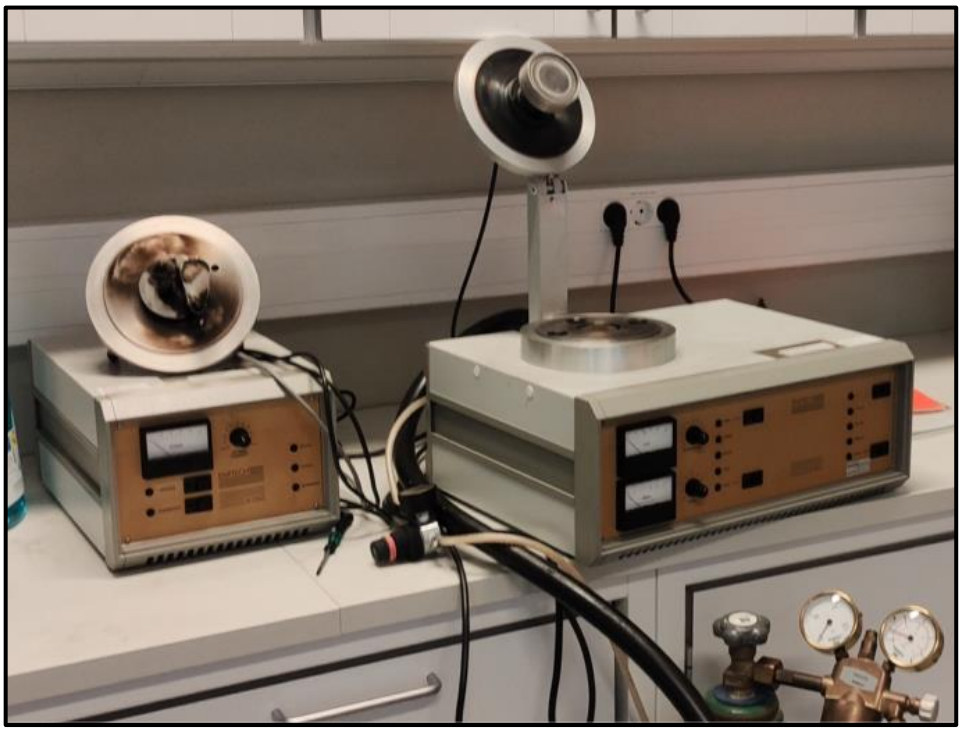

Figure 4.25 Shows the Emitech K250 Sputter Coater, that has been used for carbon coating.

In our study work we have done carbon coating for each mound/slide twice. As the one coat of carbon onto the slide did not produce enough charge for proper analysis in Scanning Electron Microscope.

4.8. SEM Analysis

The Field Emission-Scanning Electron Microscope (FE-SEM) (Fig 4.24) along with its various components gives us detailed information about the sample slides/mounds. Each component gave certain set of a characteristic or elemental information of the sample. The FE-SEM along with the sets of detectors aids in the characterization and identification of minerals also gives us the details about mineral structure, shape of the grain, fractures, different inclusions and phases within one grain. The cathodoluminescence detector (CL) gave an image of high resolution of detrital minerals separately that displays their different zonation. The backscattered electrons detectors (BSE) helped in formation of mineral maps on the surface of the sample by creating contrast

images of elemental compositions of surface of the sample being analyzed. The energy dispersive spectroscopy detector (EDS) was used to identify and semi-quantify the heavy minerals by giving the percentage of weight (wt.%) and atomic percent (at%) for each element in the mounds/sample slides being analyzed under SEM.

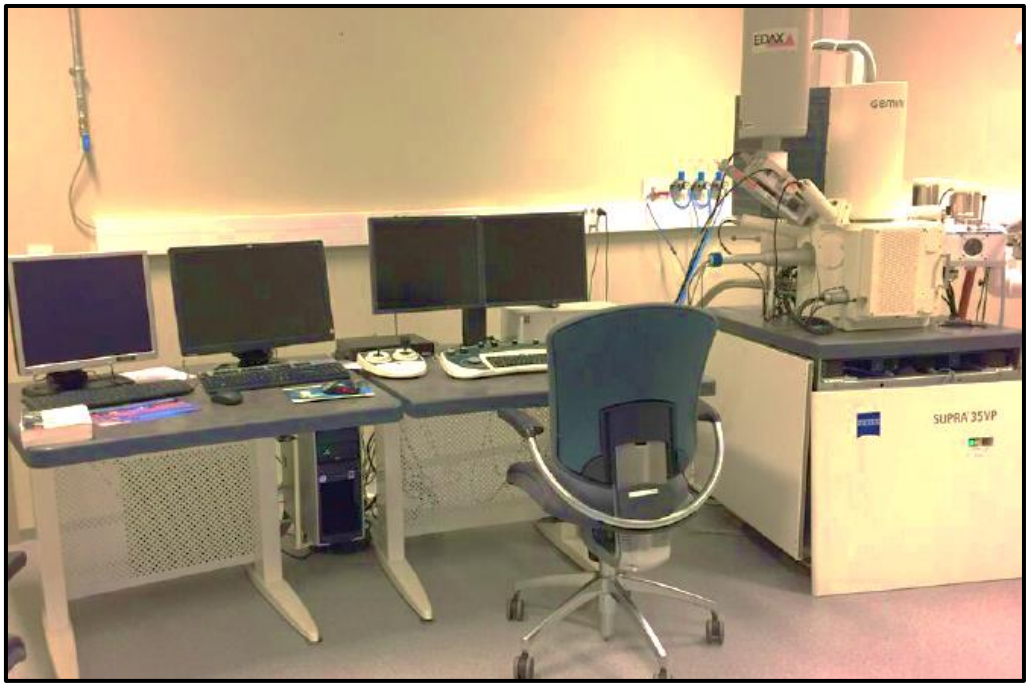

Figure 4.26 Shows the Zeiss Supra 35VP FE-SEM located at UiS.

The sample slides or mounds after carbon coating were placed on a sample holder and a carbon tape was used at both ends of the sample in order to prevent the risk of overcharging. The one or two slides were usually placed inside the vacuum chamber of FE-SEM for analysis to begin by adjusting the various components and detectors of SEM at an angle to attain desired results.

CHAPTER 05

RESULTS

5.1. Introduction

The results of this thesis work were carried out and divided into three analytical methods which are Frantz Separation, X-Ray Diffractometer analysis and Scanning Electron Microscope images. The results are discussed in detail in the next chapter (Chapter 06).

5.2. Results deduced from Frantz Magnetic Separator

Following are the images of results that have been derived after the magnetic separation of mineral grains from Frantz Isodynamic Magnetic Separator and mounted on slides. There are three samples **CR 06, R 125 and R 16**. Each sample, based on grain sizes, has further divided into three fractions:

- An original/reference sample
- Reference sample Frantz Separated
- Less than 150 microns

5.2.1. The Dernburg Formation (CR 06)

The following figures belong to sample CR 06 which is a gabbro of Neoproterozoic age. The sample grains underwent magnetic separation by Frantz after sieving which divides the sample into following fractions.

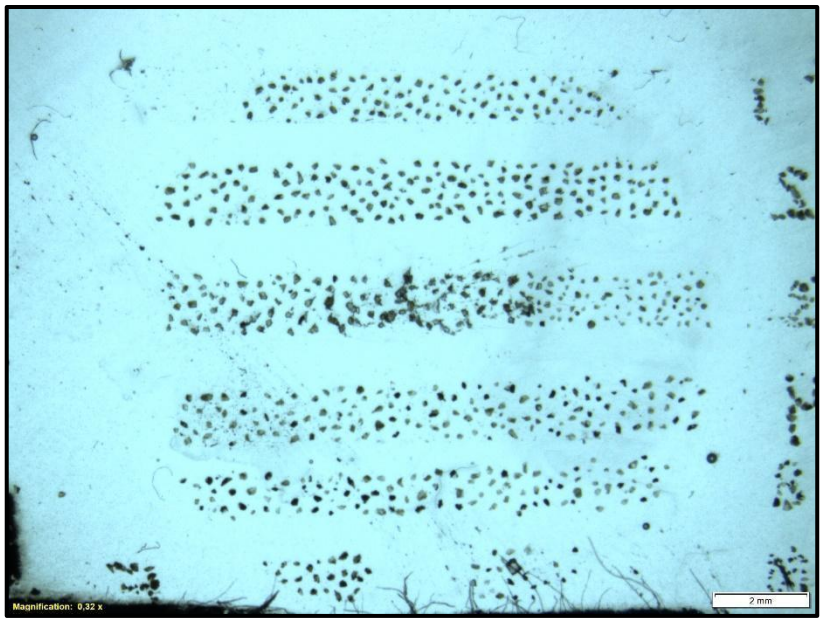

Figure 5.1 The mounted slide shows the separation of reference sample grains by Frantz (CR 06).

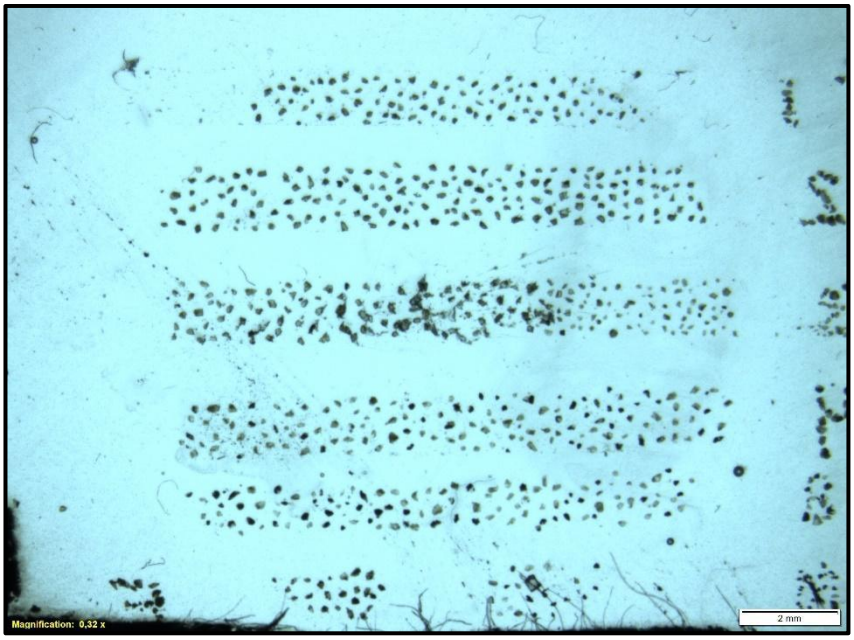

Figure 5.2 The mounted slide shows the separation of reference sample-Frantz separated grains by Frantz (CR 06).

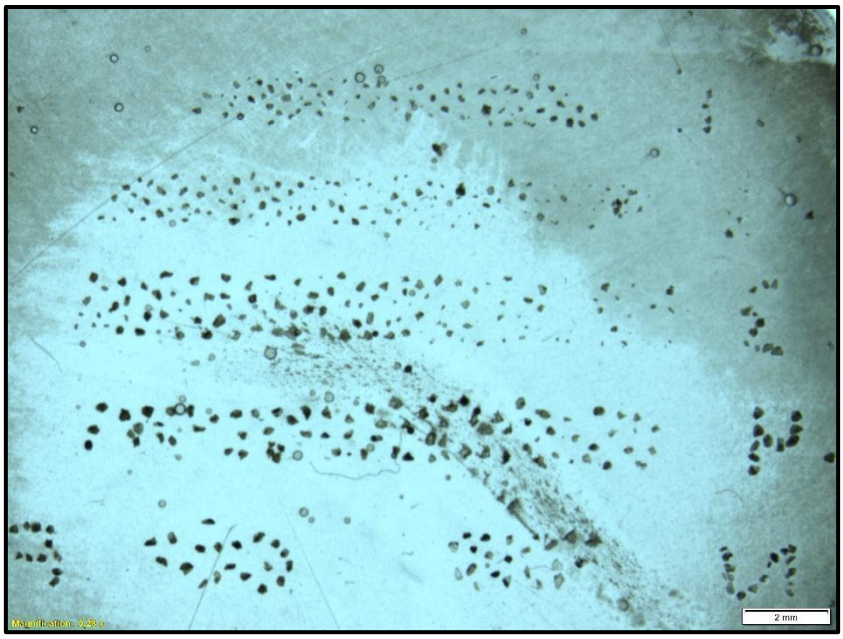

Figure 5.3 The mounted slide shows the separation of sample grains that are less than 150 microns by Frantz (CR 06).

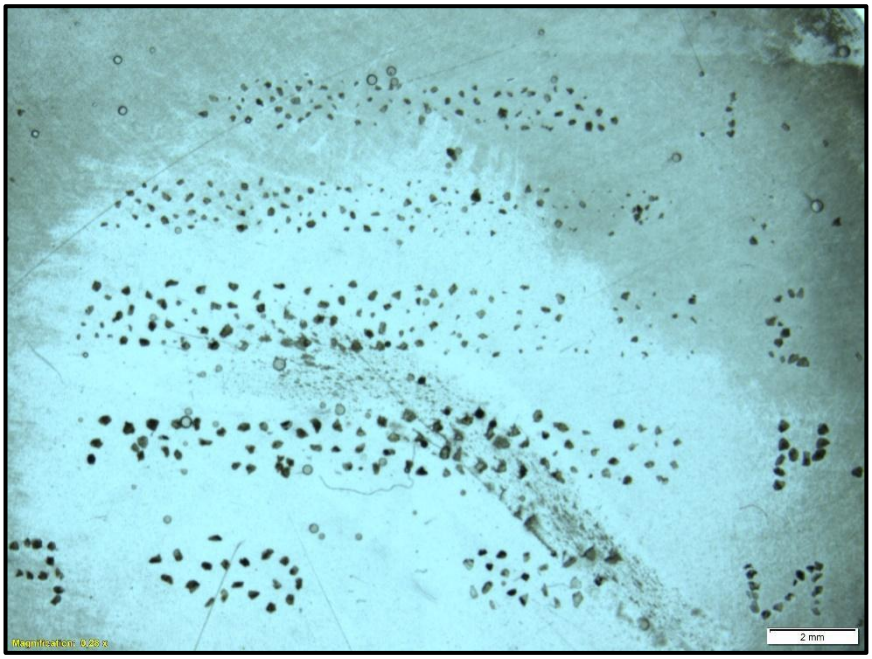

Figure 5.4 The mounted slide shows the separation of sample grains that are less than 250 microns by Frantz (CR 06).

5.2.2. The Vredefontein Formation (R 16)

The following figures belong to sample R 16 which is a lava agglomerate of Neoproterozoic age. The sample grains underwent magnetic separation by Frantz after sieving which divides the sample into following fractions.

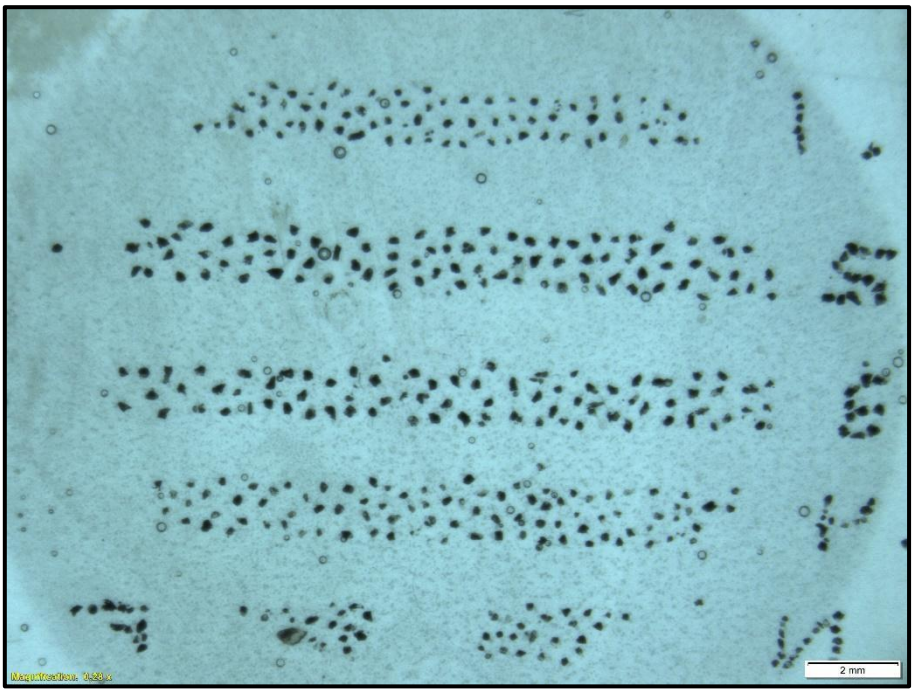

Figure 5.5 The mounted slide shows the separation of reference sample grains by Frantz (R 16).

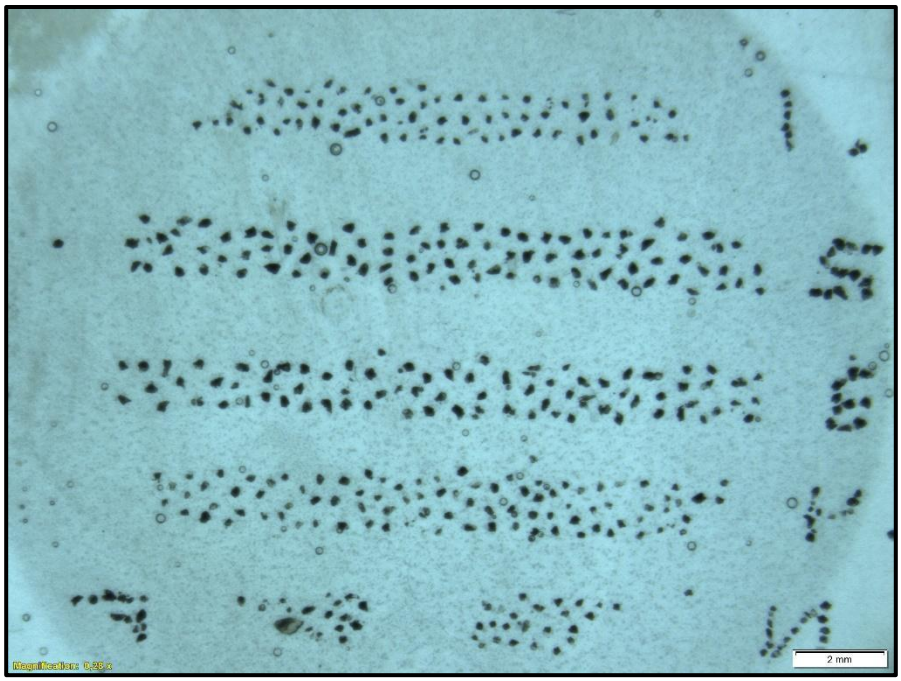

Figure 5.6 The mounted slide shows the separation of reference sample-Frantz separated grains by Frantz (R 16).

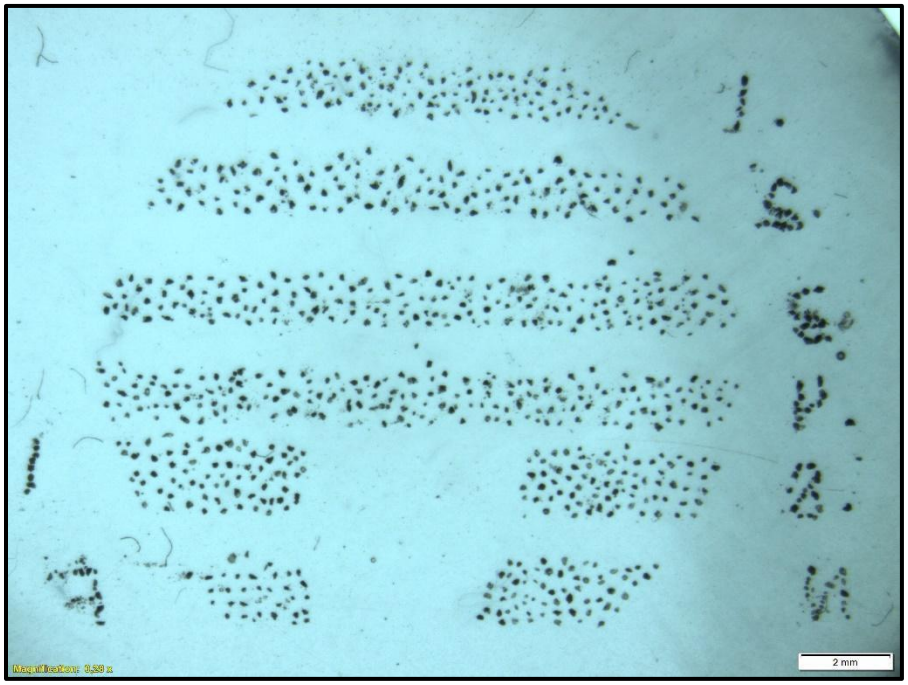

Figure 5.7 The mounted slide shows the separation of sample grains that are less than 150 microns by Frantz (R 16).

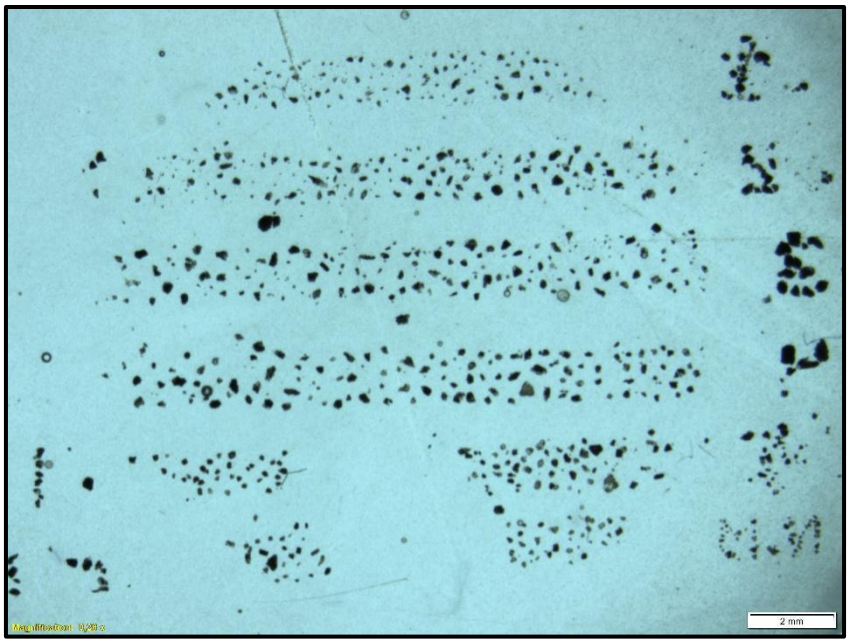

Figure 5.8 The mounted slide shows the separation of sample grains that are less than 250 microns by Frantz (R 16).

5.2.3. The Grootderm Formation

The following figures belong to sample R 125 which is a lava agglomerate of Neoproterozoic age. The sample grains underwent magnetic separation by Frantz after sieving which divides the sample into following fractions.

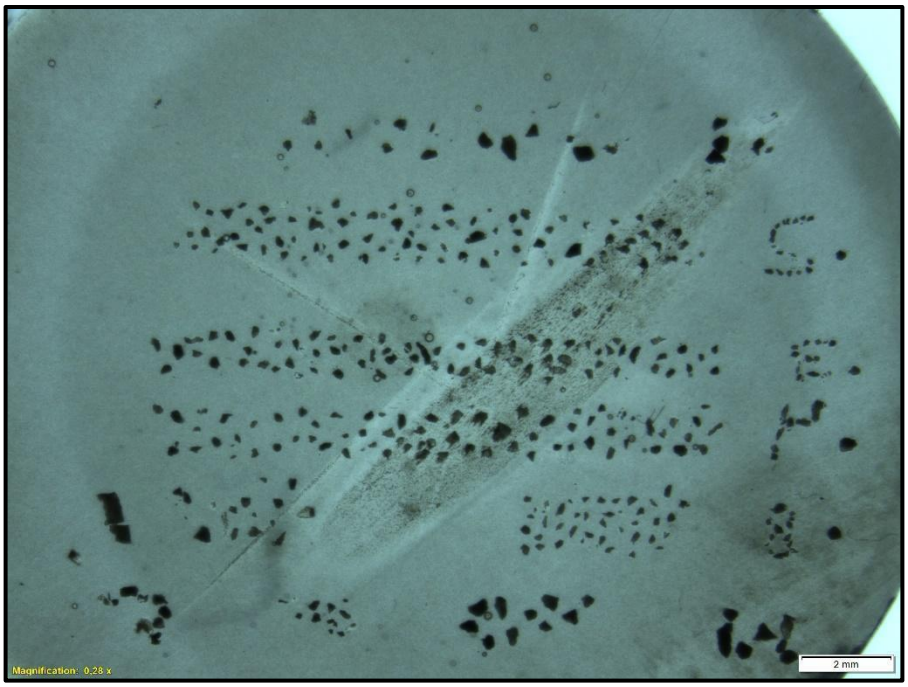

Figure 5.9 The mounted slide shows the separation of reference sample grains by Frantz (R 125).

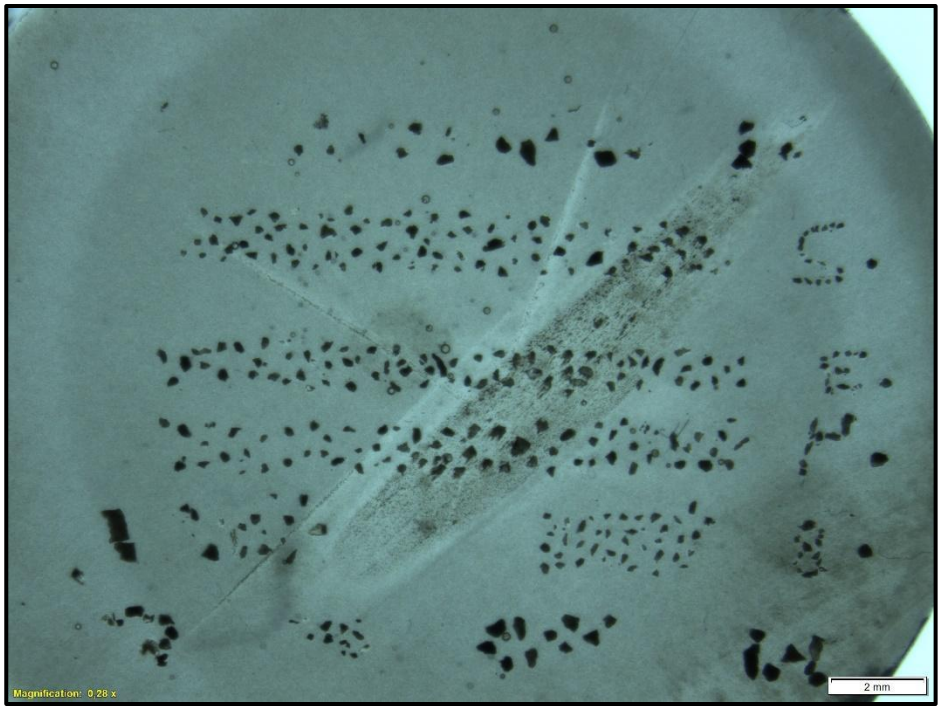

Figure 5.10 The mounted slide shows the separation of reference sample-Frantz separated grains by Frantz (R 125).

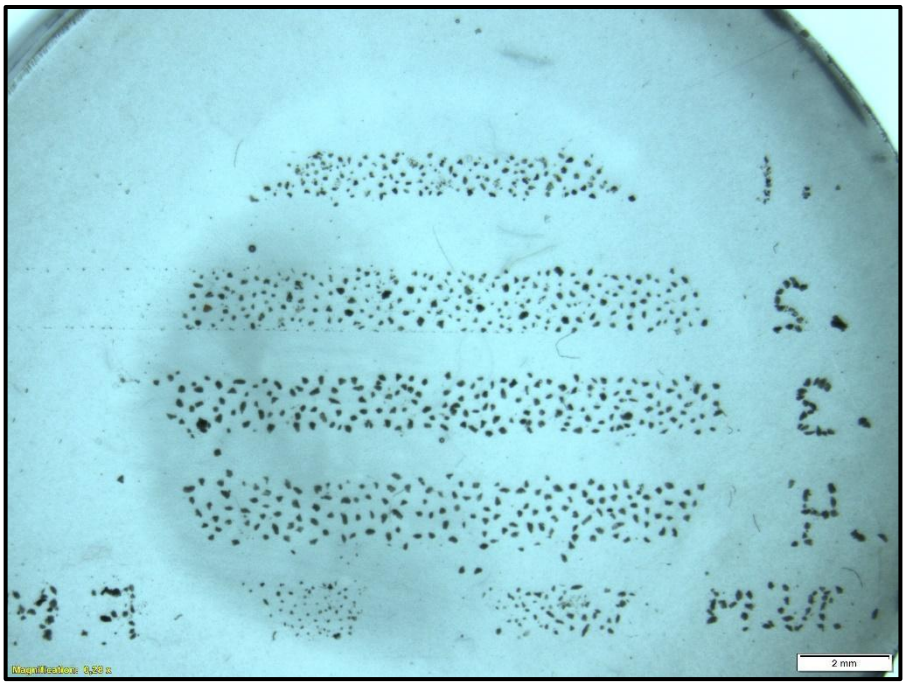

Figure 5.11 The mounted slide shows the separation of sample grains that are less than 150 microns by Frantz (R 125).

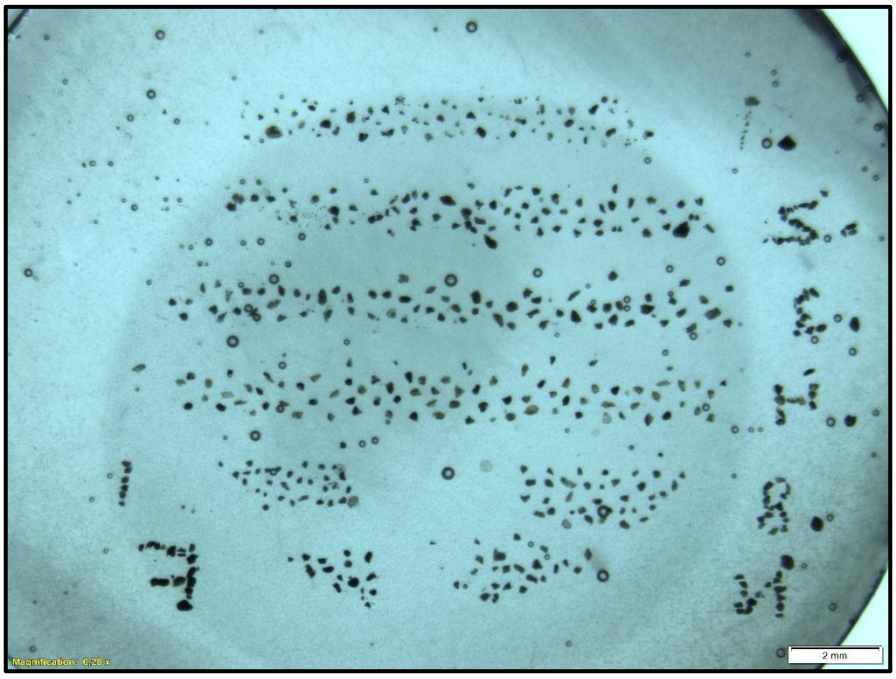

Figure 5.12 The mounted slide shows the separation of sample grains that are less than 250 microns by Frantz (R 125).

5.3. Results deduced from XRD

The separation of heavy minerals form XRD of all the three sample Formations includes Augite/Diopside, Hotsonite, Cristobalite, Baileychlore, Albite/anorthite low, Hematite, Microline, Sanidine, Magnesioferrite, Albite, Eglestonite, Epidote, Chamosite, Clinoclore and Epidote. All these minerals in sample Formations were identified by XRD. The XRD results show that the sample contains Hematite not magnetite and all other iron, oxygen, aluminum and oxygen bearing minerals mostly. The spectrum from XRD analysis for each sample is shown in the figures given below.

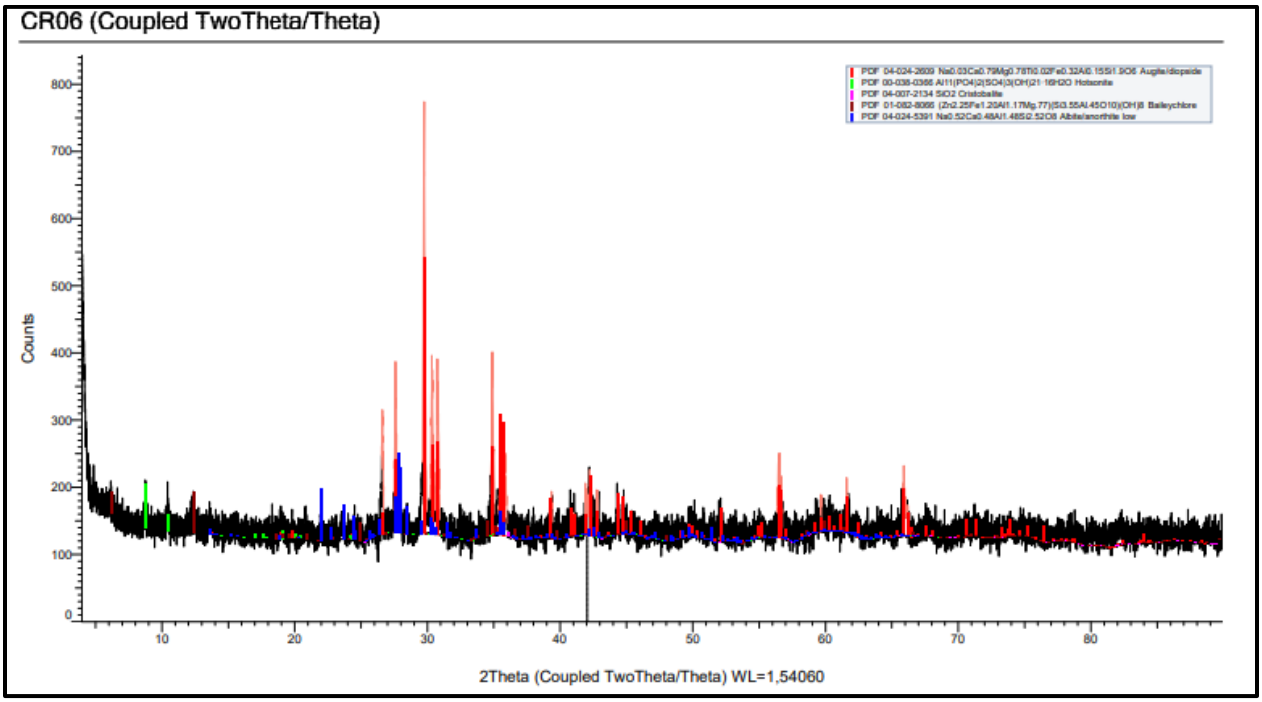

Figure 5.13 Shows the XRD results of minerals analysis of CR 06 sample.

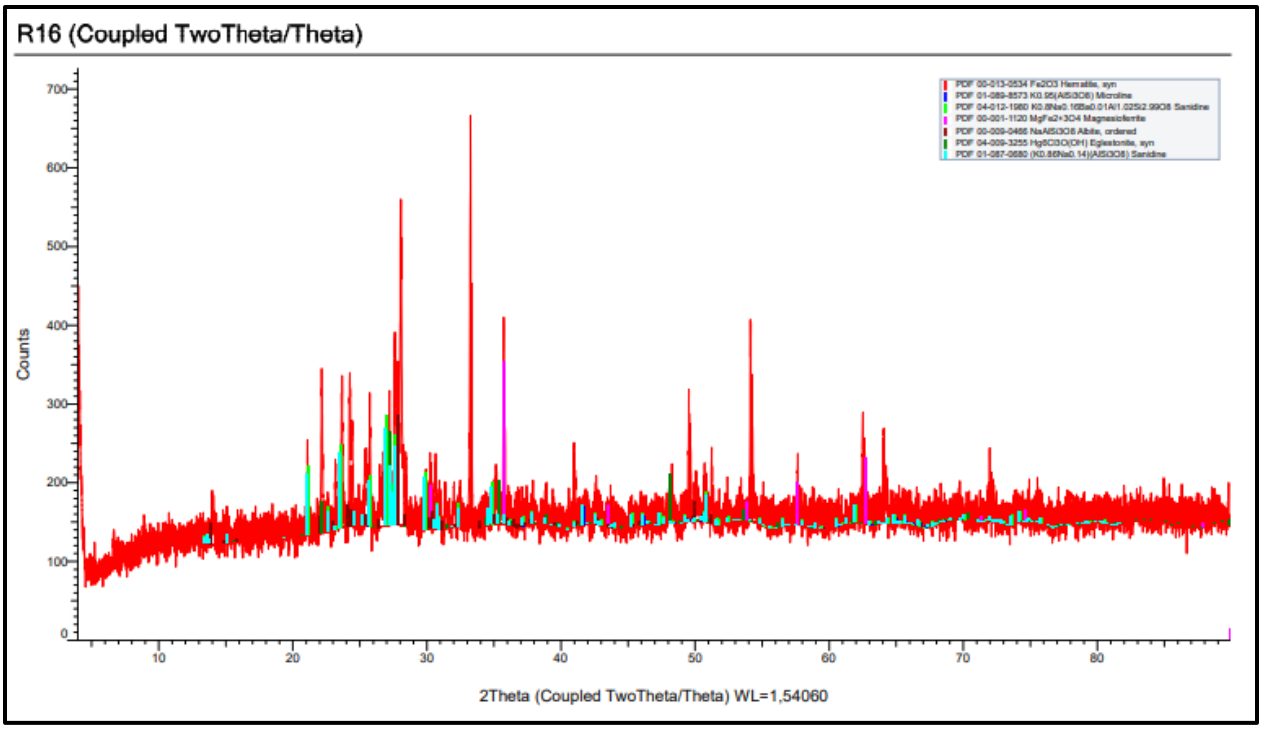

Figure 5.14 Shows the XRD results of minerals analysis of R 16 sample.

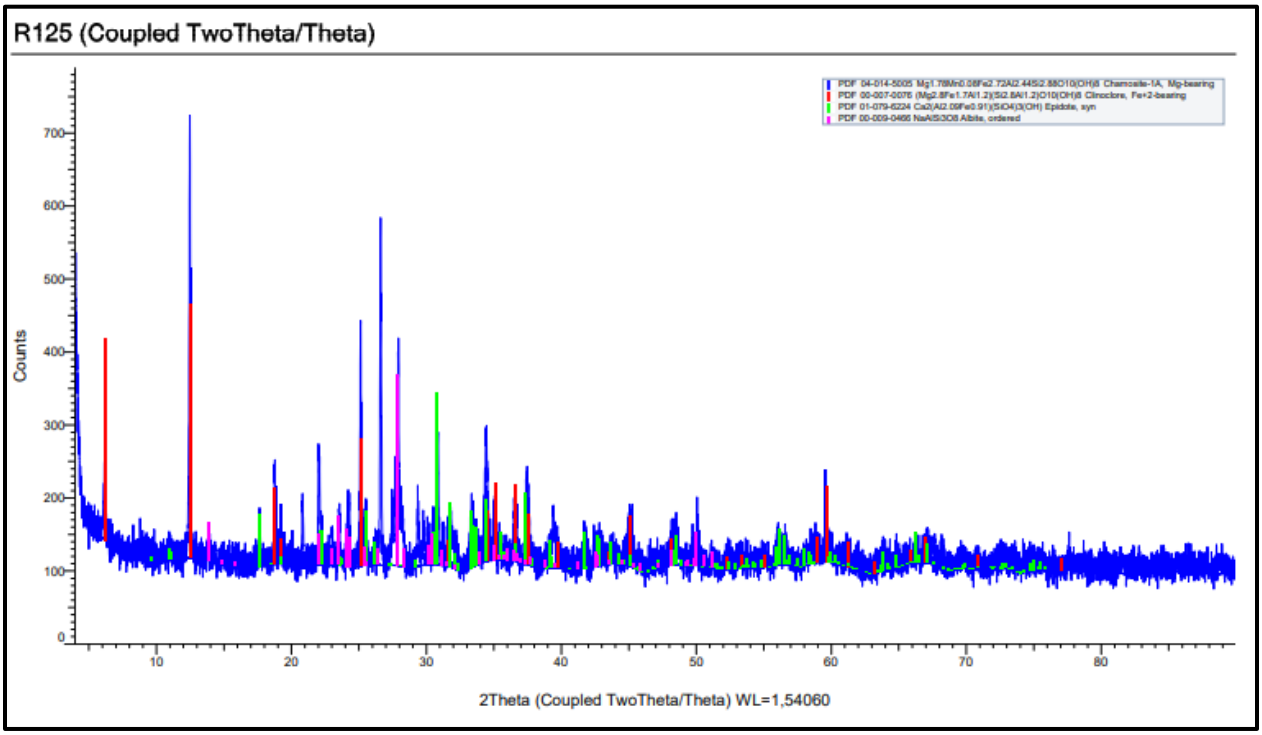

Figure 5.15 Shows the XRD results of mineral analysis of R 125 sample.

5.4. Results deduced from Scanning Electron Microscope

The minerals were identified on the basis of spectrum charts given in *Appendix A.* Variety of heavy minerals have been identified such as zircon, ilmenite, apatite, rutile, titanite, hematite, almandine garnet etc. The tables of each sample are given below, showing the percentage of each mineral in different fractions such as, reference sample, less than 150 microns, less than 250 microns and reference Frantz separated. The table include all the values of minerals including non-heavy minerals such as quartz and feldspar (having density less than 2.9 g/cm^3).

The Energy Dispersive Spectrum (EDS) spectra have been acquired from SEM results which represents a specific mineral. These spectra were then corresponded with the EDS spectra given in the book named as Energy Dispersive Spectrometry of common rock forming minerals. The minerals were then identified by matching the EDS spectra obtained from SEM with the book mentioned above. The EDS spectra of each mineral are given in *Appendix B.*

Table 5.1 Shows the list of minerals of CR 06 sample and their values in different fractions.

Minerals	Reference	Reference Frantz Separated								Less than 150 micrometers							
		0.1A	0.2A	0.3A	0.4A	0.8A	1.0A	N.M	F.M	0.1A	0.2A	0.3A	0.4A	0.8A	1.0A	N.M	F.M
Clinopyroxene	1									1							
Garnet	11									3	11	1					3
Epidote	37									1		6	6			1	1
Amphibole	24									2	7	2					1
Sphene	1																
Albite	13	1		4	5	1	1	1		3	1	6	3			2	2
Cordierite	16									2	2						
Apatite	2																
Corundum	1									1							
Lawsonite	92									7	8	25	30			5	6
Wollastonite	1											1	1				
Plagioclase	1												8				
Melilite	5																

Mica	3	1									4						
Chlorite	11									8	18						4
Titanite	4	4	5		3			1									
Zeolite	4									1							
Pumpellyite	1																
Olivine	22	6	29	14	10			3	5	8							1
Plagioclase	27	5	13	28	31	16	8	5	3							3	
Hematite	2	3							2	1							
Ilmenite	2									3							
Nepheline																	
Orthoclase	4			1	1							1				4	
Kalsisite	1			2													
Quartz or Cristobalite	4			1		1				1	1	3	1				
Tourmaline	2											1					
Rutile	2																1
UI	4						1		2				2				3

Table 5.2 Shows the list of minerals of R 16 sample and their values in different fractions.

Minerals	**Reference**	**Reference Frantz Separated**								**Less than 150 micrometers**							
		0.1A	0.2A	0.3A	0.4A	0.8A	1.0A	N.M	F.M	0.1A	0.2A	0.3A	0.4A	0.8A	1.0	N.M	F.M
Anorthoclase	22		3	1	1					2	5		4				
Apatite	26		1	2	10	6	2		1	1	1	14	27	6	1		
Albite	43	10	13	12	13	3	2	1	6	8	13	5	2	2		1	4
Orthoclase	19		2	2	1					5	5	5					2
Rutile	17		2	1	13	9	7	4				9	9	5	8	5	1
Tephroite	4																
Hematite	42	6	8	3	1				5	17	6		4				5
Ferrosilite	5																

Microcline	36	10	6	12	6	3			1	4	7	9	2	2			2
Plagioclase	4			2					1								
Sphene	2													1			
Quartz	1	1		1	1	2				1			1	1	1		
Nepheline	8		2								2	2	2			1	2
Pyrolusite	6			3								2					
Garnet	2				1												
Epidote	3			1													
Titanite	12						4	5					2	4	11	13	
Ilmenite	5			4							3						
Olivine	1											1					
Zircon	3			1									1				
UI	5	1		1	1						1	4	2				1

Table 5.3 Shows the list of minerals of R 125 sample and their values in different fractions.

Minerals	**Reference**	**Reference Frantz Separated**								**Less than 150 micrometers**							
		0.1A	0.2A	0.3A	0.4A	0.8A	1.0A	NM	FM	0.1A	0.2A	0.3A	0.4A	0.8A	1.0A	NM	FM
Garnet	9	2									1	2					
Anorthoclase	4				7							2			1		1
Mica	4	3									1						
Amphibole	38	21	10	52	6	8			8		6						
Clinopyroxenes	115	22	10	2	1	3				12	30	22			2	1	14
Orthopyroxenes	18		3			1				2							2
Epidote	2																
Quartz or Cristobalite	2		1		1	2							1		1		
Olivine	4		1			1				1			7		3	4	
Ulvospinel	1																
Plagioclase Feldspar	35	9	34	8	22	13				3		9	21		6	1	4

Tourmaline	3					1				1							
Orthoclase	8	3	2	2	2	3						5	9		1	2	1
Zeolite	1					1					1						
Pumpellyite	2																
Nepheline	7			2	8	3				2							
Pyrite	4			4	4	2			3								
Vivianite	8				6	9											
Rutile	3								1								
Microcline	2								1								

CHAPTER 06

DISCUSSION AND CONCLUSION

The three of the rock samples under study are analyzed through three qualitative and quantitative methods including Frantz Magnetic Separator, X-Rays Diffraction Method and Scanning Electron Microscope. The results obtained from these methods are attached in the previous chapter which are discussed one by one for each sample in this chapter.

6.1. R16 (The Vredefontein Formation - Lava)

It is important to know about standard Magnetic susceptibilities of minerals which are observed in this sample separated by Frantz separator. They are as follows:

Table 6.4 Shows the magnetic susceptibilities of minerals found in sample R 16.

Mineral Name	Total Range (AMPS)	Best Range (AMPS)
Anorthoclase/Sanidine	>1.70	>1.70
Orthoclase	>1.70	>1.70
Apatite	1.4 - >1.70	>1.70
Albite	>1.70	>1.70
Hematite	0.025 – 0.5	0.10 – 0.30
Rutile	0.80 - >1.70	>1.70
Ferrosilite	0.10 – 0.90	0.60 – 0.80
Microcline	>1.70	>1.70
Plagioclase	>1.70	>1.70
Sphene/Titanite	0.70 - >1.70	0.80 - >1.70
Quartz	>1.70	>1.70
Nepheline	N/A	N/A
Pyrolusite	0.10 – 0.70	0.40 – 0.50
Garnet	0.20 – 0.80	0.50 – 0.60
Epidote	0.30 – 1.0	0.4 – 0.7
Ilmenite	0.25 – 0.4	0.20 – 0.30

Olivine	0.10 – 0.60	0.20 – 0.30
Zircon	>1.70	>1.70

The SEM results showed same mineral identifications as those of XRD spectrum which are hematite, microcline anorthoclase and sanidine. The XRD spectrum can be visualized in the previous chapter of this thesis. Iron bearing minerals (hematite, ferrosilite, ilmenite and garnets) and potassium bearing minerals (microcline, sanidine and orthoclase) are observed in majority in this sample. Chemistry is the controlling factor in determining magnetic susceptibility of minerals. (Rosenblum & Brownfield, 2000). Below is the illustartion of R16 original sample in graphical form:

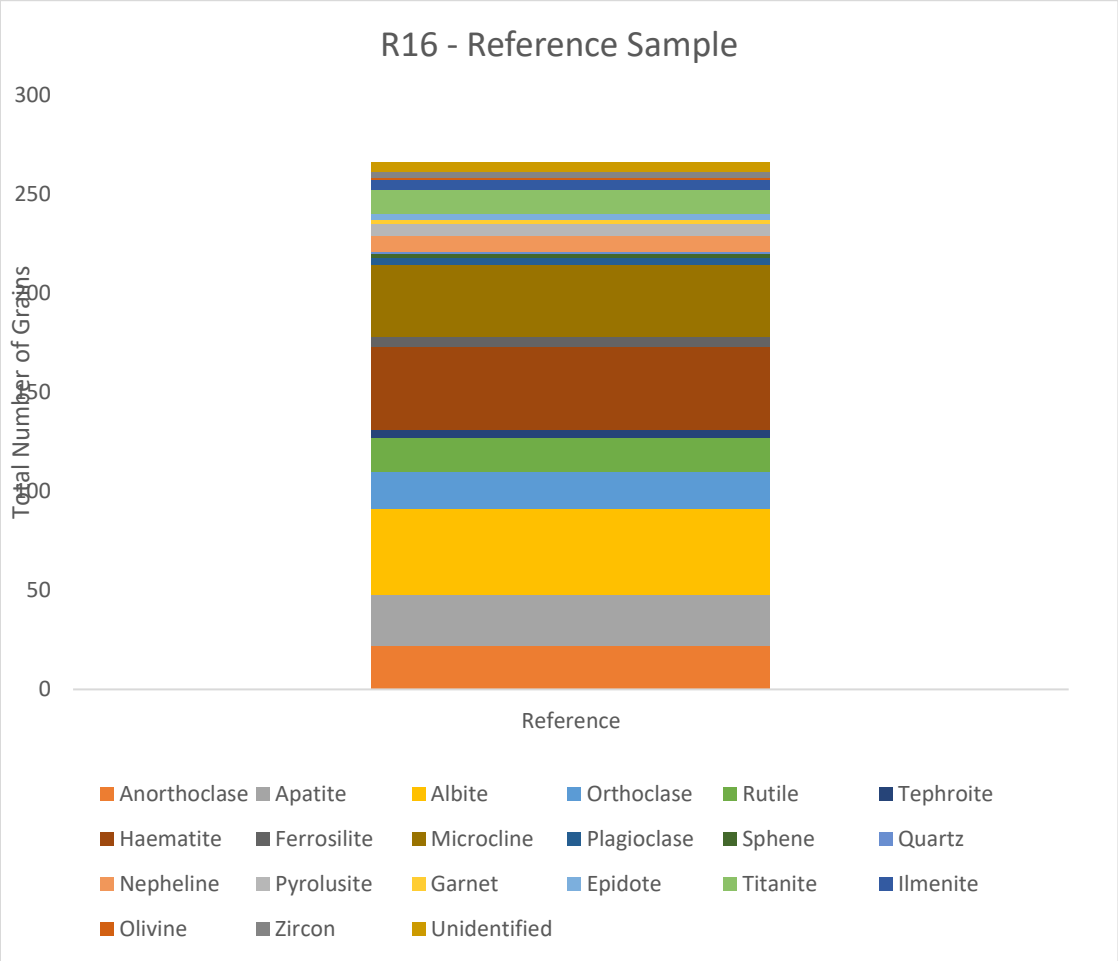

Figure 6. 1 Concentration of of different minearls in reference sample of R-16.

According to the table 5.2 in results section, Frantz has done considerable separation of minerals in this sample according to their magnetic susceptibilities. The graphical representation of the amount of minerals obtained after passing the original sample through Frantz separator are as follows:

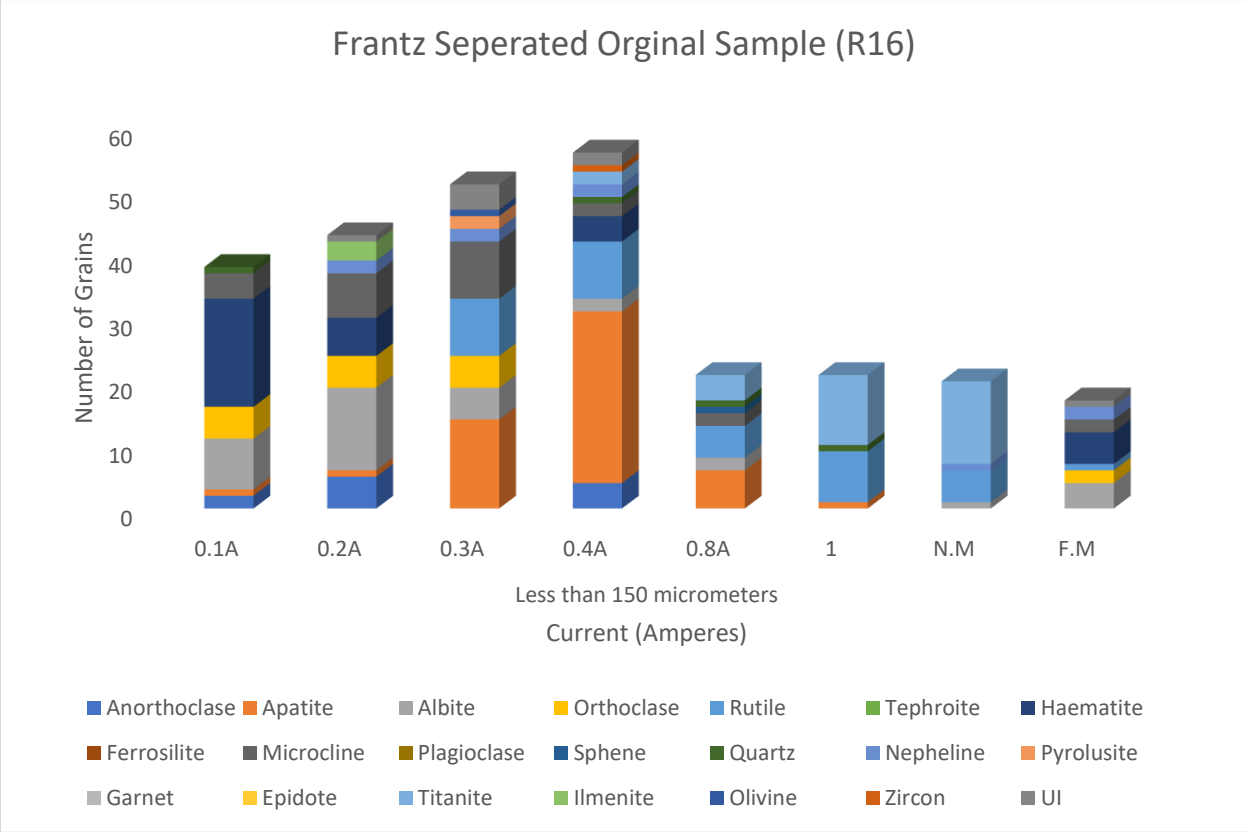

Figure 6. 2 Concentration of of different minearls in Frantz seperated reference sample of R-16.

It can be clearly seen in the above chart that almost complete package of minerals was observed when we had our current at 0.4 amperes. It is important to note that we also found albite, orthoclase some rutile in proportion separated by hand magnet. They can be seen in F.M (Ferromagnetic) side. This may because of the presence of large amount iron in our minerals. These minerals are present in lithoclasts form. So, if there is an iron bearing mineral attached with some mineral having higher magnetic susceptibility then it can be attached to the hand magnet due to that iron.

The results clearly demonstrate that the minerals in the original sample are present in lithoclasts form because all those minerals which are separated on lower magnetic susceptibilities (0.1,0.2,0.3 and 0.4) actually have magnetic susceptibilities greater than one as shown in the table 6.4. So, they

should not be present on these magnetic ranges. This is all because of the great amount of iron present in the lava. For example, Potassium feldspar can only be separated if we have our current supplied in Frantz machine greater than 1.70 amperes, but it is also found on 0.2, 0.3 and 0.4 amperes in our results because of the presence of iron bearing minerals with it as a lithoclasts. Although, it is in less amount in Frantz separated reference sample, but it is available in good quantity in grains less than 150 micrometers as shown in the graph below:

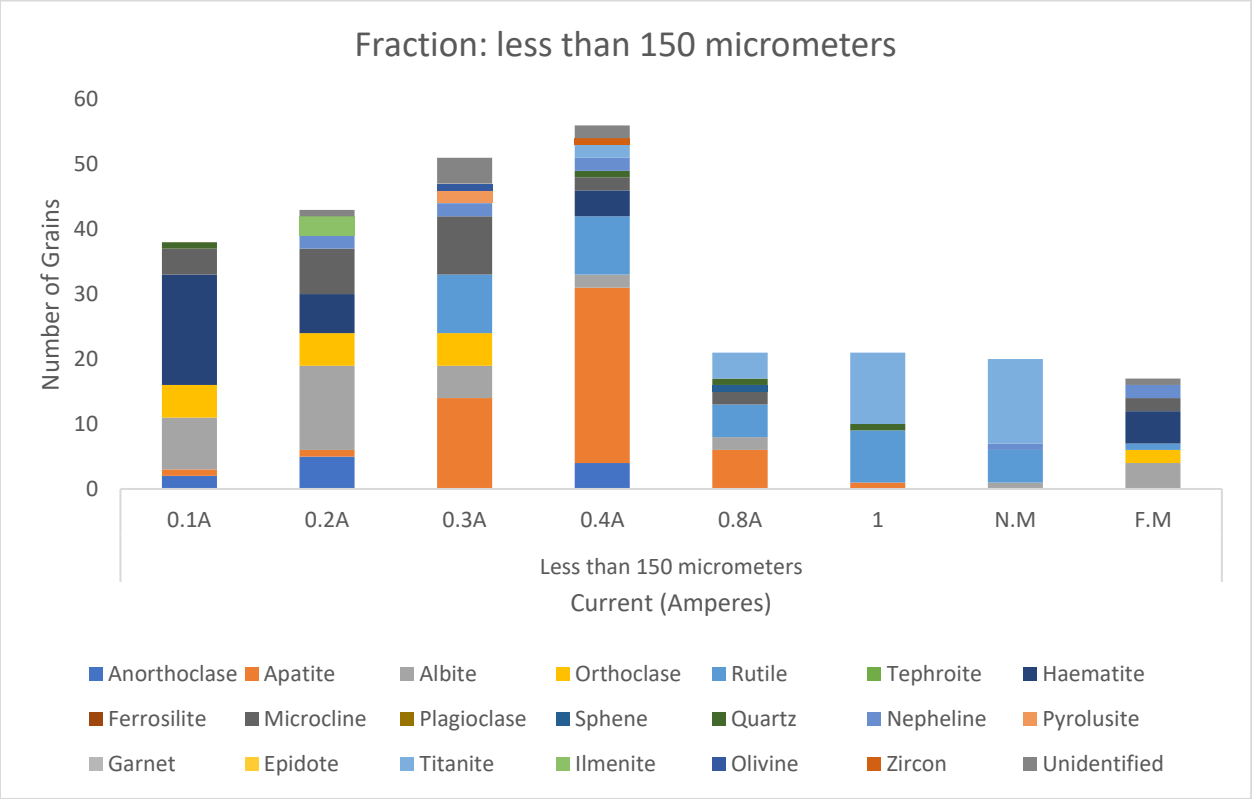

Figure 6. 3 Concentration of of different minearls in fraction of sample of R-16 less than 150 um.

This is because the hematite grains present in this rock sample are mostly less than 150 micrometers sizes. The highest proportion of Apatite mineral is observed at 0.3 ampere and 0.4 ampere. In this fraction of less than 150 micrometers also, a most of our minerals from the reference sample are separated at 0.4 amperes. Even the zircon which has a standard magnetic susceptibility of >1.7 ampere is also separated on 0.4 ampere current. Orthoclase shows a consistent trend from 0.1 to 0.3 amperes, but it is found at higher magnetic susceptibilities. This is because of the weathering of feldspar minerals. Epidote is also found when we have current between 0.2 and 0.3 amperes.

6.2. R125 (Grootderm Formation - Lava)

The minerals separated in this sample section are mentioned in following table with their standard magnetic susceptibilities:

Table 6.5 Shows the magnetic susceptibilities of minerals found in sample R 125.

Minerals	Total Range (AMPS)	Best Range (AMPS)
Pyroxenes	0.10 – 0.50	0.20 – 0.40
Garnet	0.20 – 0.80	0.50 – 0.60
Amphibole	0.30 – 0.90	0.40 – 0.80
Epidote	0.60 – 1.70	1.10 - >1.70
Albite	>1.70	>1.70
Cordierite	N/A	N/A
Apatite	1.4 – 1.70	>1.70
Corundum	>1.70	>1.70
Lawsonite	0.60 – 1.70	1.10 - >1.70
Wollastonite	>1.70	>1.70
Plagioclase	>1.70	>1.70
Melilite	0.6 - >1.70	0.80 – 0.90
Mica	0.30 – 1.40	0.70 – 1.30
Chlorite	0.10 – 0.9	0.2 – 0.5
Titanite	0.70 - >1.70	0.80 - >1.70
Zeolite	0.1 – 1.7	7.0 – 1.2
Pumpellyite	0.5 – 1.10	0.8 – 0.9
Olivine	0.1 – 1.2	0.5 – 1.0
Hematite	0.25 – 0.5	0.1 – 0.3
Ilmenite	0.25 – 0.4	0.20 – 0.30
Orthoclase	>1.70	>1.70
Quartz or Cristobalite	>1.70	>1.70
Rutile	0.8 - >1.70	>1.70

SEM results showed similar mineral identifications as those of the XRD Spectra Analysis. Mineral grains in the R125 Original sample are as follows:

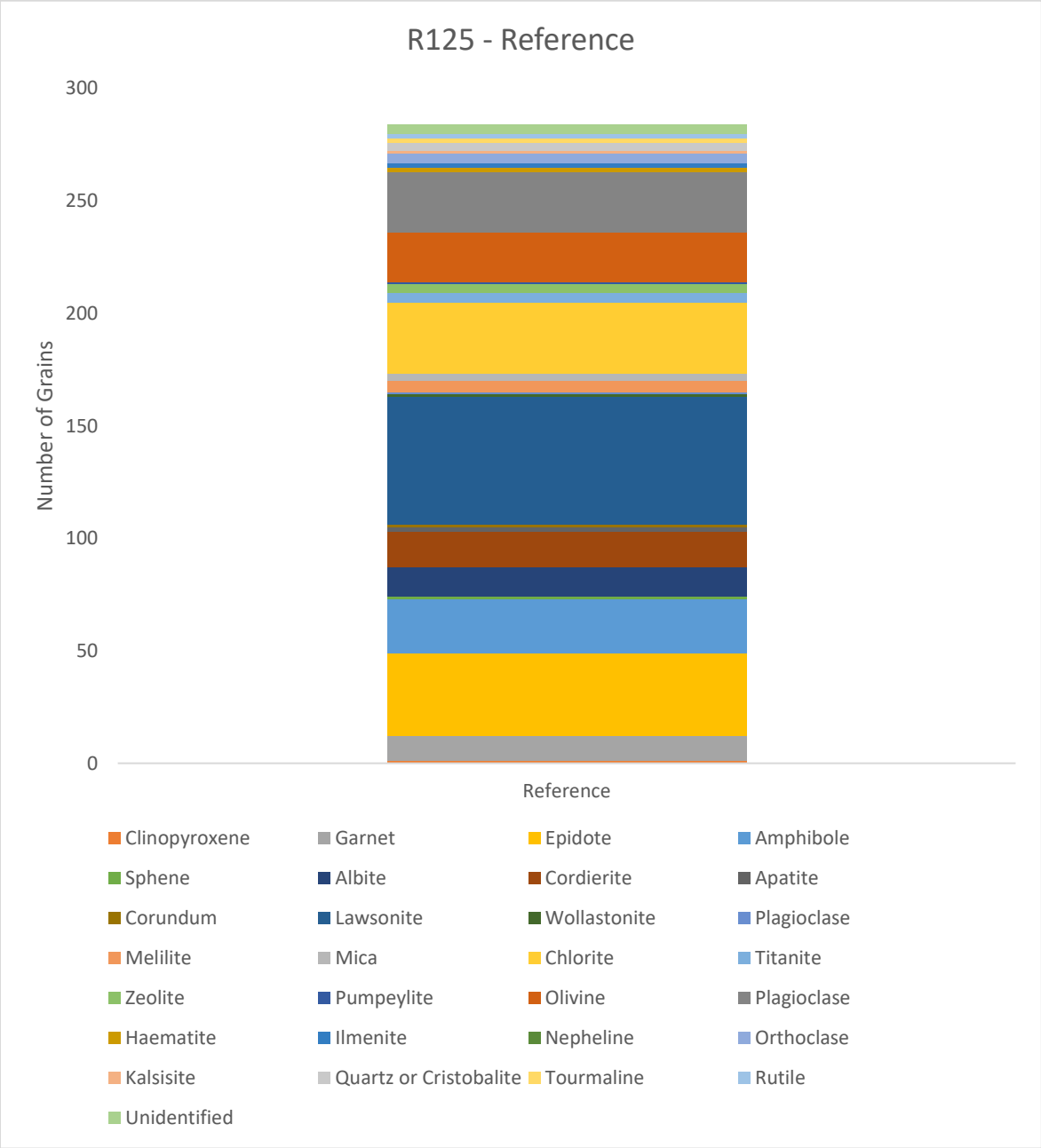

Figure 6. 4 Concentration of different minerals in reference sample of R125.

Epidotes and chlorite minerals are the most abundant in this rock sample as shown in the reference chart above. Plagioclase and Amphiboles stand on second position. In this Frantz seperated sample, it is important to note that minerals like epidotes, lawsonites, chlorites and amphiboles are not found in the fraction amperes above 150 micrometers sizes. This is because

these mineral grains are present in smaller sizes less than 150 micrometers and can only be separated on that scale. It is as follows:

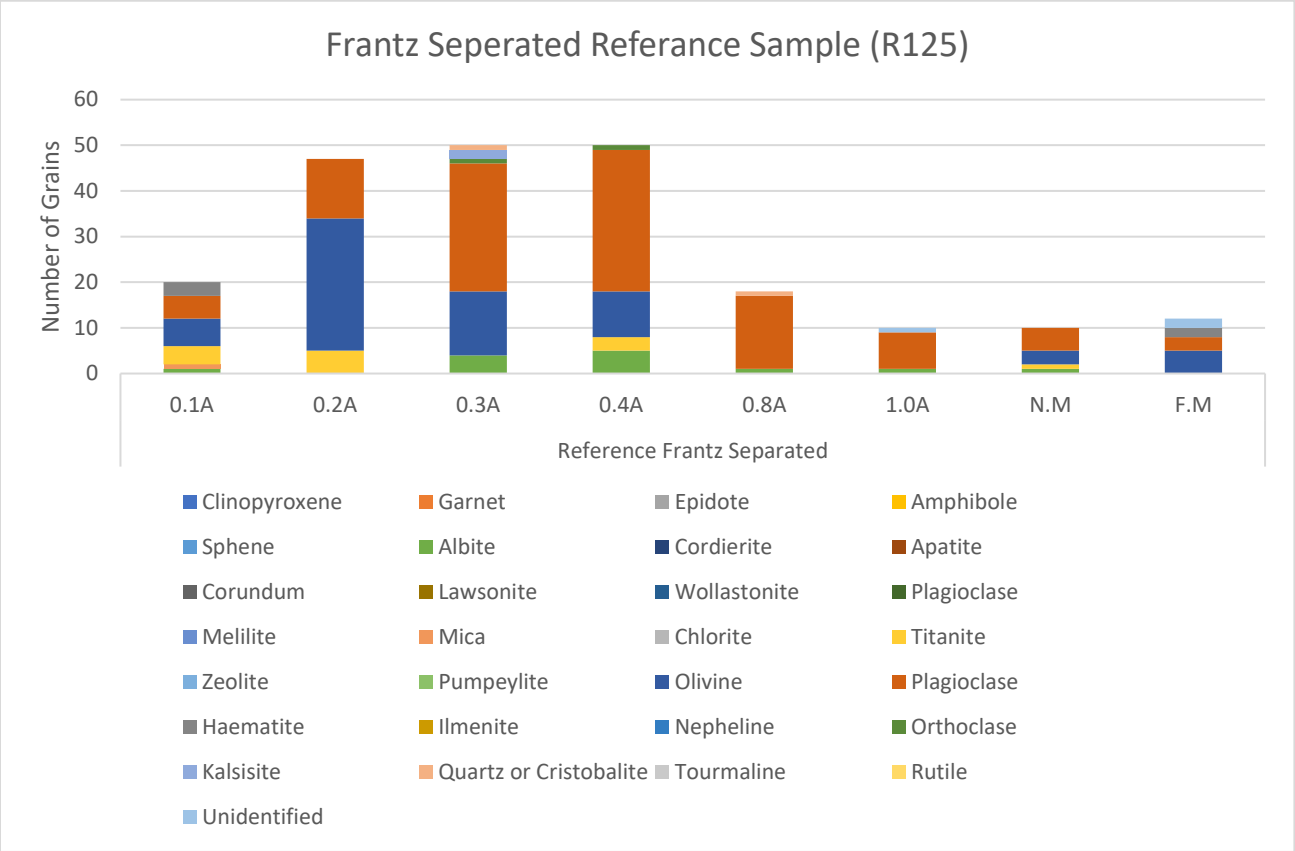

Figure 6. 5 Concentration of different minerals in Frantz Separated reference sample of R125.

Moreover, the plagioclase and olivine are in majority when we observe the sample separated on sizes greater than 150 micrometers.

The minerals of fraction less than 150 micrometers are separated by Frantz Separator and are as follows in terms of their quantities:

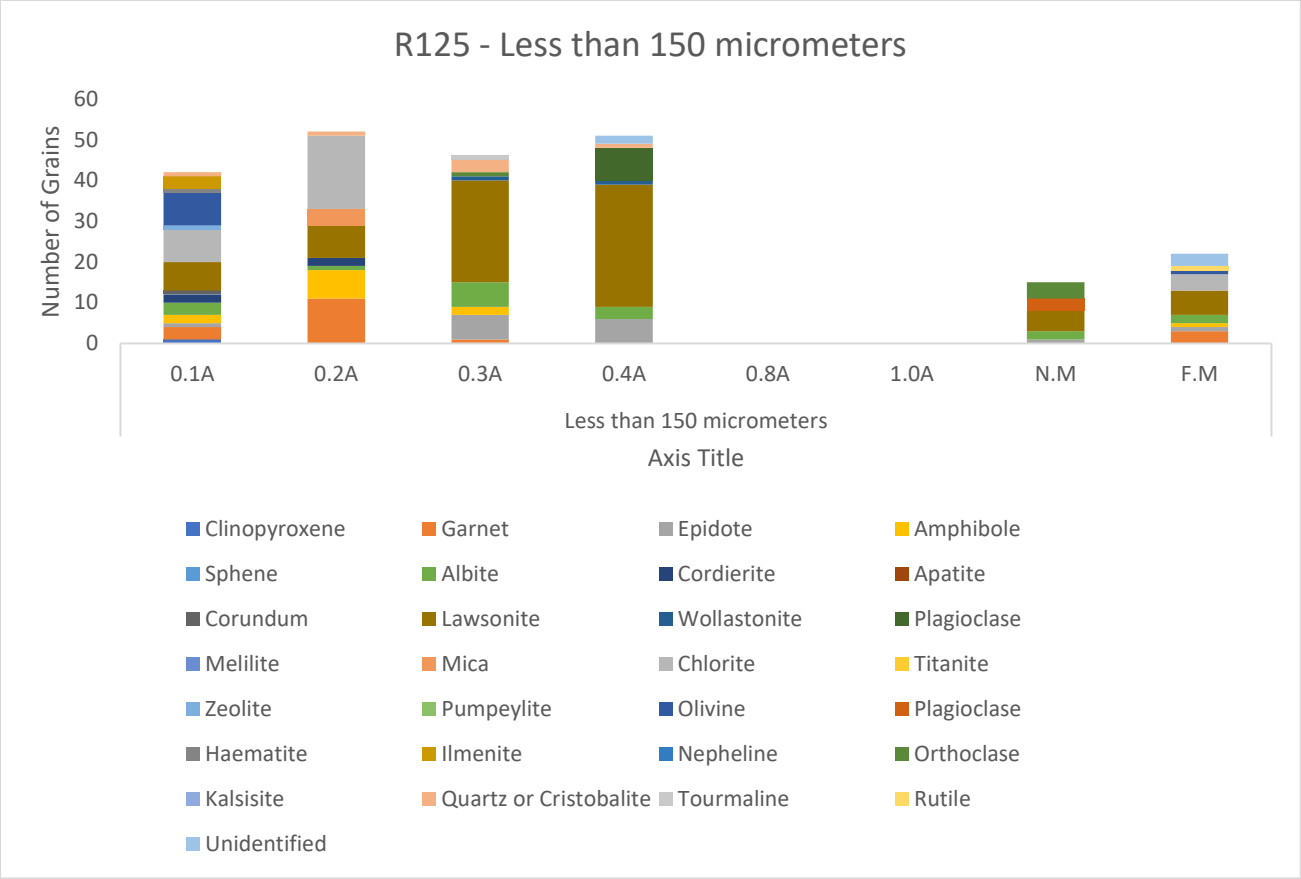

Figure 6. 6 Concentration of different minerals in Fraction of R125 less than 150um.

At 0.1 ampere charge unit, we can observe a whole package of minerals originally found in our reference sample in varying amounts. Garnet, epidotes, amphiboles and lawsonites are found at range of 0.1 to 0.4 charge units. Epidotes and lawsonites are mainly separated at 0.4 ampere unit. Chlorites and olivine's are separated mainly on lower amperes (0.1 and 0.2) because they are iron rich minerals and this also clarifies that the olivine's present under 150 micrometers sizes are mainly fayalites. The only plagioclase feldspar we had in our results was separated on 0.4 amperes.

No mineral grain can be separated on 0.8 and 1.0 ampere charge units because all the sample available was already separated on lower currents considerably. It shows Frantz Separator we used, has done a considerable separation of minerals for a fraction less than 150 micrometers sizes in a range of 0.1 to 0.4 amperes.

6.3. CR 06 (Dernburg Formation – Gabbro)

Minerals in this sample are separated and analyzed by their standard magnetic susceptibilities as follows:

Table 6.6 Shows the magnetic susceptibilities of minerals found in sample CR 06.

Minerals	Total Range (AMPS)	Best Range (AMPS)
Garnet	0.2 – 0.8	0.5 – 0.6
Anorthoclase/Sanidine	>1.70	>1.70
Glauconite	0.2 – 0.6	0.4
Pumpellyite	0.5 – 1.10	0.8 – 0.9
Actinolite-Amphibole	0.3 – 0.9	0.4 – 0.8
Clinopyroxene-Hedenbergite	0.1 – 0.5	0.2 – 0.4
Epidote-Piemonite	0.3 – 1.0	0.4 – 0.7
Quartz or Cristobalite	>1.70	>1.70
Nepheline	N/A	N/A
Augite	0.2 – 1.2	0.4 – 0.9
Phlogopite Mica	0.3 – 1.0	0.7 – 1.3
Forsterite	0.4 – 1.2	0.5 – 1.0
Ulvospinel	0.1 – 1.0	0.5 – 1.0
Zinnwaldite Mica	0.3 – 0.7	0.4 – 0.5
Albite	>1.70	>1.70
Hypersthene	0.20 – 0.60	0.40
Orthoclase	>1.70	>1.70
Pectolite	>1.70	>1.70
Plagioclase Feldspar	>1.70	>1.70
Tourmaline	>1.70	>1.70
Pyrite	>1.70	>1.70
Rutile	0.80 - >1.70	>1.70
Microcline	>1.70	>1.70
Vivianite	0.10 - .50	0.20 – 0.30

Fayalite	0.10 – 0.6	0.2 – 0.3

SEM results of sample CR06 also shows the same minerals which are interpreted in Xray's Diffraction Method and separated by Frantz Separator. However, Hotsonite and baileychlore are not representative minerals in XRD because our XRD graph is generated on low intensity so they can be phyllosilicates. The specimen contains abundant clinopyroxenes, amphiboles, and plagioclase feldspar as shown in the graph below:

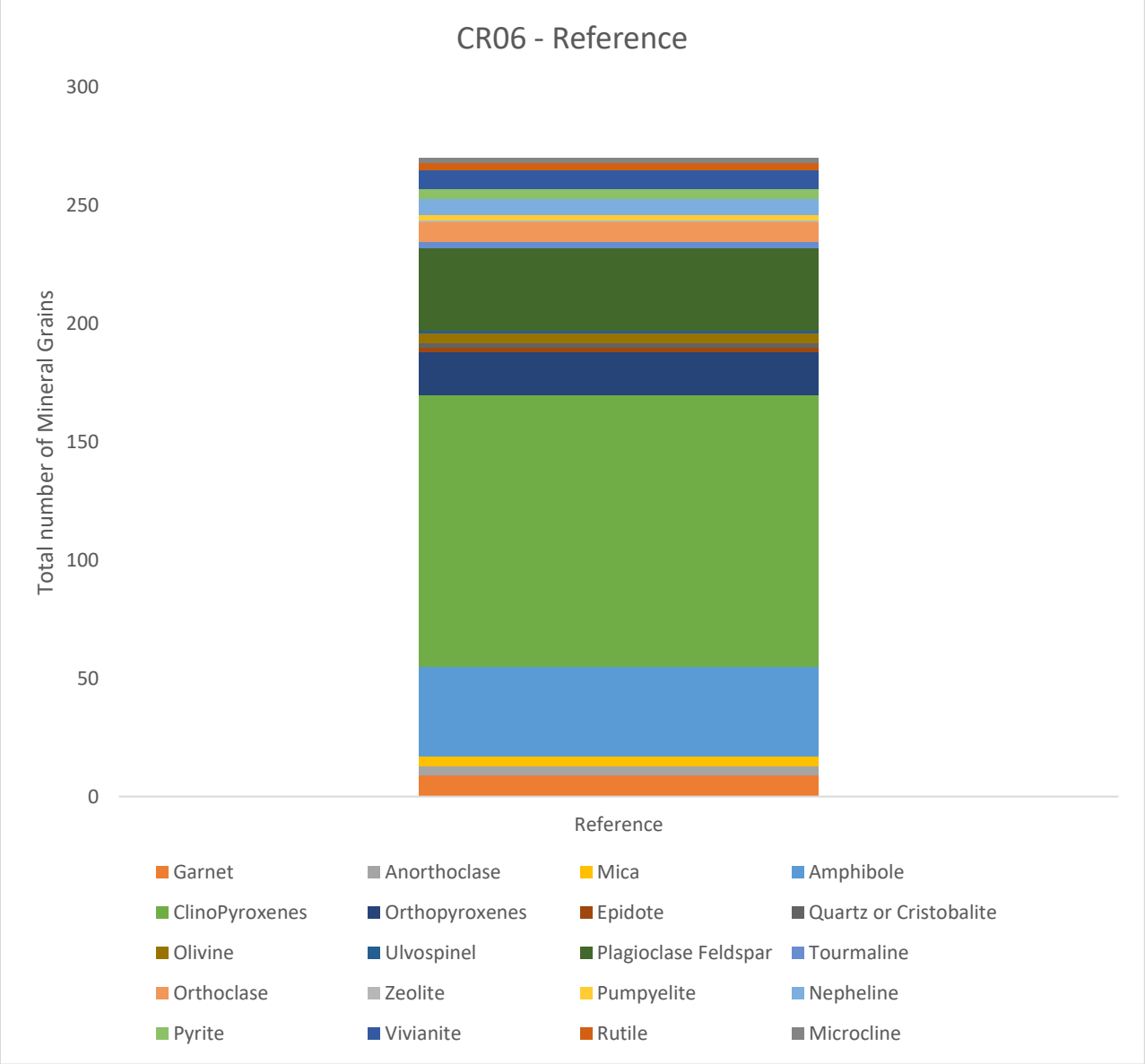

Figure 6. 7 Concentration of different minerals in reference sample of CR06.

Minor amounts of potassium feldspar and garnets are also found. A total of 20 species of different minerals was available in the CR06 (original sample).

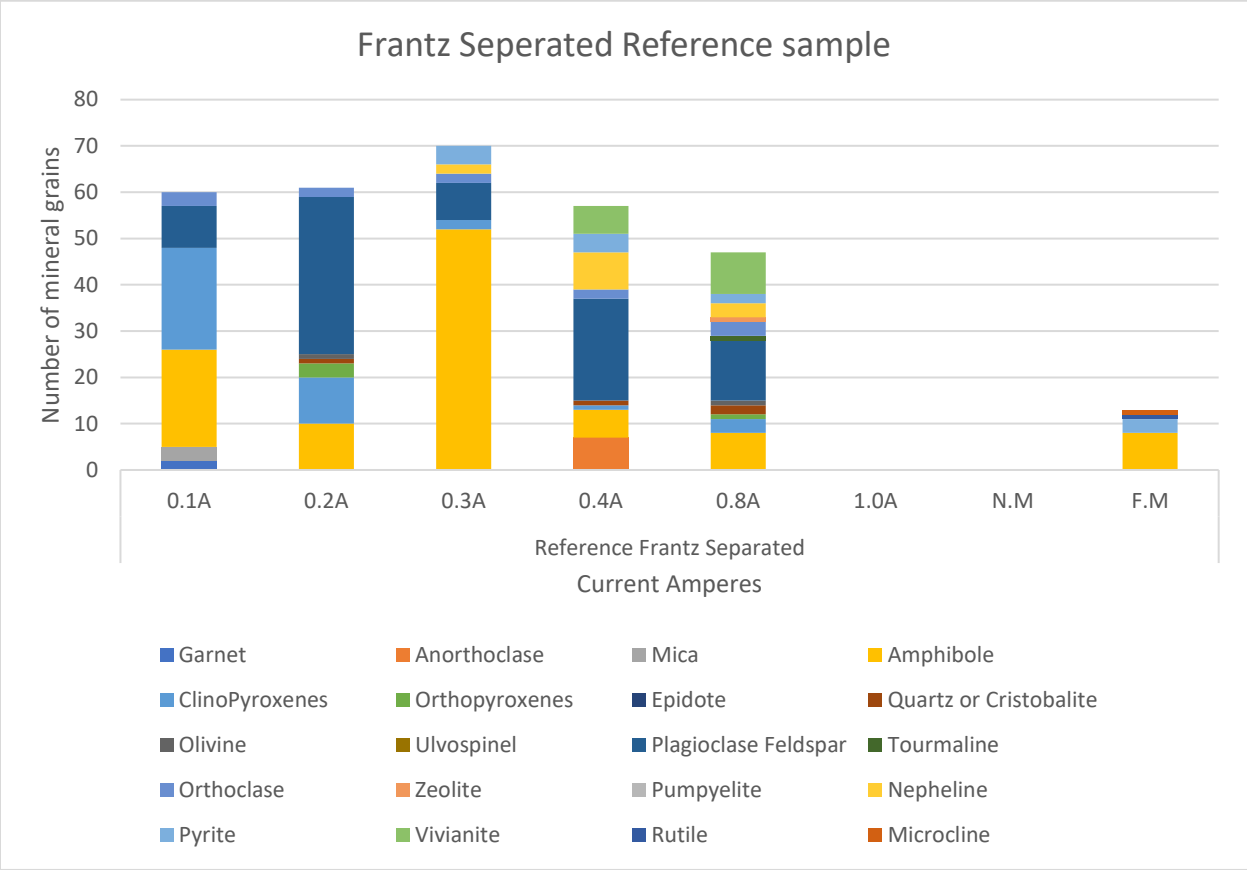

Figure 6. 8 Concentration of different minerals in Frantz separated reference sample of CR06.

For the original sample separated by Frantz, Amphiboles, Clinopyroxenes, and plagioclase feldspars are widely distributed in almost every range of amperes used till 0.8 charge unit. This is because all three of them have magnetic susceptibility greater than 1.70 amperes, so they just spread out in lower magnetic susceptibilities. At 0.8 ampere current, we can find an excellent package of almost all minerals separated by Frantz, also present in Original sample CR06. Clinopyroxenes are separated mainly at 0.1 A, plagioclase at 0.2, and amphiboles at 0.3 A. Although these minerals have standard of high magnetic susceptibilities as shown Table 6.6 but still, they can be found on lower charge units because they are present in the form of lithoclasts.

Also, they become less abundant when we observe the fraction containing less than 150 micrometers sizes as follows:

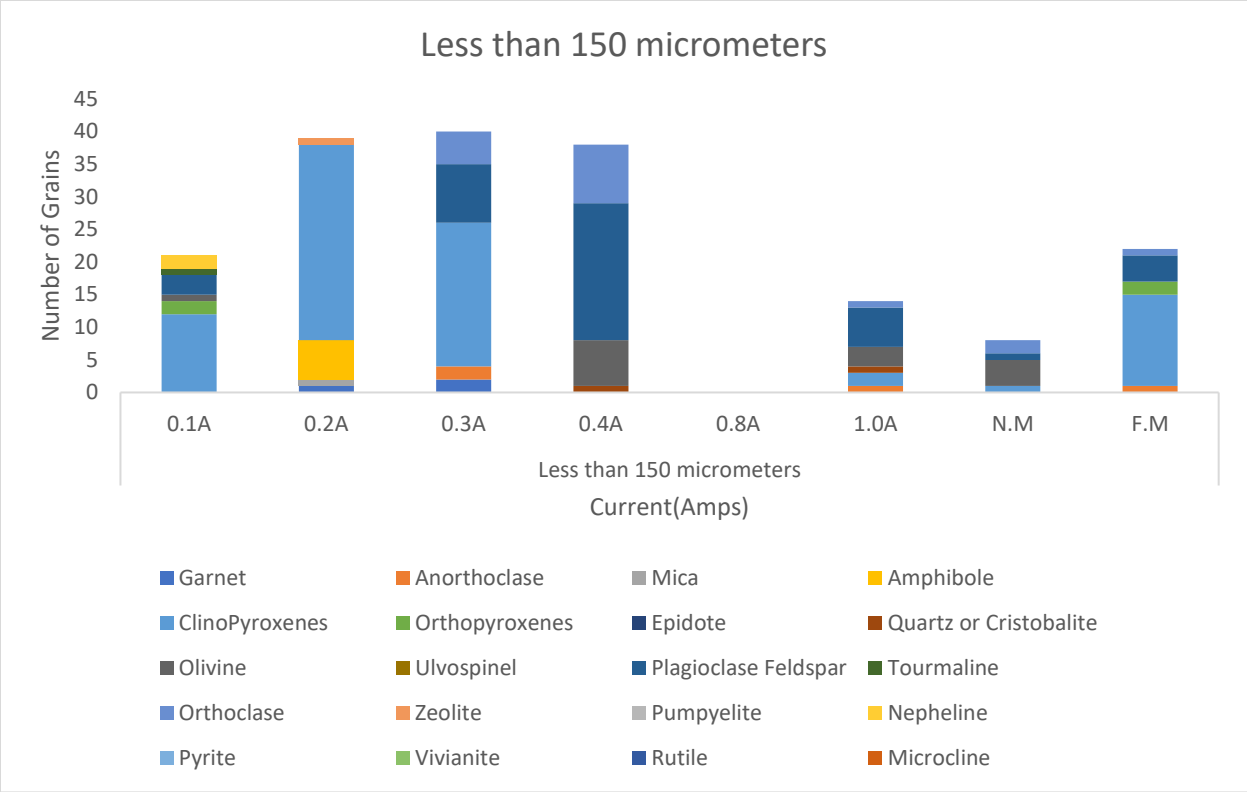

Figure 6. 9 Concentration of different minerals in Fraction of sample CR06 less than 150um.

The Fraction, less than 150 micrometers size, is separated mainly on 0.1 ampere but clinopyroxenes are abundant at 0.2 and 0.3 charge units and plagioclase at 0.4 amperes.

On the other hand, Clinopyroxenes are more abundant in smaller sizes than the reference sample CR06.

6.4. Conclusion

From the results and discussion stated in the above chapter, two factors control the purity of separate: the composition of the host rock and the quality of the grain itself. Rocks often contain more than one paramagnetic mineral. When they are analyzed through Frantz, the susceptible phases may separate together at the same magnetic setting as we had in our samples. The amphiboles found in our sample CR06 were of two types: one is actinolite and the other is hornblende. According to Rosenblum and Brownfield (1999), both these minerals can be separated between 0.3 and 0.6 amperes, but only one of them, hornblende, can be used for age dating. So, in this case Frantz would not be a considerable approach to separate the rock minerals.

Also, the plutonic and volcanic nature of the rocks comes under this point related to the composition of the host rock as the results in this thesis show that for the lava-type rocks (R16 and R125), the lower current amperes (0.3 and 0.4) are more suitable to get all the minerals separated by Frantz. Volcanic rocks will be easily weathered and converted into more iron-bearing or manganese-bearing rocks and thus will have lower magnetic susceptibilities (0.1,0.2,0.3 and 0.4 Amperes) in the Frantz Separator. Similarly, for the plutonic rock like gabbro (CR06), charge units of more than 0.7 amperes would be used to have all mineral assemblages separated in one place.

Monomineralic grains will have a different type of separation than the lithoclasts or included grains (Discussed previously in discussion). From our results, it is demonstrated that the quality of grains affects the separation of minerals. For example, in rock sample R16, the zircon is separated only when it was present in size less than 150 micrometers. So, if there is a need to separate zircons from R16 rock sample then one needs to disaggregate the compound grains by using mortar and pestle into monomineralic grains and then use it for Frantz separation to separate zircons for age dating purposes.

REFERNECES

- Basei, M. A. S., Frimmel, H. E., Nutman, A. P., Preciozzi, F., & Jacob, J. (2005). A connection between the Neoproterozoic Dom Feliciano (Brazil/Uruguay) and Gariep (Namibia/South Africa) orogenic belts–evidence from a reconnaissance provenance study. Precambrian Research, 139(3-4), 195-221.
- Basei, M. A. S., Frimmel, H. E., Nutman, A. P., Preciozzi, F., & Jacob, J. (2005). A connection between the Neoproterozoic Dom Feliciano (Brazil/Uruguay) and Gariep (Namibia/South Africa) orogenic belts–evidence from a reconnaissance provenance study. Precambrian Research, 139(3-4), 195-221.
- Bunaciu, A. A., UdriŞTioiu, E. G., & Aboul-Enein, H. Y. (2015). X-ray diffraction: instrumentation and applications. Critical reviews in analytical chemistry, 45(4), 289-299.
- Connolly, J. R. (2007). Elementary crystallography for X-ray diffraction. EPS400-001, Introduction to X-Ray Powder Diffraction, Spring.
- Dunlap, M., & Adaskaveg, J. E. (1997). Introduction to the scanning electron microscope. Theory, practice, & procedures. Facility for Advance Instrumentation. UC Davis, 52.
- Frimmel, H. E., & Frank, W. (1998). Neoproterozoic tectono-thermal evolution of the Gariep Belt and its basement, Namibia and South Africa. Precambrian Research, 90(1-2), 1-28.
- Frimmel, H. E., & Hartnady, C. J. H. (1992). Blue amphiboles and their significance for the metamorphic history of the Pan-African Gariep belt, Namibia. Journal of metamorphic Geology, 10(5), 651-669.
- Frimmel, H. E., Basei, M. S., & Gaucher, C. (2011). Neoproterozoic geodynamic evolution of SW-Gondwana: a southern African perspective. *International Journal of Earth Sciences*, *100*(2), 323-354.
- Frimmel, H. E., Fölling, P. G., & Eriksson, P. G. (2002). Neoproterozoic tectonic and climatic evolution recorded in the Gariep Belt, Namibia and South Africa. Basin Research, 14(1), 55-67.
- Frimmel, H. E., Hartnady, C. J., & Koller, F. (1996). Geochemistry and tectonic setting of magmatic units in the Pan-African Gariep Belt, Namibia. Chemical Geology, 130(1-2), 101-121.

- Gilchrist, A. R., Kooi, H., & Beaumont, C. (1994). Post-Gondwana geomorphic evolution of southwestern Africa: Implications for the controls on landscape development from observations and numerical experiments. Journal of Geophysical Research: Solid Earth, 99(B6), 12211-12228.
- Guma, T. N., Madakson, P. B., Yawas, D. S., & Aku, S. Y. (2012). X-ray diffraction analysis of the microscopies of some corrosion-protective bitumen coatings. Int. J. Mod. Eng. Res, 2, 4387-4395.
- Hartnady, C. J. H., Von Veh, M. W., & Rogers, J. (1990). Tectonostratigraphic and structural history of the Late Proterozoic-early Palaeozoic Gariep belt, Cape Province, South Africa. Geological Society of South Africa.
- Hartnady, C., Joubert, P., & Stowe, C. (1985). Proterozoic crustal evolution in southwestern Africa. Episodes, 8(4), 236-244.
- Li, Z.X., Bogdanova, S.V., Collins, A.S., Davidson, A., De Waele, B., Ernst, R.E., Fitzsimons, I.C.W., Fuck, R.A., Gladkochub, D.P., Jacobs, J. and Karlstrom, K.E., 2008. Assembly, configuration, and break-up history of Rodinia: a synthesis. *Precambrian research*, *160*(1-2), pp.179-210.
- Macdonald, F. A., Strauss, J. V., Rose, C. V., Dudás, F. Ő., & Schrag, D. P. (2010). Stratigraphy of the Port Nolloth Group of Namibia and South Africa and implications for the age of Neoproterozoic iron formations. American Journal of Science, 310(9), 862-888.
- Middlemost, E. A. K. (1963). Geology of the south-eastern Richtersveld (Doctoral dissertation, University of Cape Town).
- Murty, M. S. (1963, June). Magnetic susceptibilities of orthopyroxenes in the Frantz Isodynamic separator. In Proceedings of the Indian Academy of Sciences-Section A (Vol. 57, No. 6, pp. 337-342). Springer India.
- Rosenblum, S., & Brownfield, I. K. (2000). Magnetic susceptibilities of minerals. US Department of the Interior, US Geological Survey.
- Severin, K. P. (2004). Energy dispersive spectrometry of common rock forming minerals (p. 19). Dordrecht, The Netherlands: Kluwer Academic.
- Smith, K. C. A., & Oatley, C. W. (2004). The Scanning Electron Microscope and Its Fields of Application. Adv. Imaging Electron Phys, 133, 111-125.

- Stanistreet, I. G., Kukla, P. A., & Henry, G. (1991). Sedimentary basinal responses to a late Precambrian Wilson cycle: The Damara orogen and Nama foreland, Namibia. Journal of African Earth Sciences (and the Middle East), 13(1), 141-156.
- Strong, T. R., & Driscoll, R. L. (2016). A process for reducing rocks and concentrating heavy minerals (No. 2016-1022). US Geological Survey.
- Swapp, S. (2014). University of Wyoming.(2013). Scanning Electron Microscopy (SEM).
- Von Veh, M. W. (1988). The stratigraphy and structural evolution of the Late Proterozoic Gariep Belt in the Sendelingsdrif-Annisfontein area, northwestern Cape Province.
- Zhao, G., Sun, M., Wilde, S.A., Li, S. and Zhang, J., 2006. Some key issues in reconstructions of Proterozoic supercontinents. Journal of Asian Earth Sciences, 28(1), pp.3-19.
- Zimmermann, U. (2018). The provenance of selected Neoproterozoic to lower Paleozoic basin successions of Southwest Gondwana: A review and proposal for further research. Geology of Southwest Gondwana, 561-591.
- Zimmermann, U., Tait, J., Crowley, Q. G., Pashley, V., & Straathof, G. (2011). The Witputs diamictite in southern Namibia and associated rocks: constraints for a global glaciation?. International Journal of Earth Sciences, 100(2), 511-526.

- Zimmermann, U., Tait, J., Crowley, Q. G., Pashley, V., & Straathof, G. (2011). The Witputs diamictite in southern Namibia and associated rocks: constraints for a global glaciation?. International Journal of Earth Sciences, 100(2), 511-526.

APPENDICES

Appendix A: Shows the pie charts of mineral count in each line of sample fraction.

Appendix B: Shows the EDS spectra of each mineral collaborated with Energy Dispersive Spectrometry of common rock forming minerals.

APPENDIX A

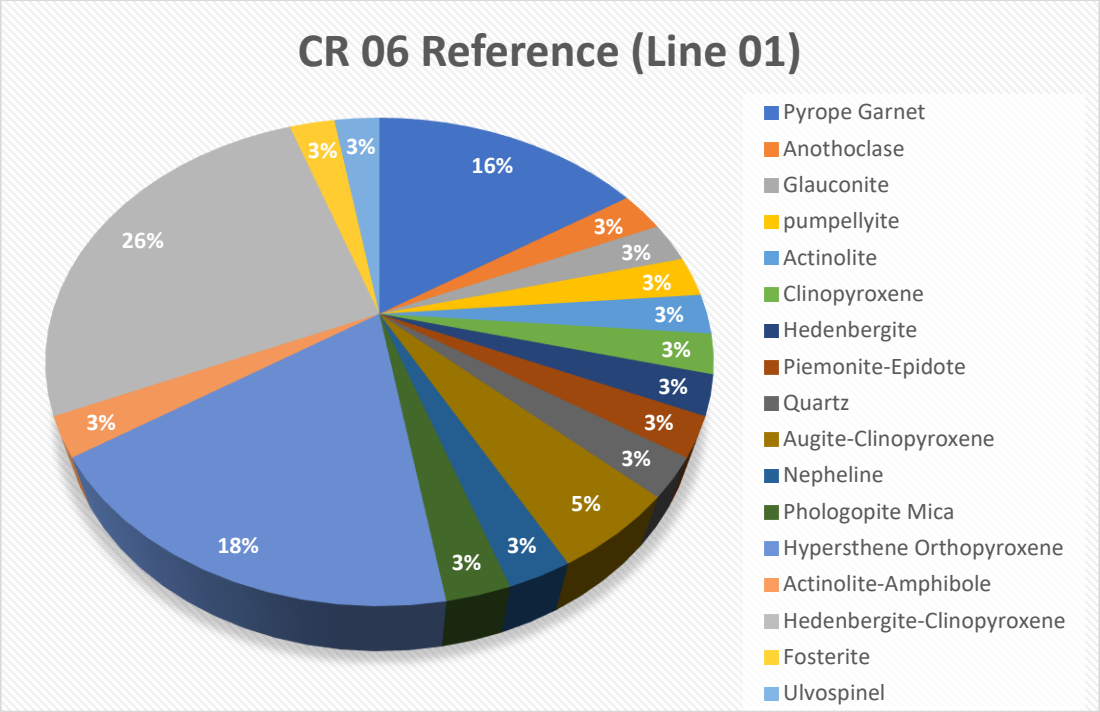

Figure 1 Shows the mineral count of line 01 of reference CR 06 sample.

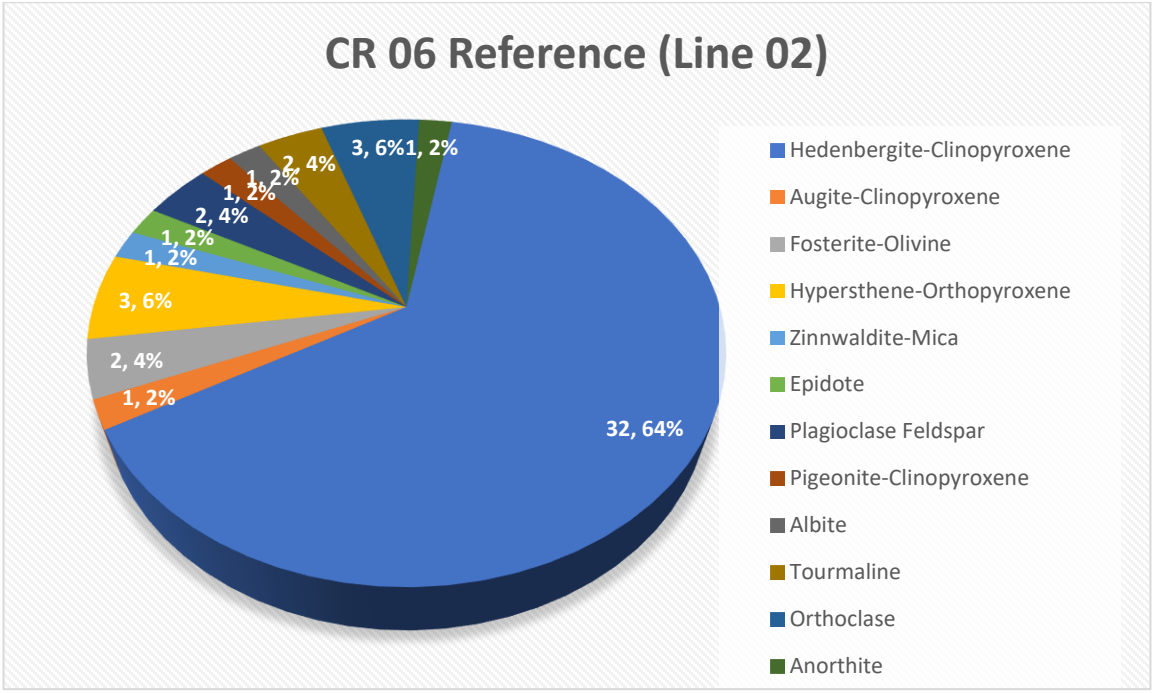

Figure 2 Shows the mineral count of line 02 of reference CR 06 sample.

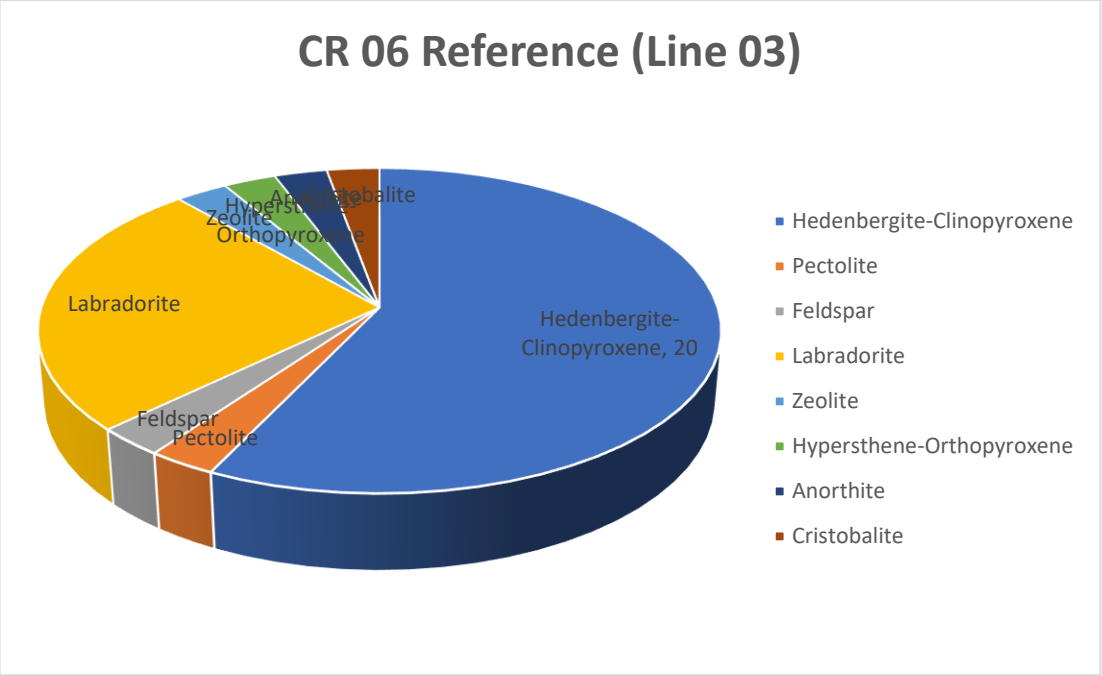

Figure 3 Shows the mineral count of line 03 of reference CR 06 sample.

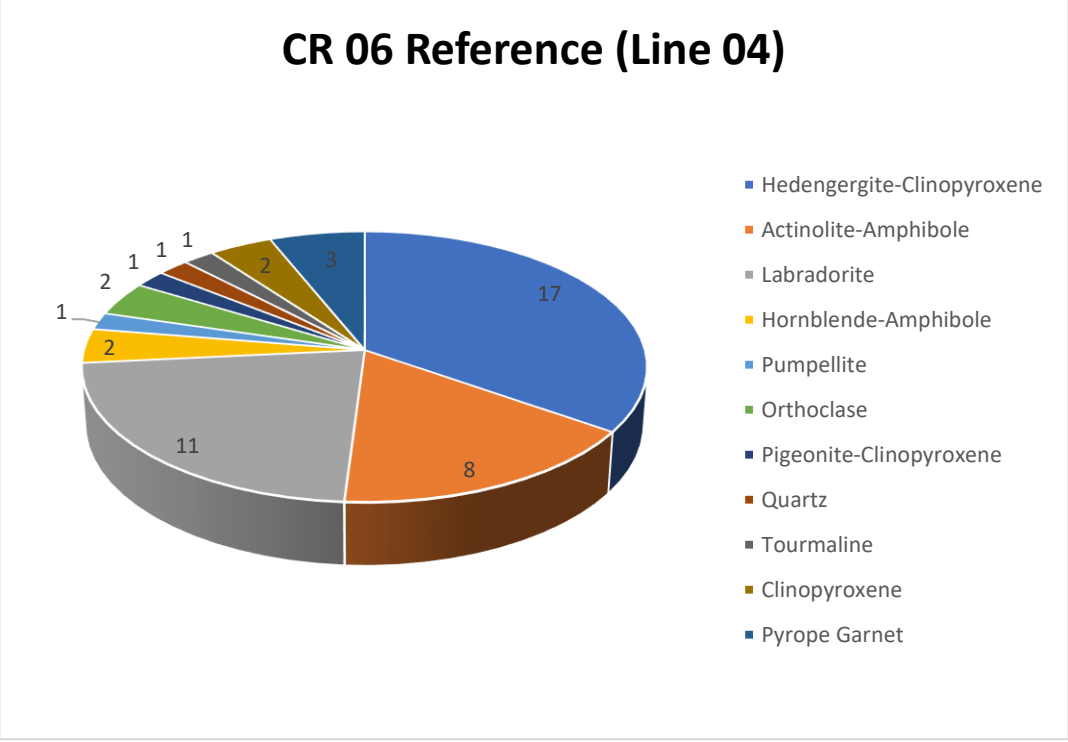

Figure 4 Shows the mineral count of line 04 of reference CR 06 sample.

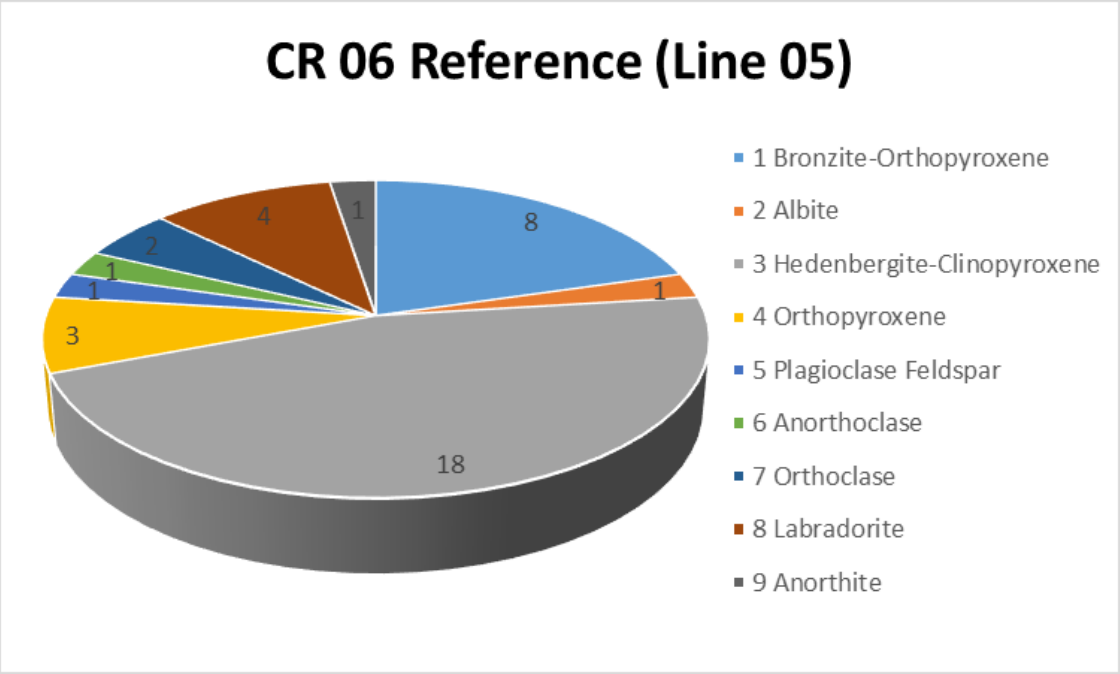

Figure 5 Shows the mineral count of line 05 of reference CR 06 sample.

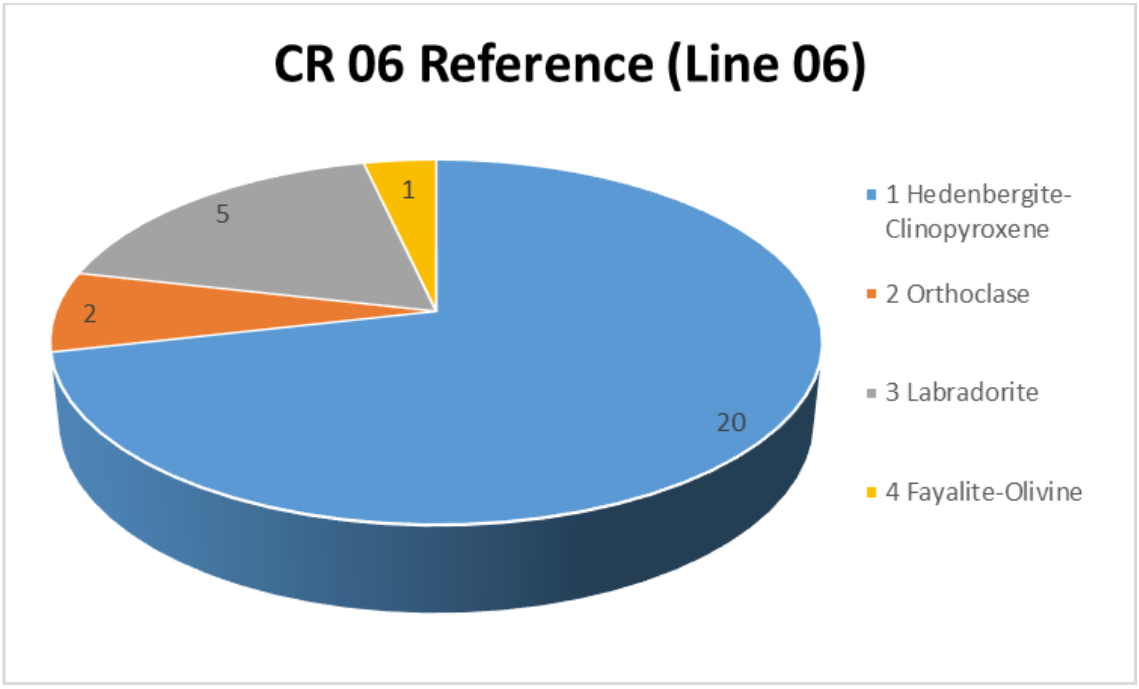

Figure 6 Shows the mineral count of line 06 of reference CR 06 sample.

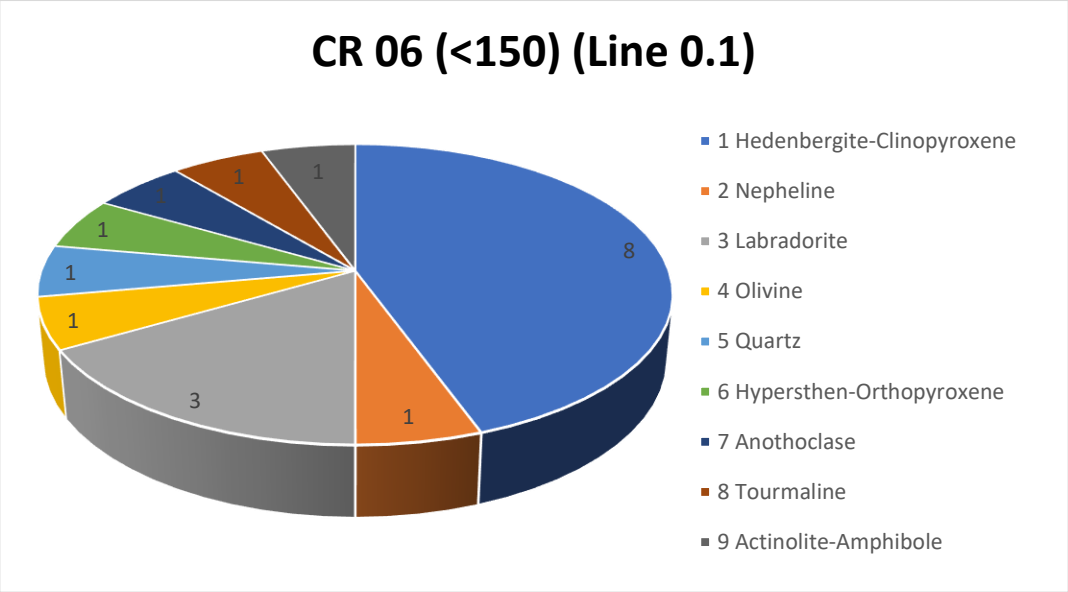

Figure 7 Shows the mineral count of line 0.1 of less than 150 microns fraction of CR 06 sample.

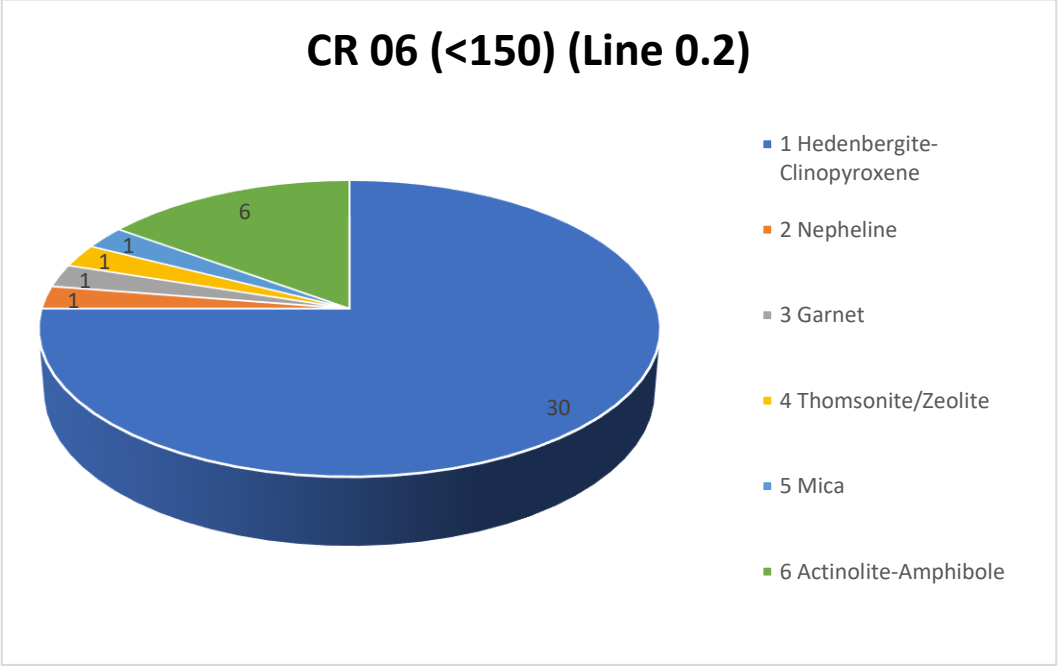

Figure 8 Shows the mineral count of line 0.2 of less than 150 microns fraction of CR 06 sample.

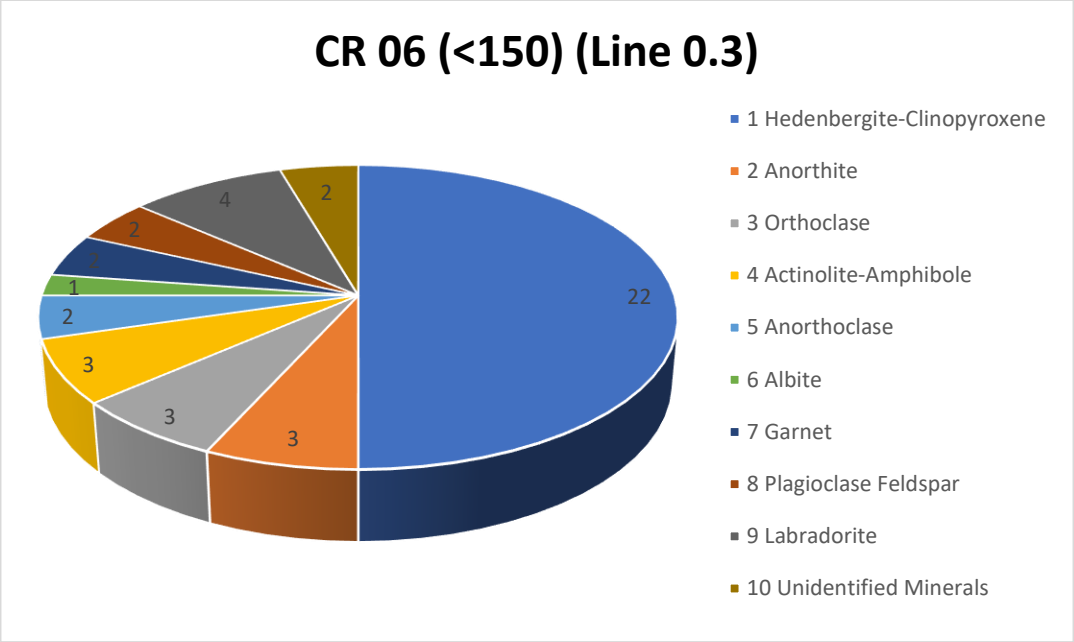

Figure 9 Shows the mineral count of line 0.3 of less than 150 microns fraction of CR 06 sample.

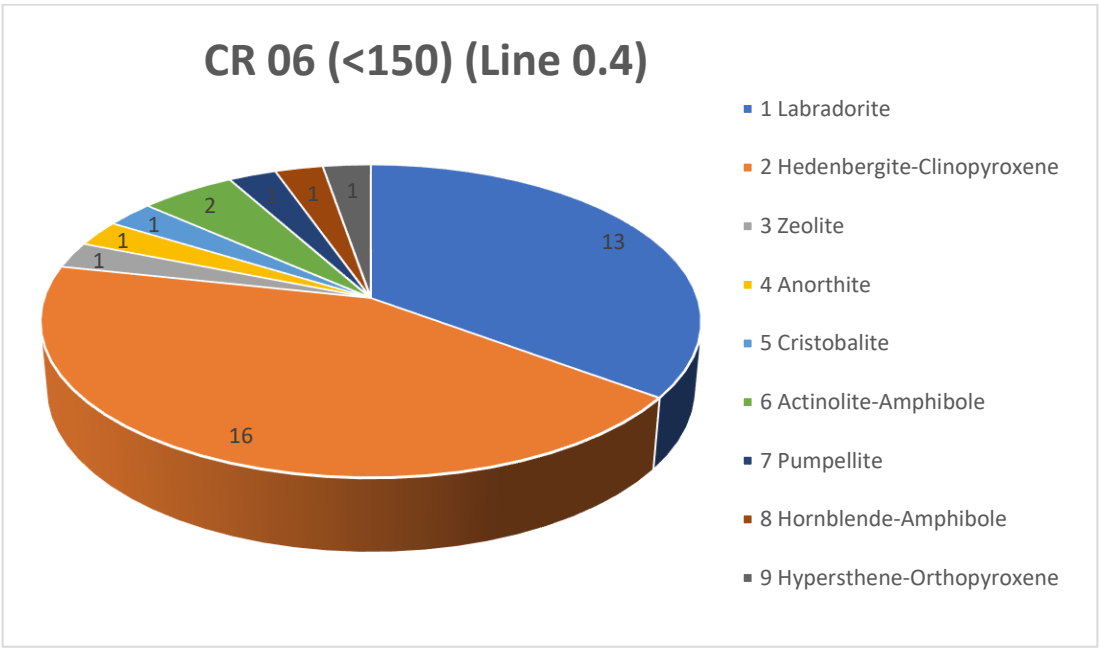

Figure 10 Shows the mineral count of line 0.4 of less than 150 microns fraction of CR 06 sample.

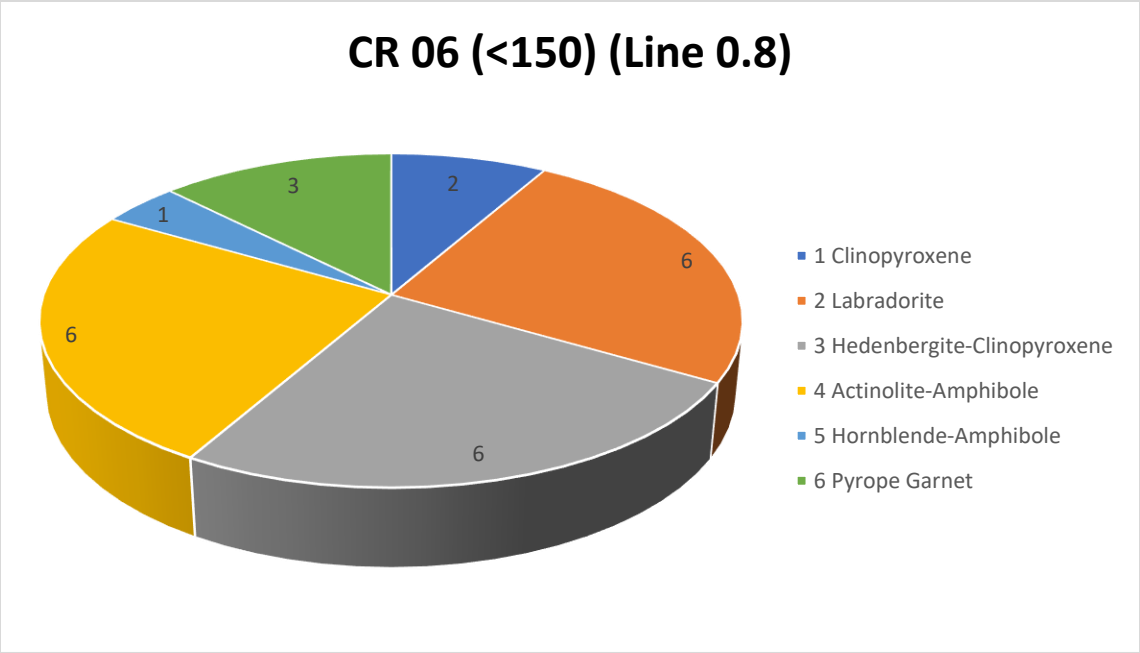

Figure 11 Shows the mineral count of line 0.8 of less than 150 microns fraction of CR 06 sample.

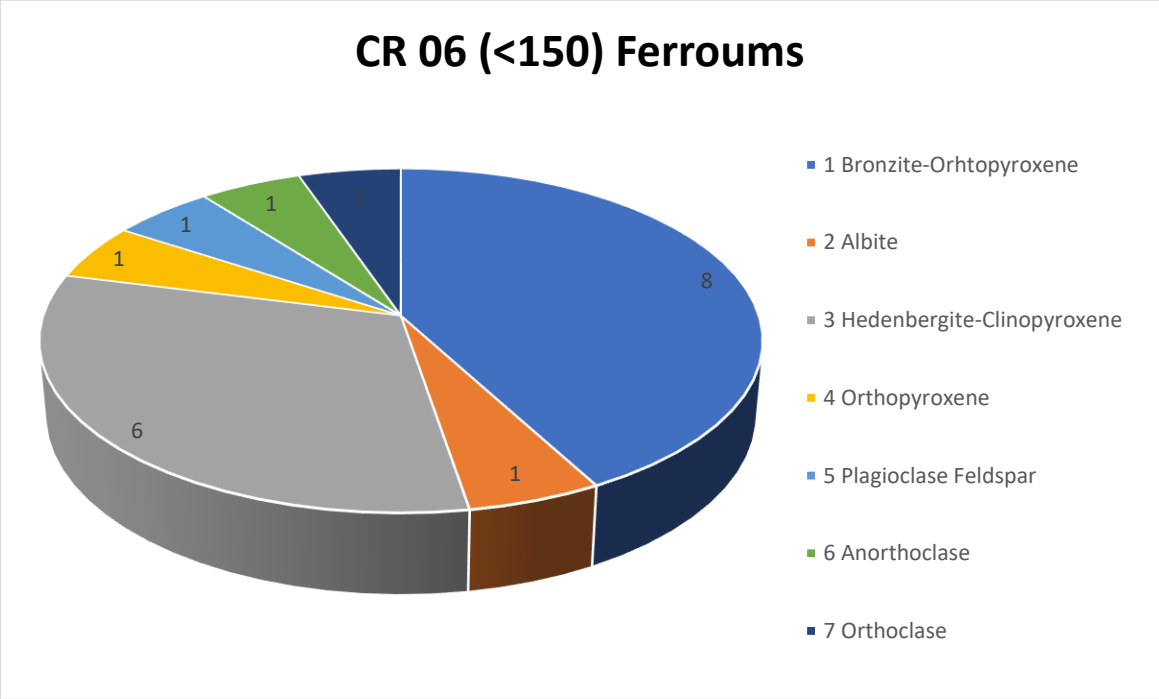

Figure 12 Shows the mineral count of Ferrous line of less than 150 microns fraction of CR 06 sample.

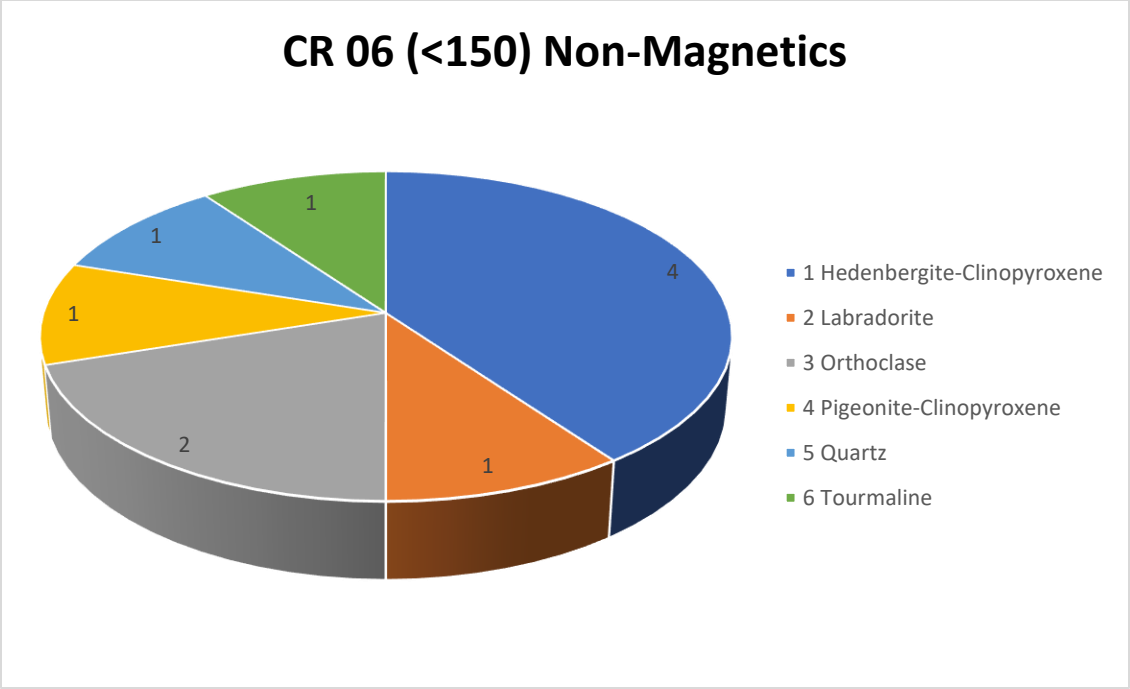

Figure 13 Shows the mineral count of non-Magnetics line of less than 150 microns fraction of CR 06 sample.

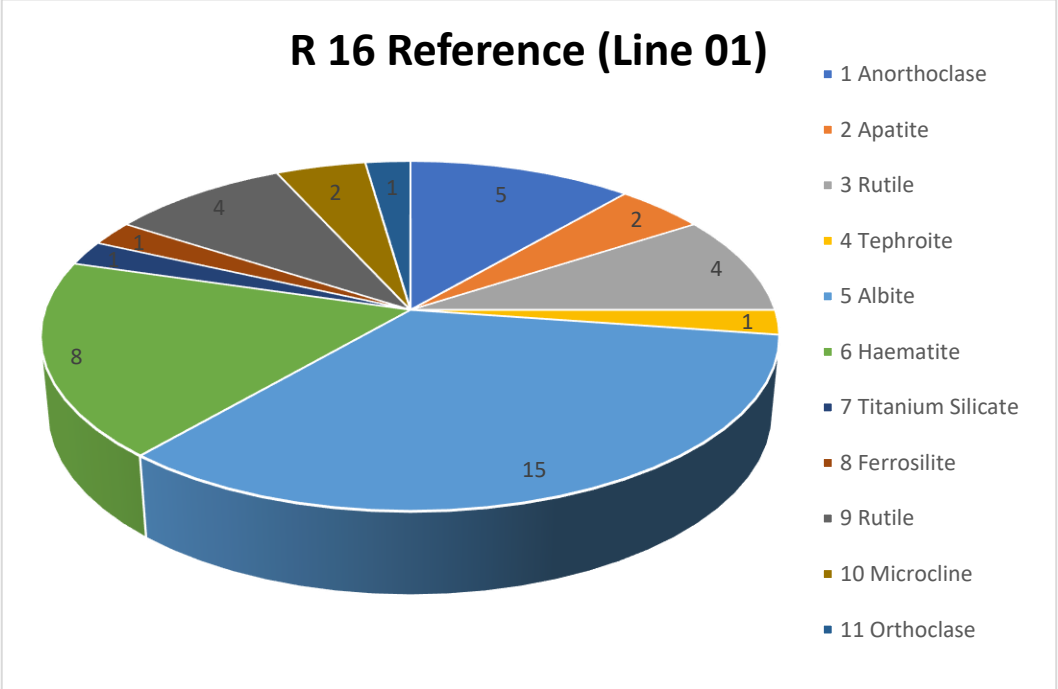

Figure 14 Shows the mineral count of line 01 of reference R 16 sample.

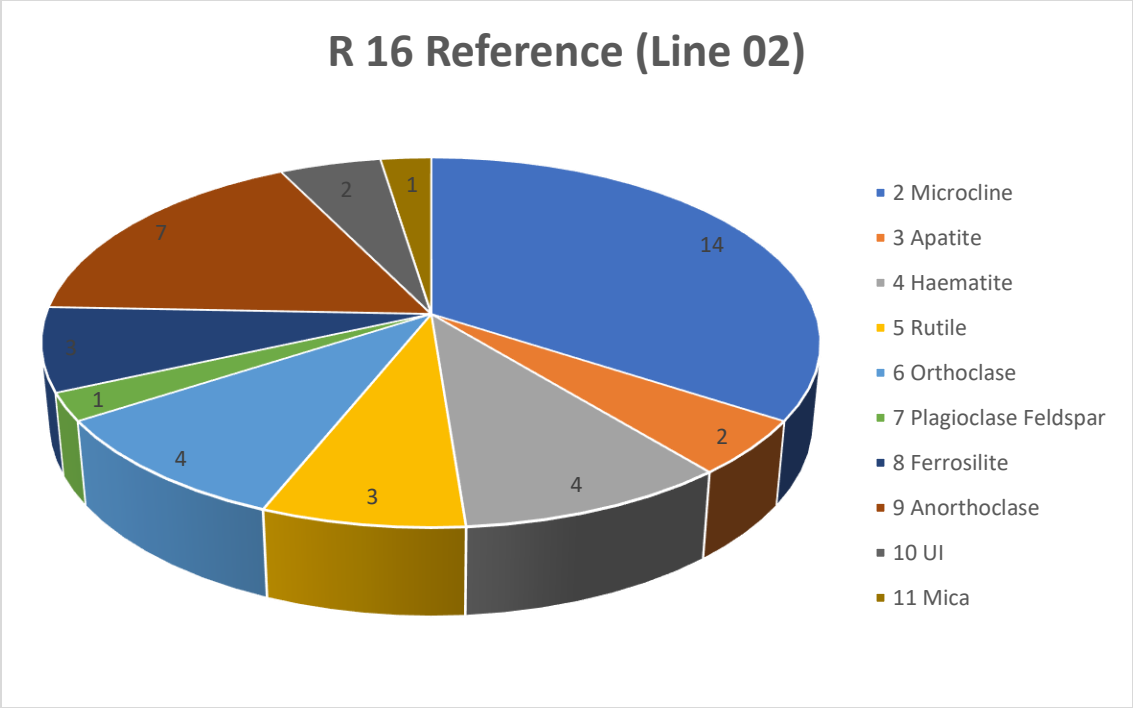

Figure 15 Shows the mineral count of line 02 of reference R 16 sample

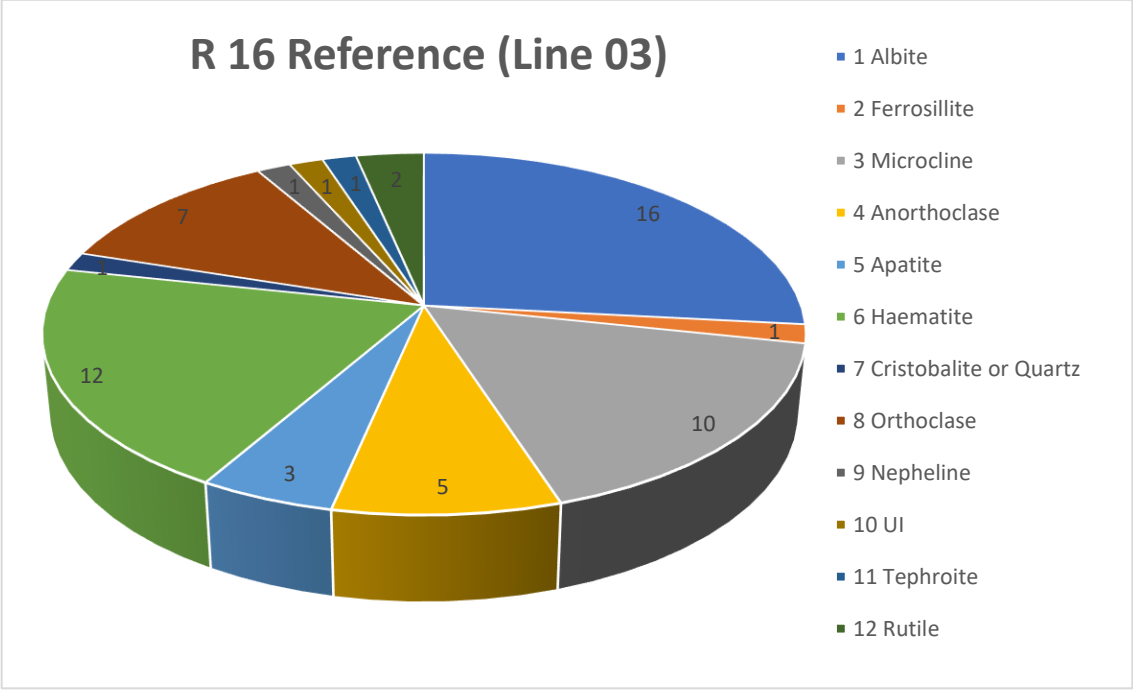

Figure 16 Shows the mineral count of line 03 of reference R 16 sample

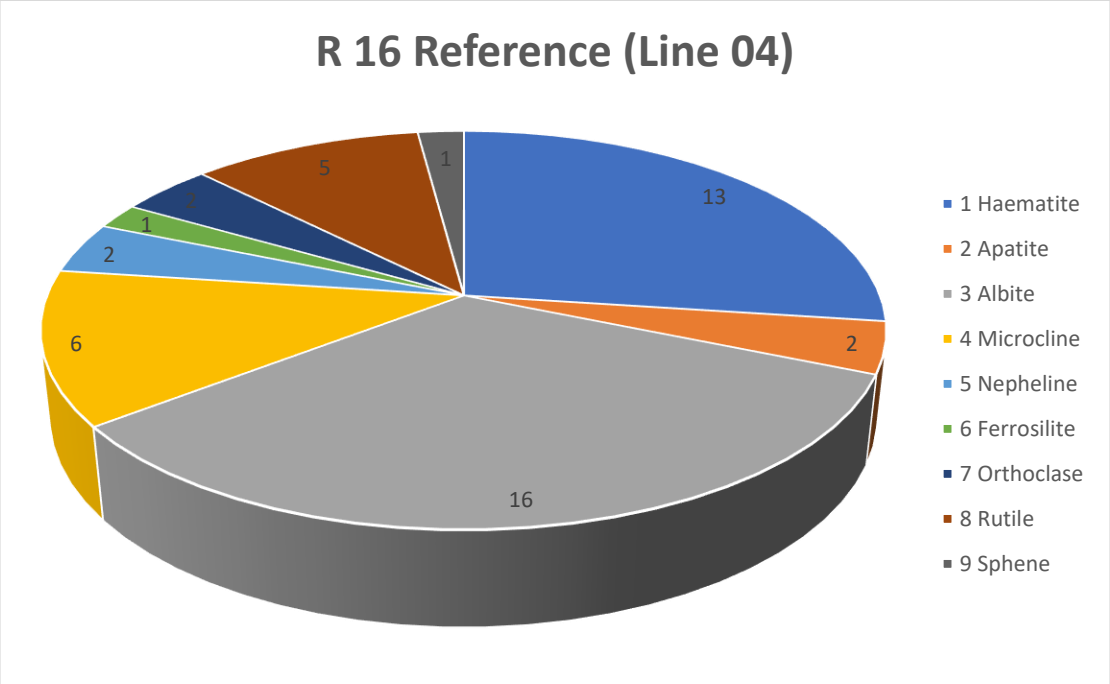

Figure 17 Shows the mineral count of line 04 of reference R 16 sample

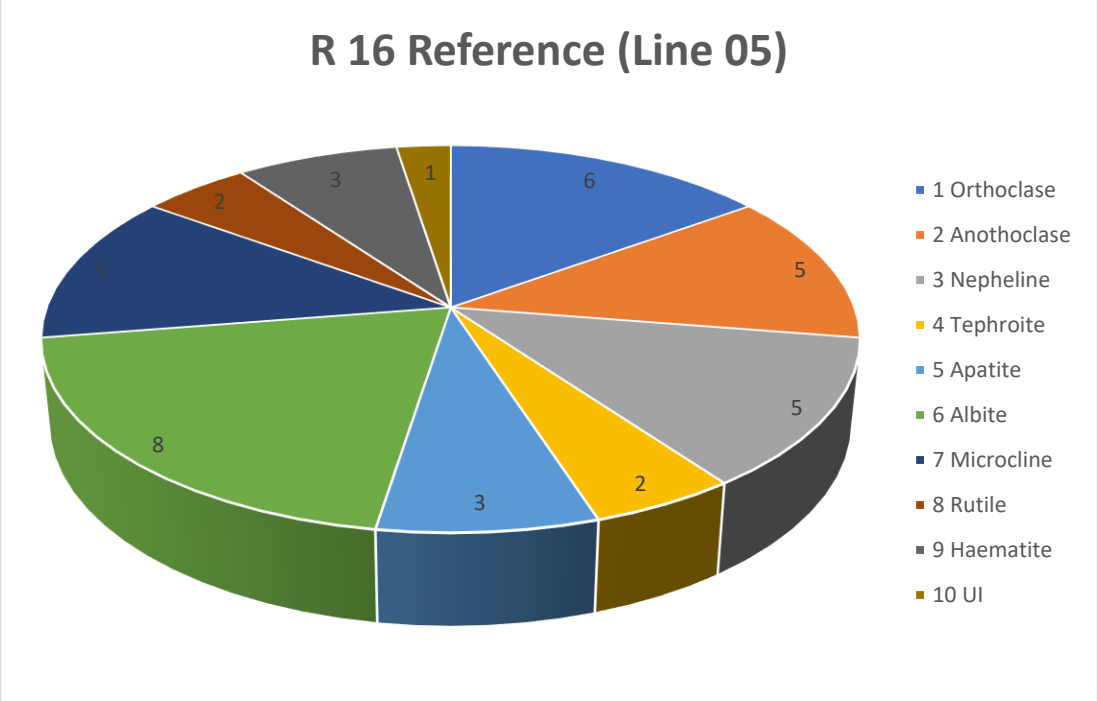

Figure 18 Shows the mineral count of line 05 of reference R 16 sample

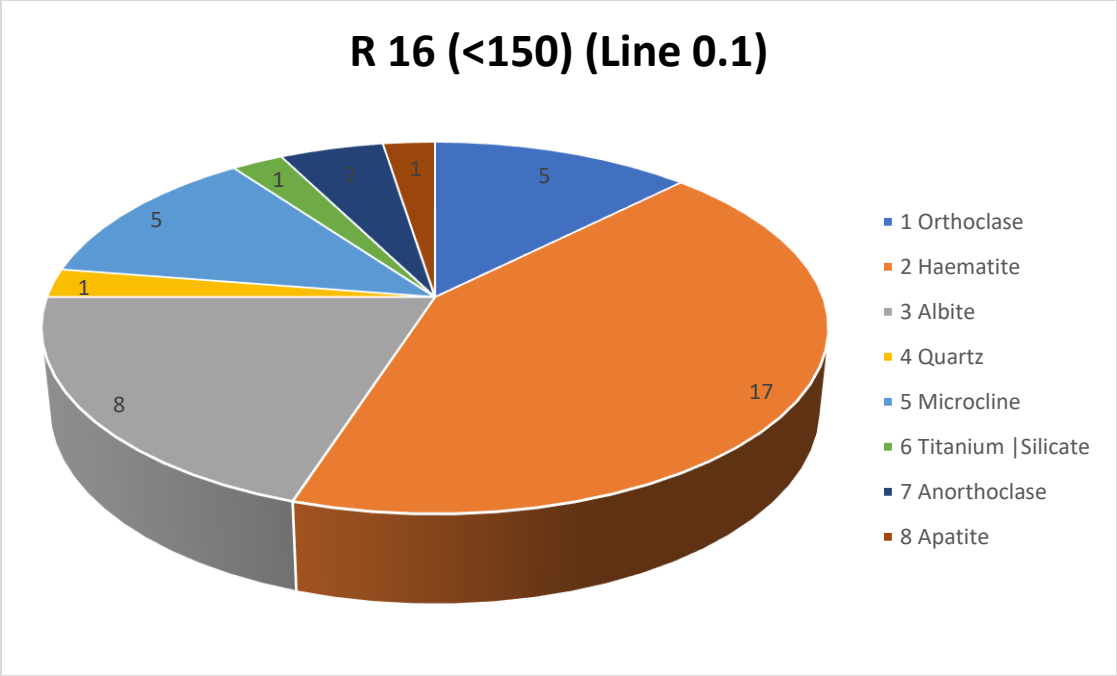

Figure 19 Shows the mineral count of line 0.1 of less than 150 microns fraction of R 16 sample

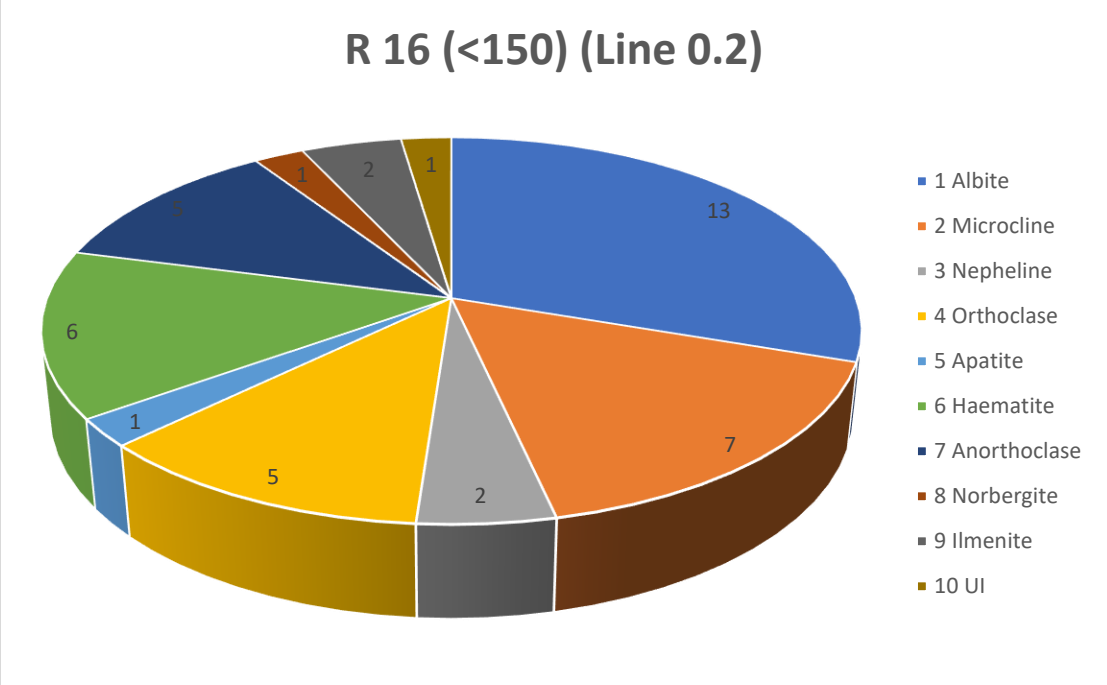

Figure 20 Shows the mineral count of line 0.2 of less than 150 microns fraction of R 16 sample

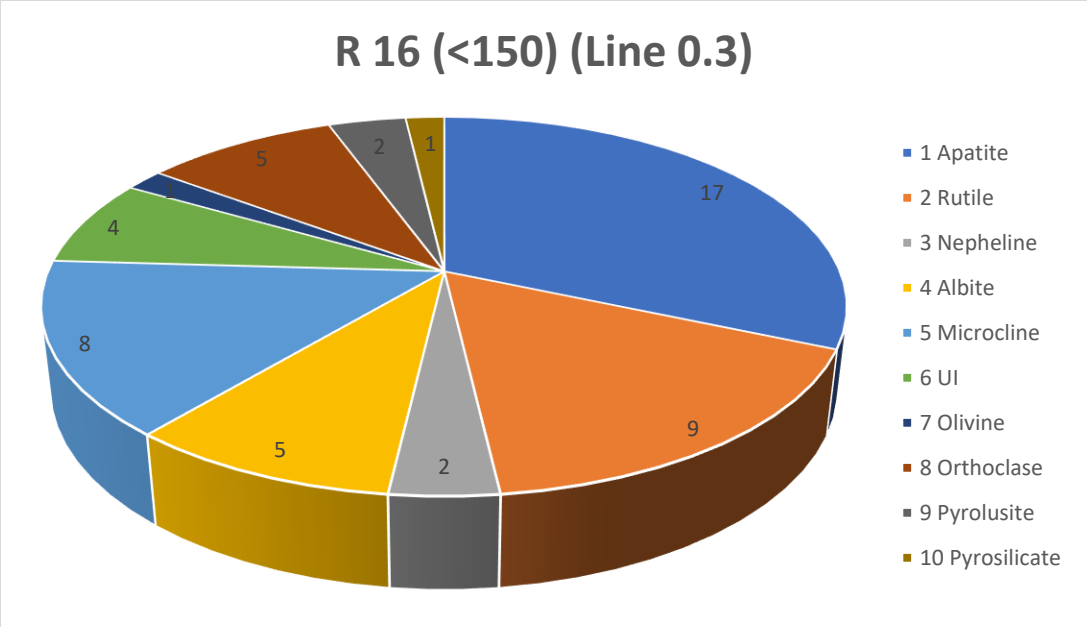

Figure 21 Shows the mineral count of line 0.3 of less than 150 microns fraction of R 16 sample

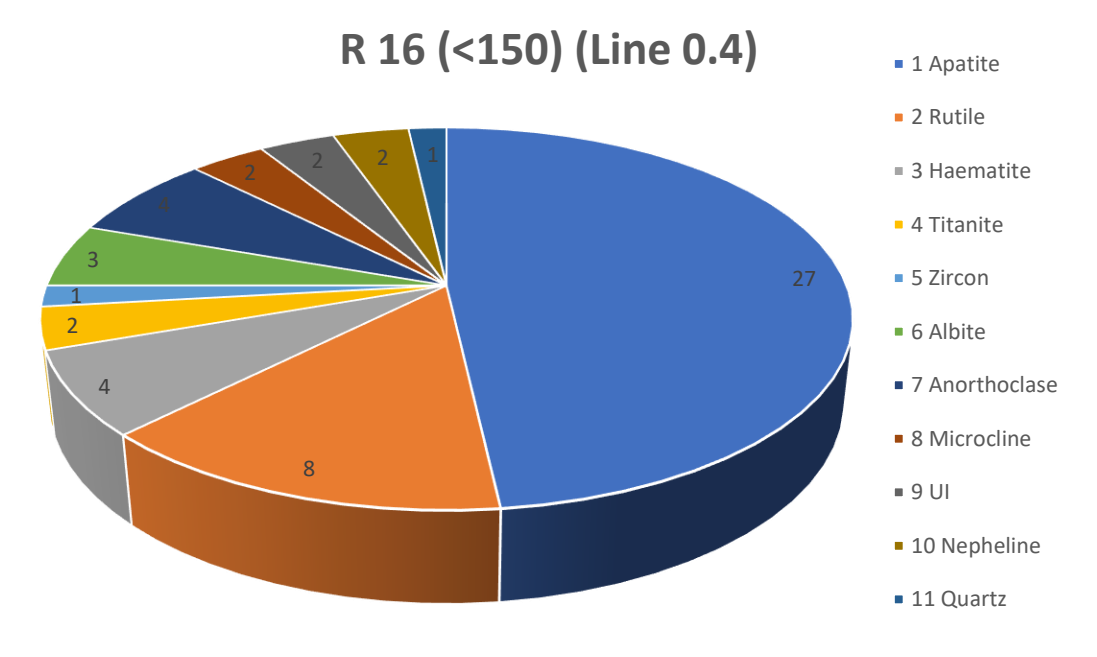

Figure 22 Shows the mineral count of line 0.4 of less than 150 microns fraction of R 16 sample

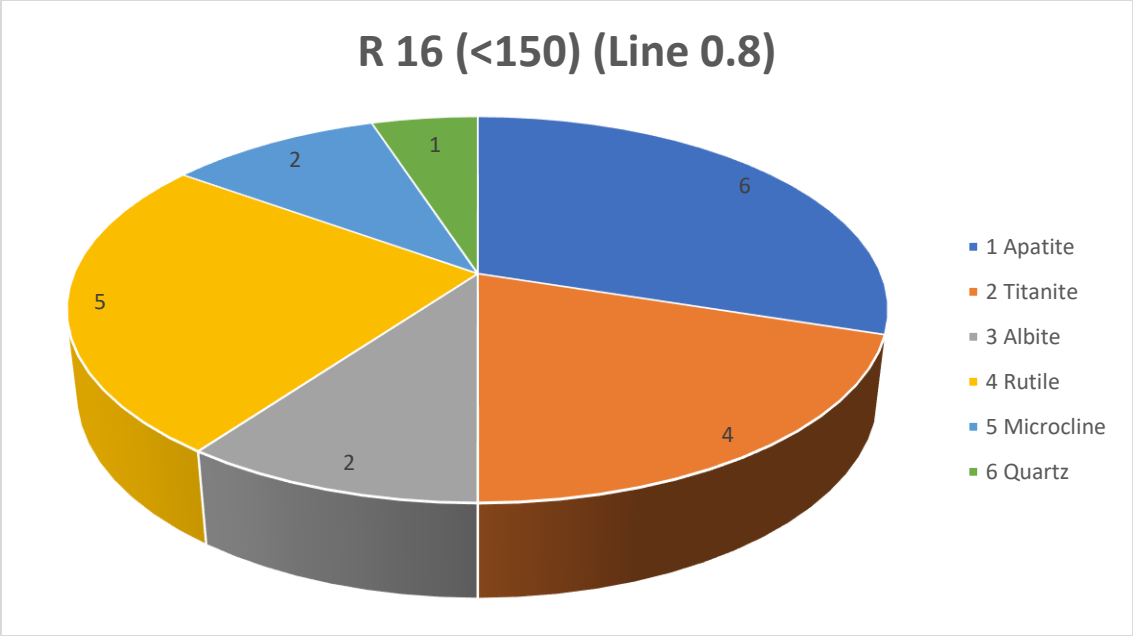

Figure 23 Shows the mineral count of line 0.8 of less than 150 microns fraction of R 16 sample

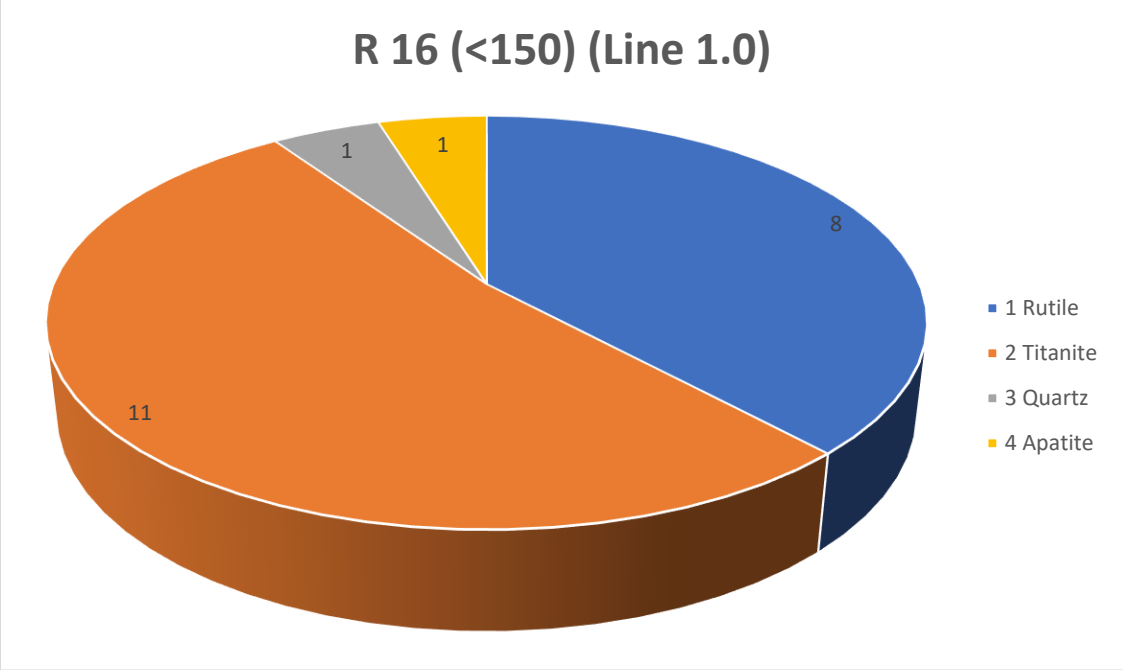

Figure 24 Shows the mineral count of line 1.0 of less than 150 microns fraction of R 16 sample

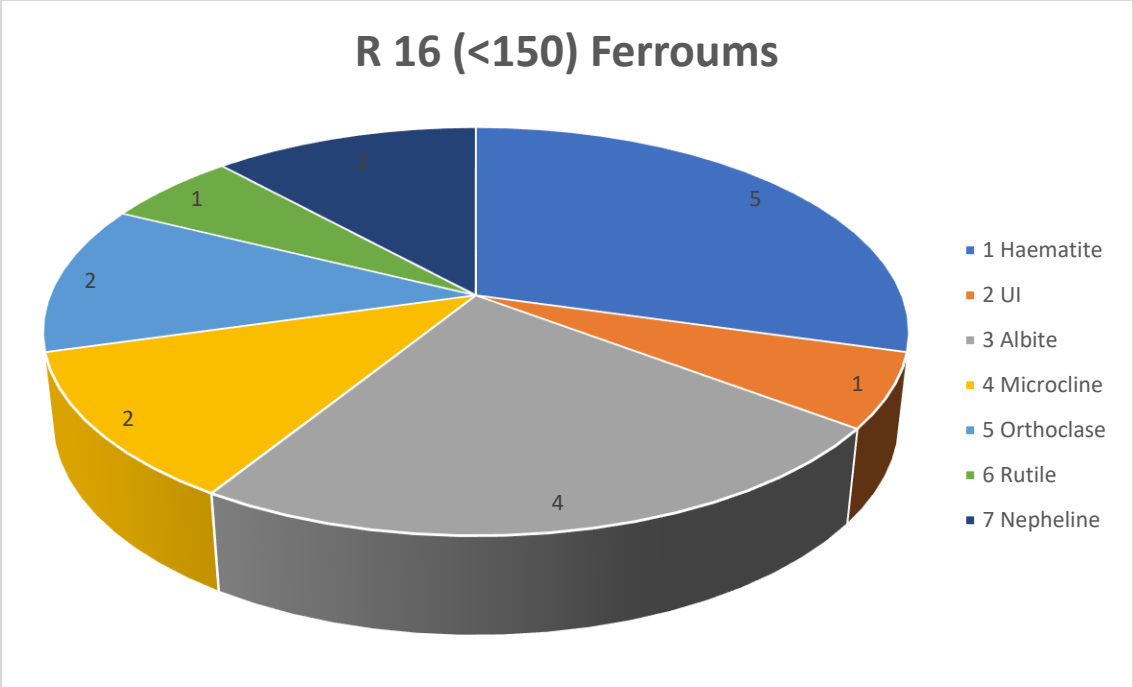

Figure 25 Shows the mineral count of Ferrous line of less than 150 microns fraction of R 16 sample.

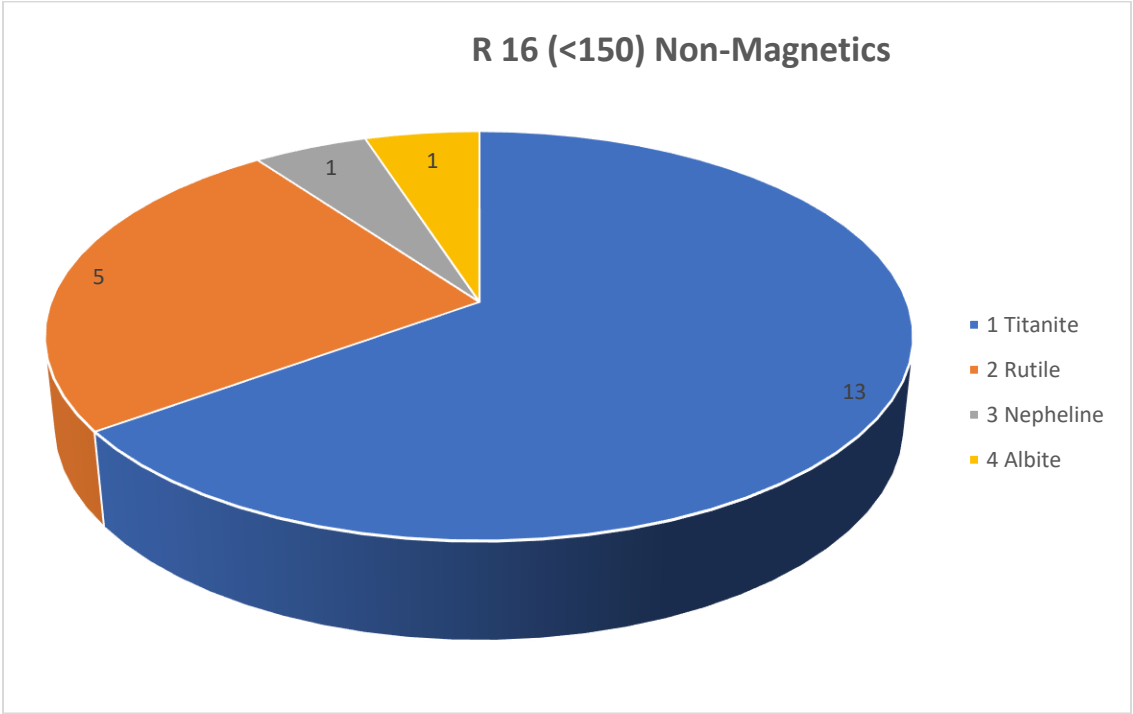

Figure 26 Shows the mineral count of non-Magnetics line of less than 150 microns fraction of R 16 sample.

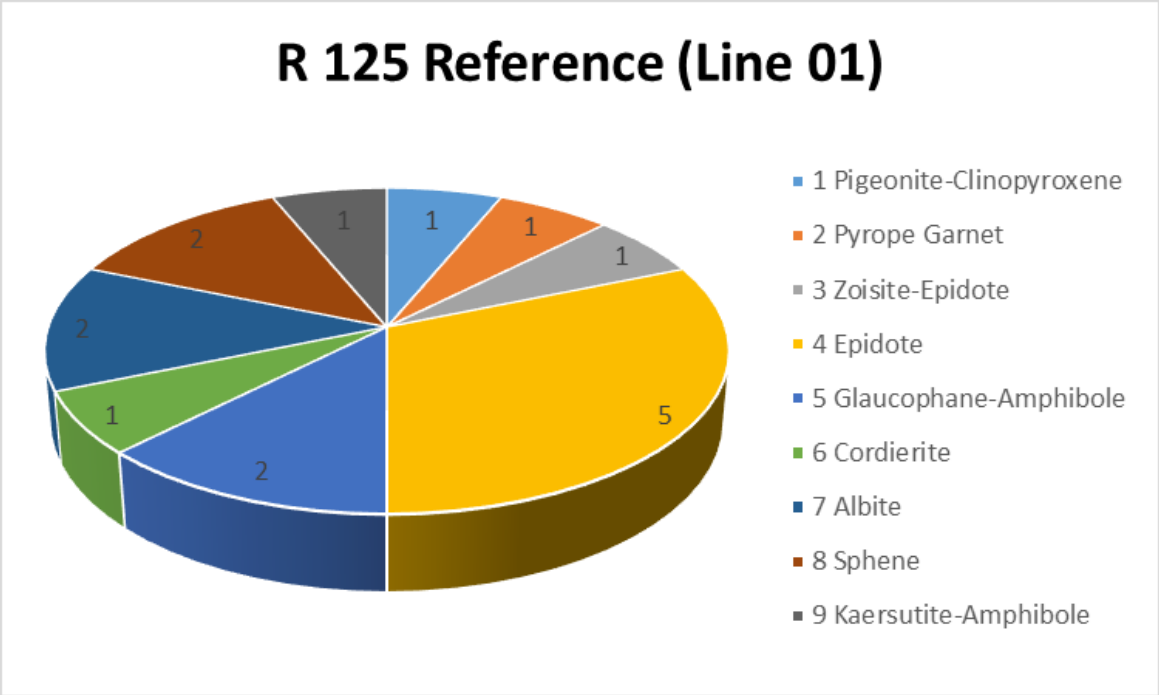

Figure 27 Shows the mineral count of line 01 of reference R 125 sample

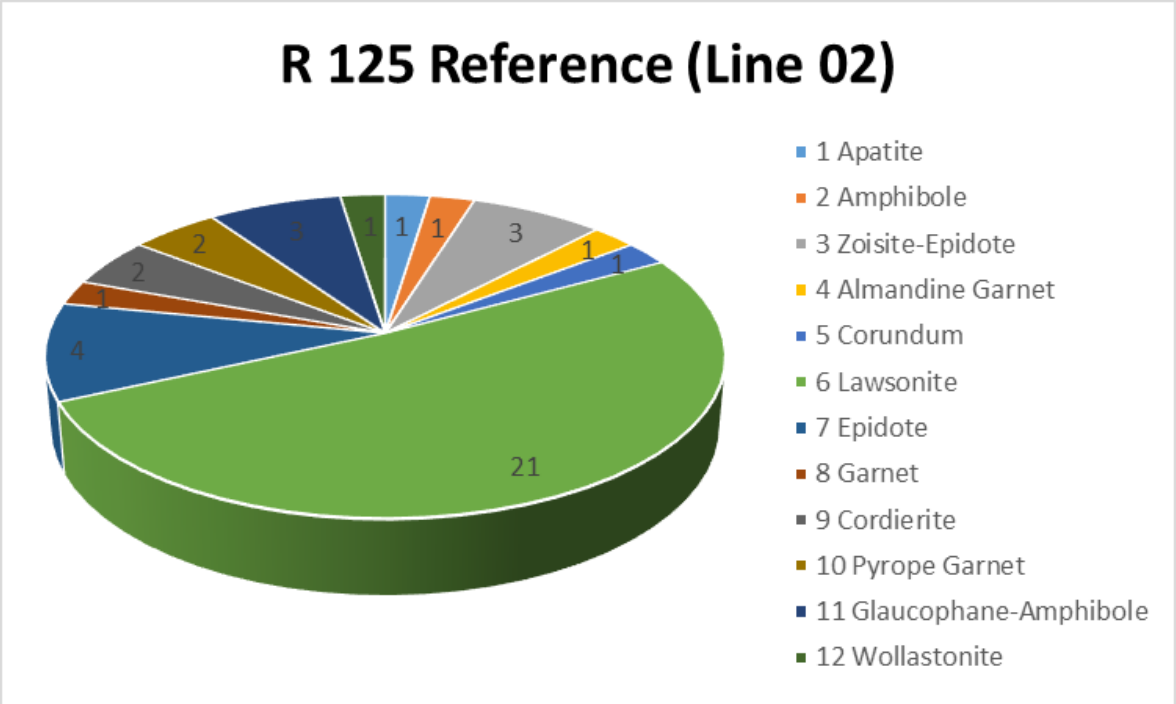

Figure 28 Shows the mineral count of line 02 of reference R 125 sample

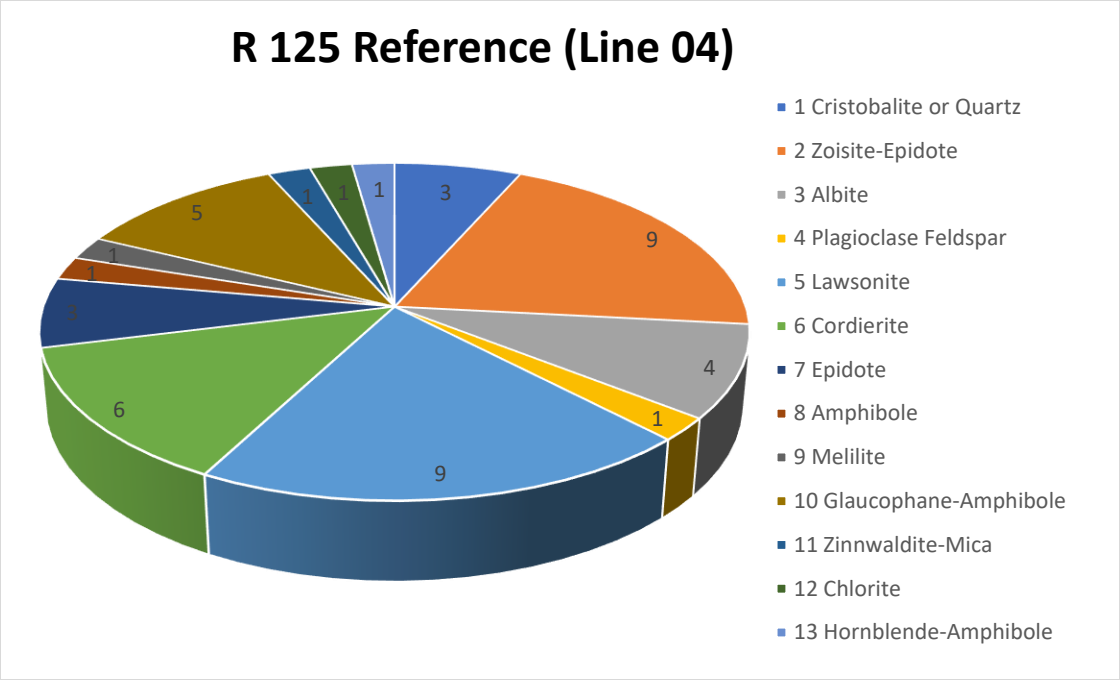

Figure 29 Shows the mineral count of line 04 of reference R 125 sample

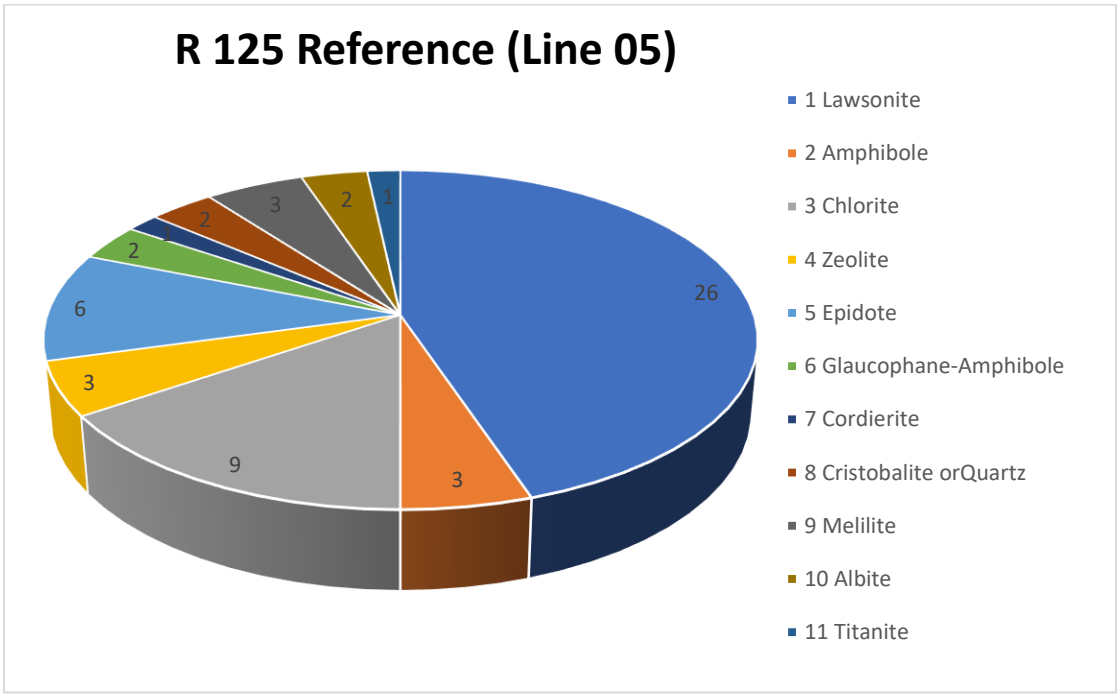

Figure 30 Shows the mineral count of line 05 of reference R 125 sample

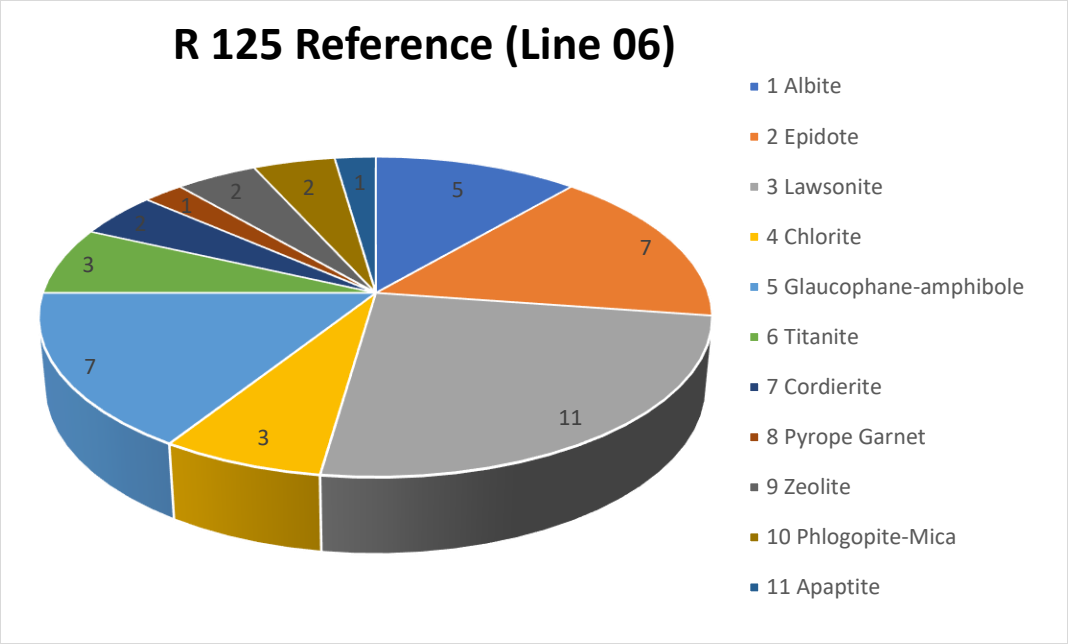

Figure 31 Shows the mineral count of line 06 of reference R 125 sample

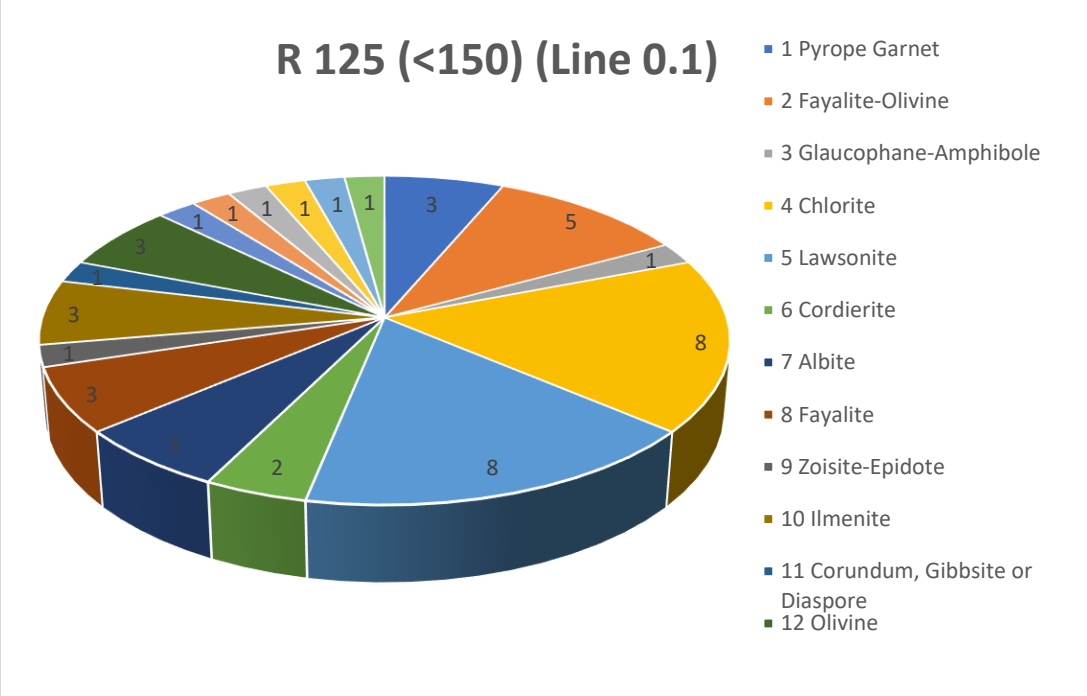

Figure 32 Shows the mineral count of line 0.1 of less than 150 microns fraction of R 125 sample

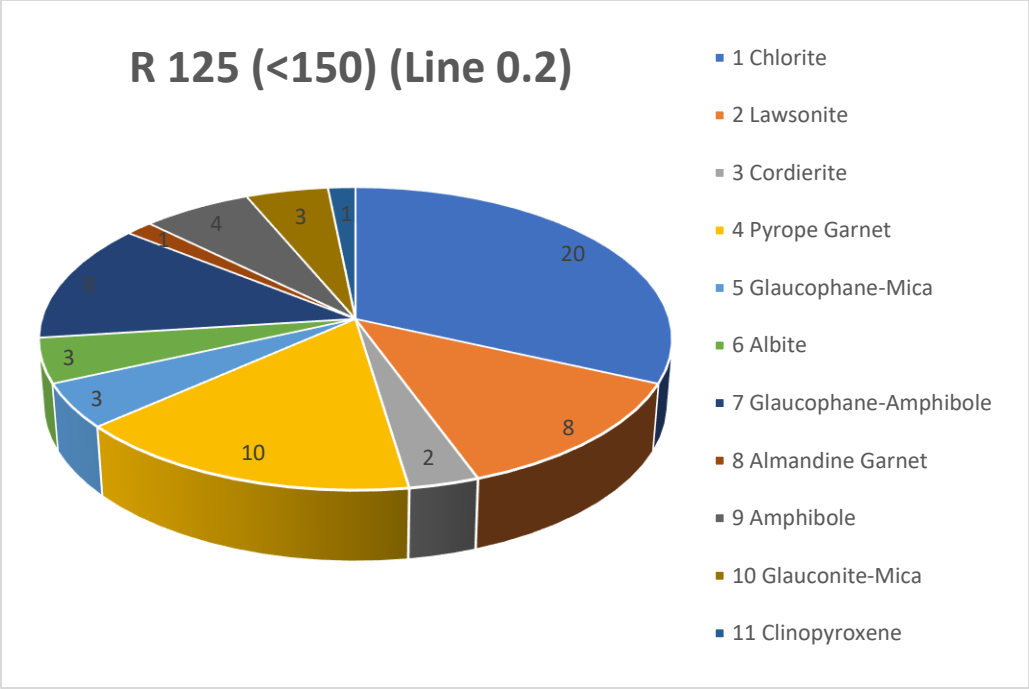

Figure 33 Shows the mineral count of line 0.2 of less than 150 microns fraction of R 125 sample

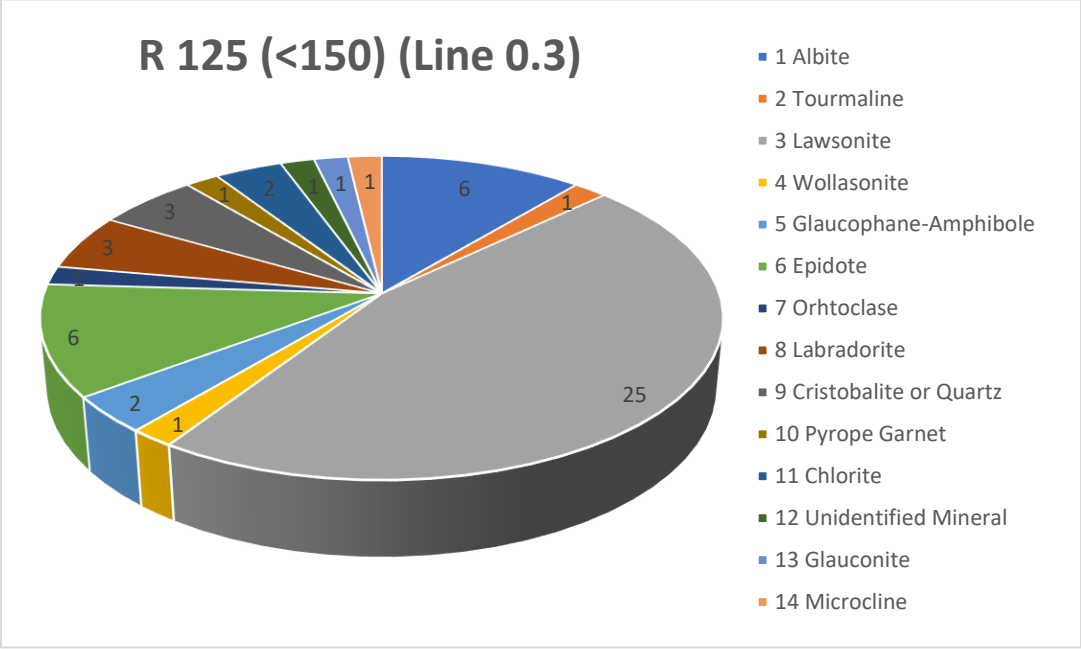

Figure 34 Shows the mineral count of line 0.3 of less than 150 microns fraction of R 125 sample

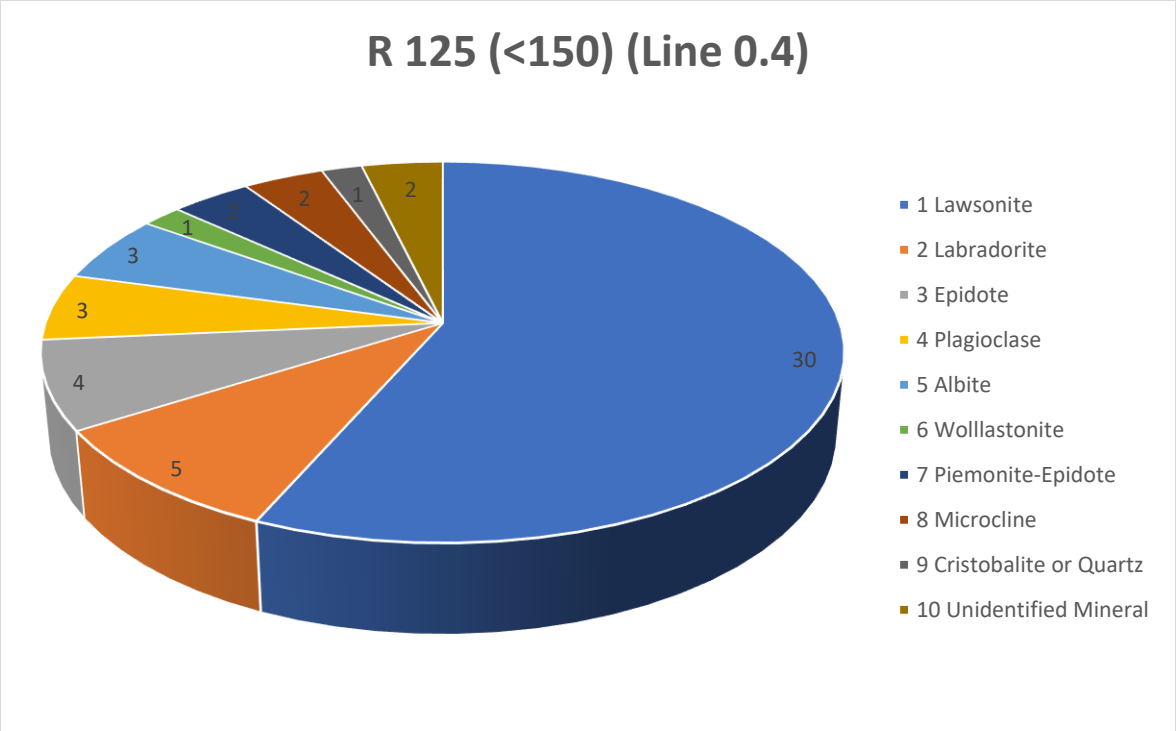

Figure 35 Shows the mineral count of line 0.4 of less than 150 microns fraction of R 125 sample

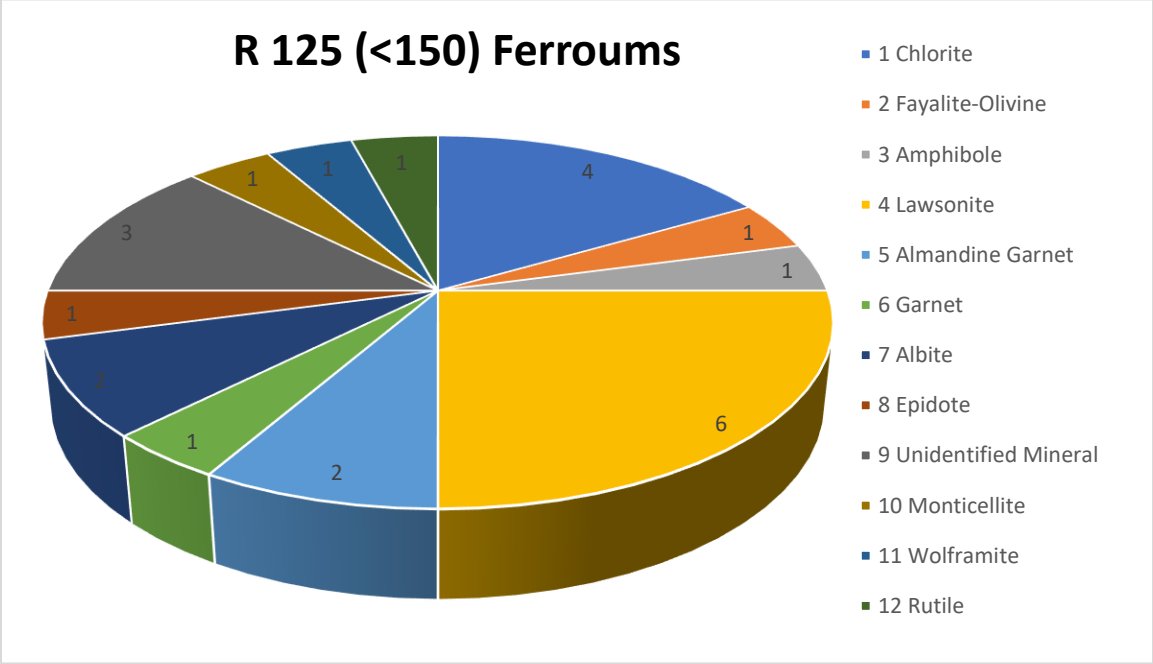

Figure 36 Shows the mineral count of Ferrous line of less than 150 microns fraction of R 125 sample.

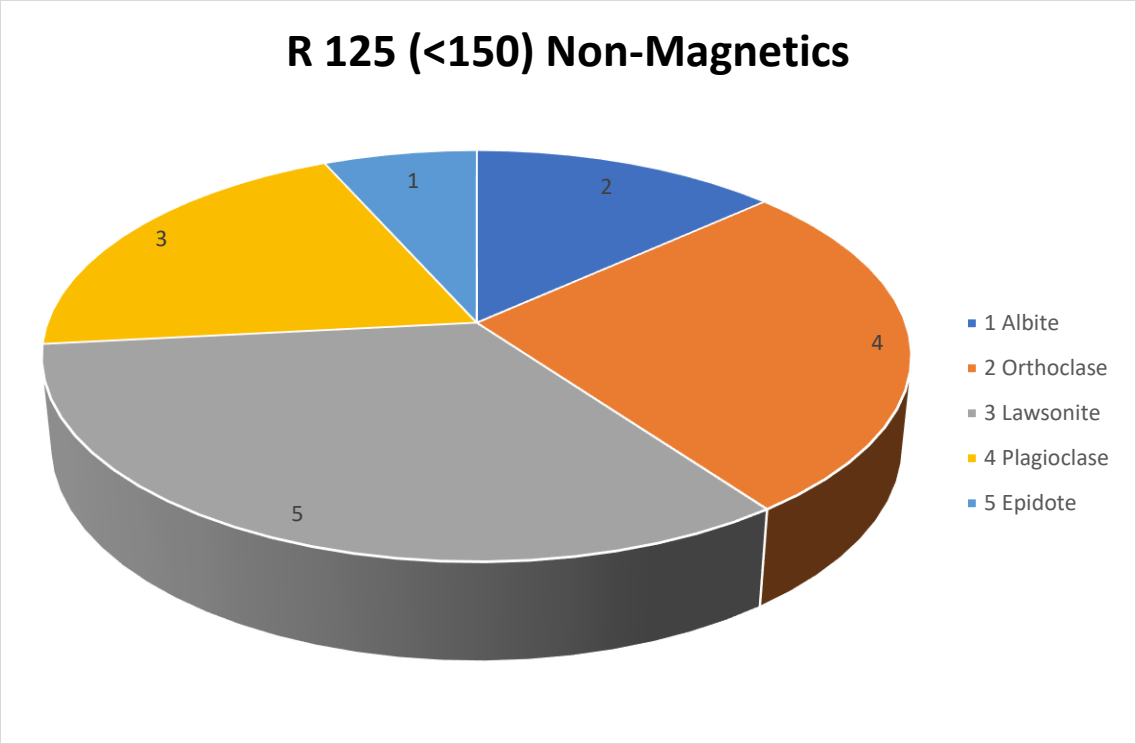

Figure 37 Shows the mineral count of non-Magnetics line of less than 150 microns fraction of R 125 sample.

APPENDIX B

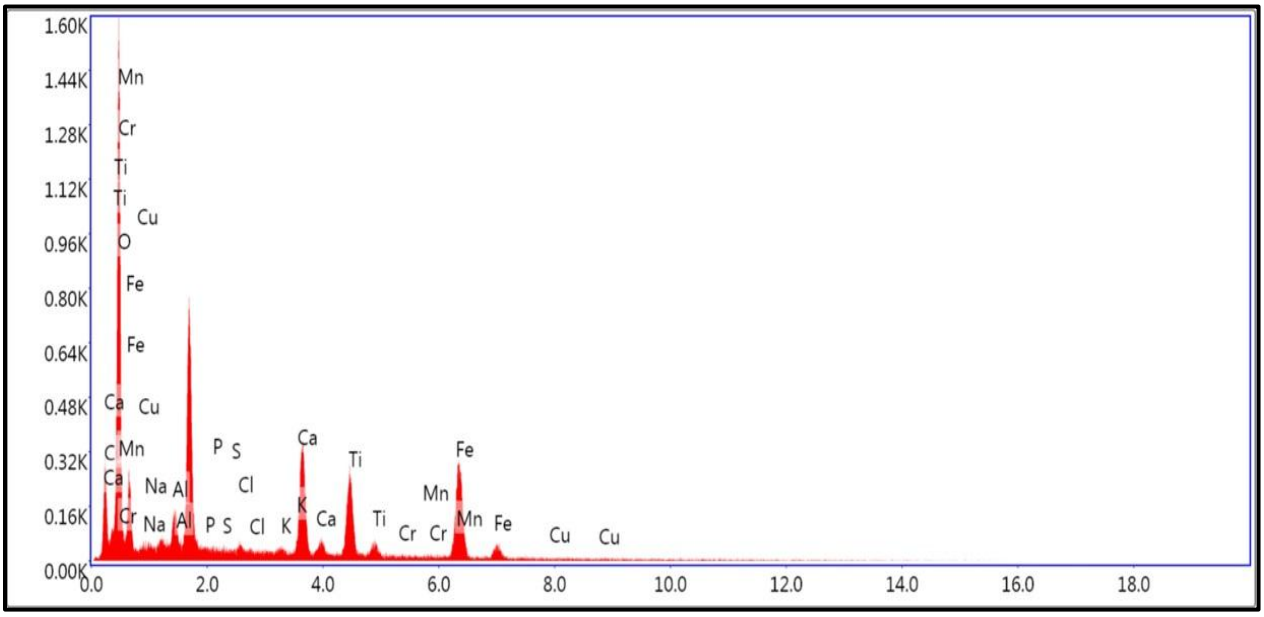

Figure 38 Shows the EDS spectra of Amphibole mineral, acquired from SEM.

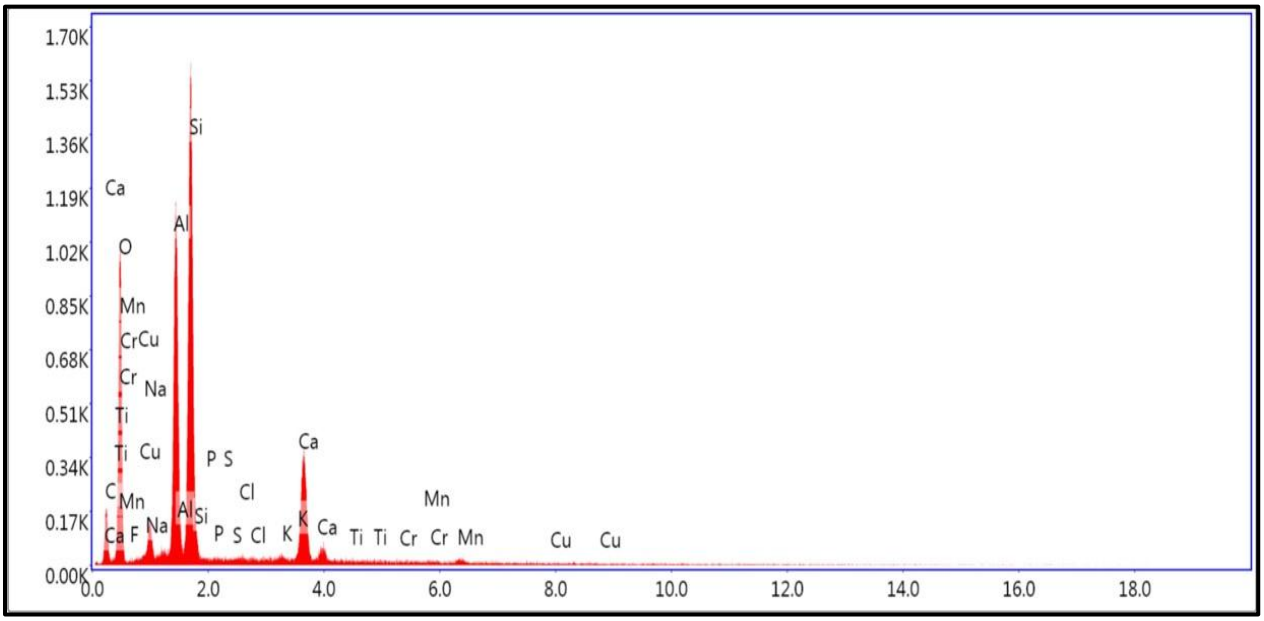

Figure 39 Shows the EDS spectra of Anorthite mineral, acquired from SEM.

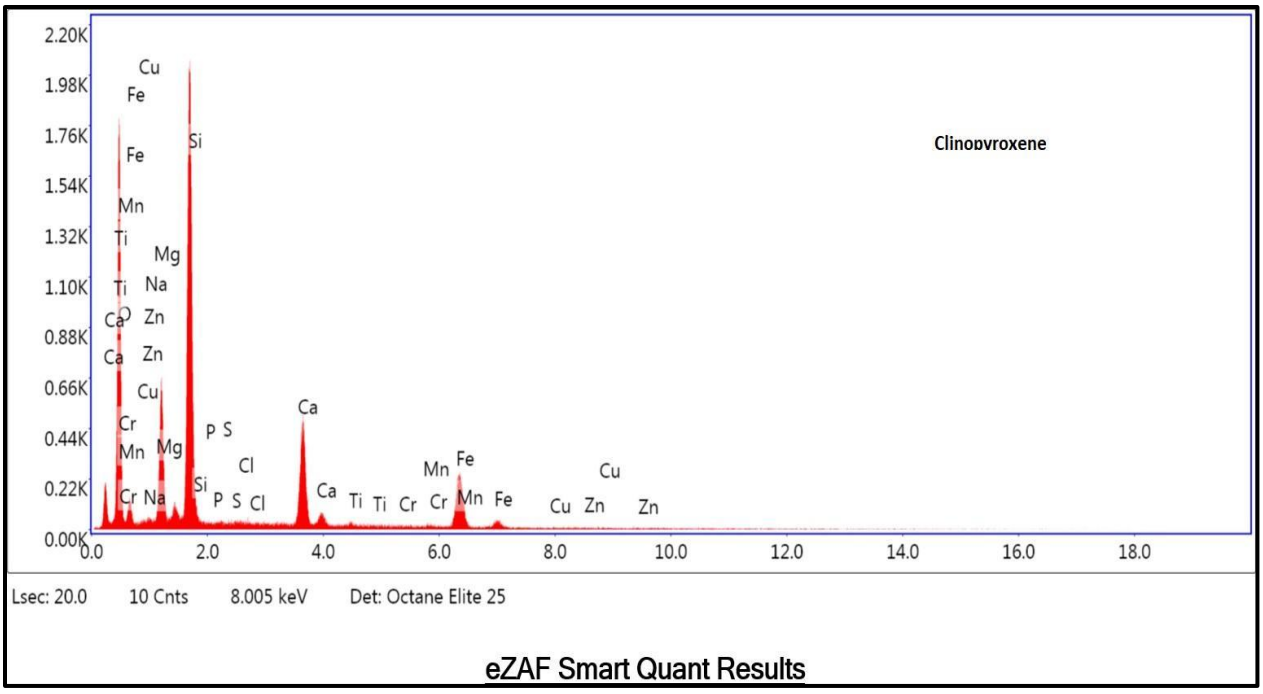

Figure 40 Shows the EDS spectra of Hedenbergite Clinopyroxene mineral, acquired from SEM.

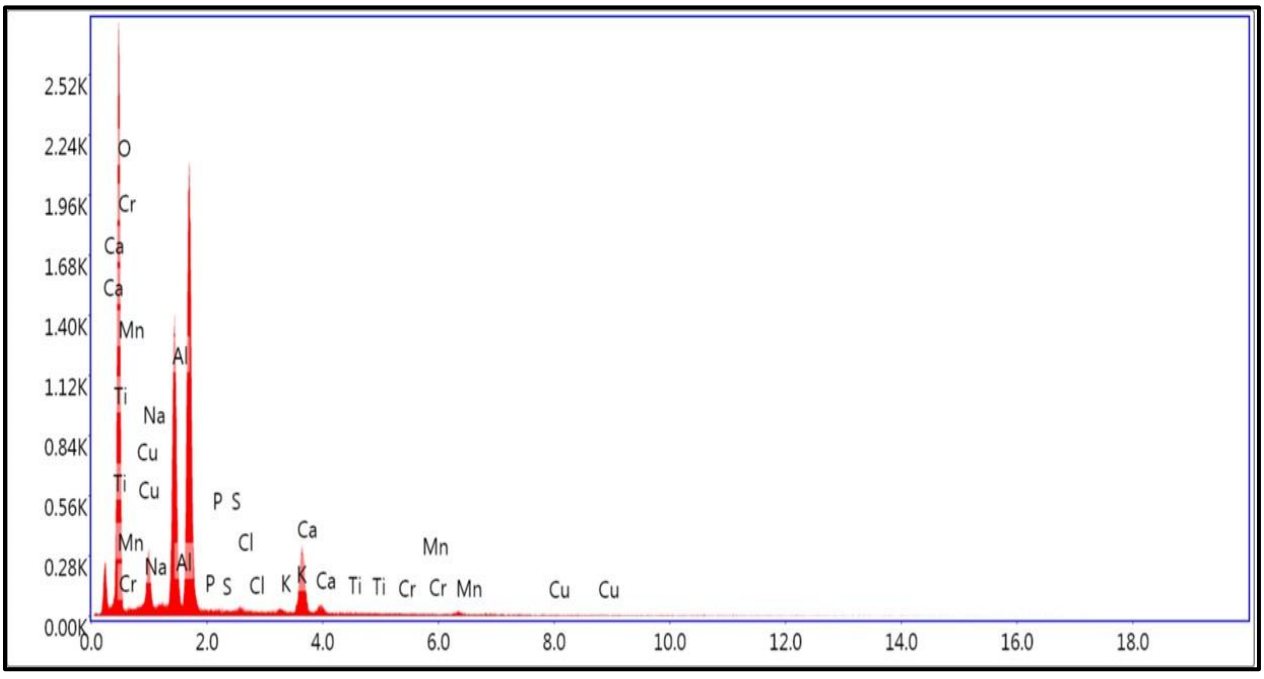

Figure 41 Shows the EDS spectra of Labradorite mineral, acquired from SEM.

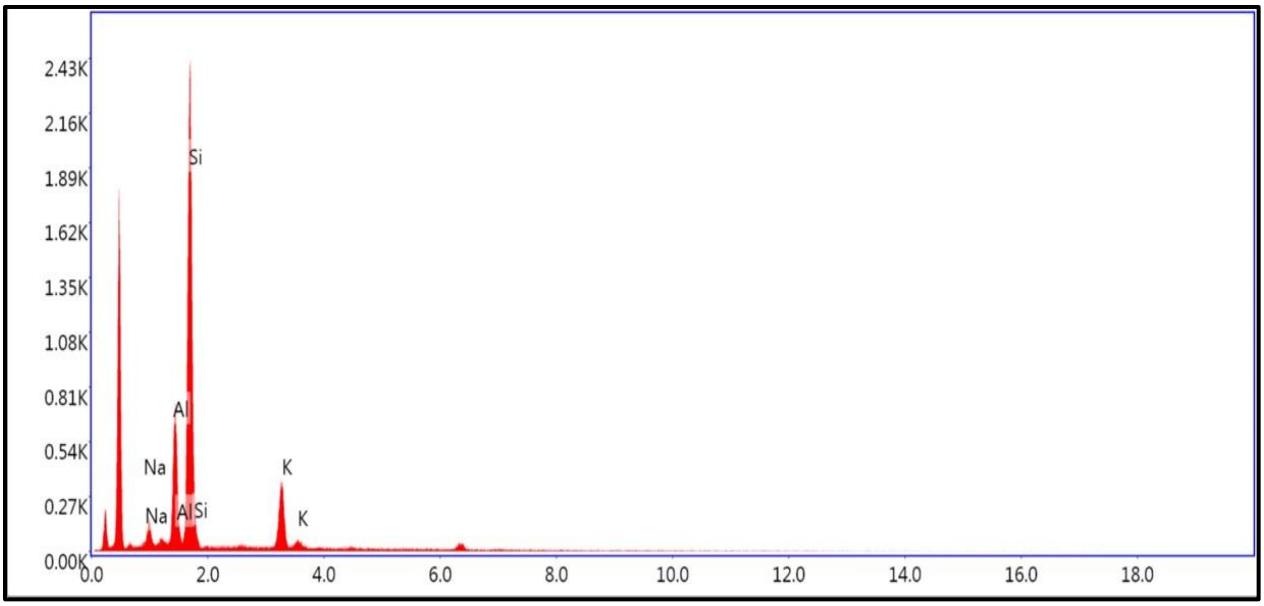

Figure 42 Shows the EDS spectra of Orthoclase mineral, acquired from SEM.

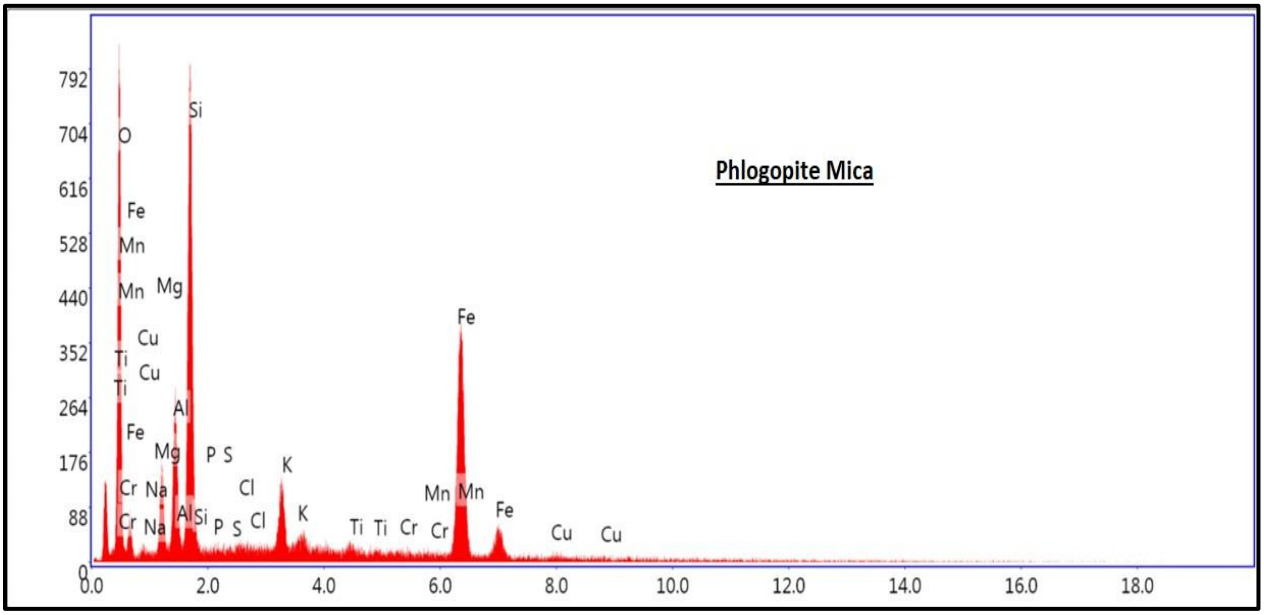

Figure 43 Shows the EDS spectra of Phlogopite Mica mineral, acquired from SEM.

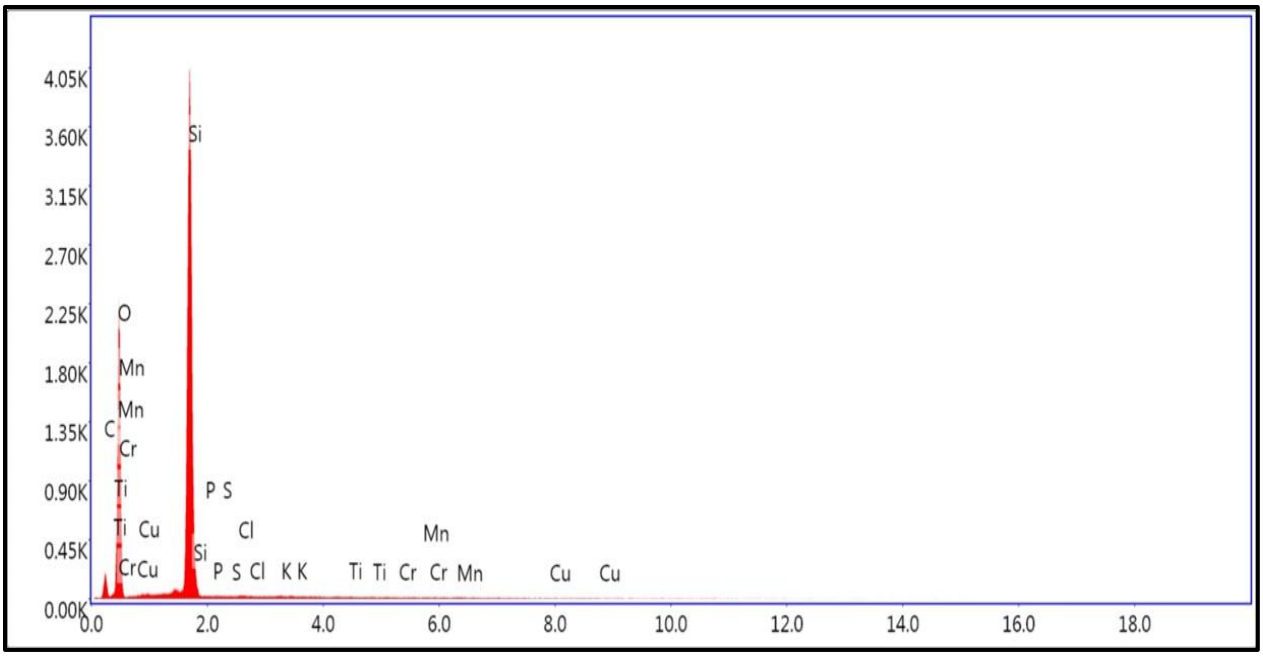

Figure 44 Shows the EDS spectra of Silica mineral, acquired from SEM.

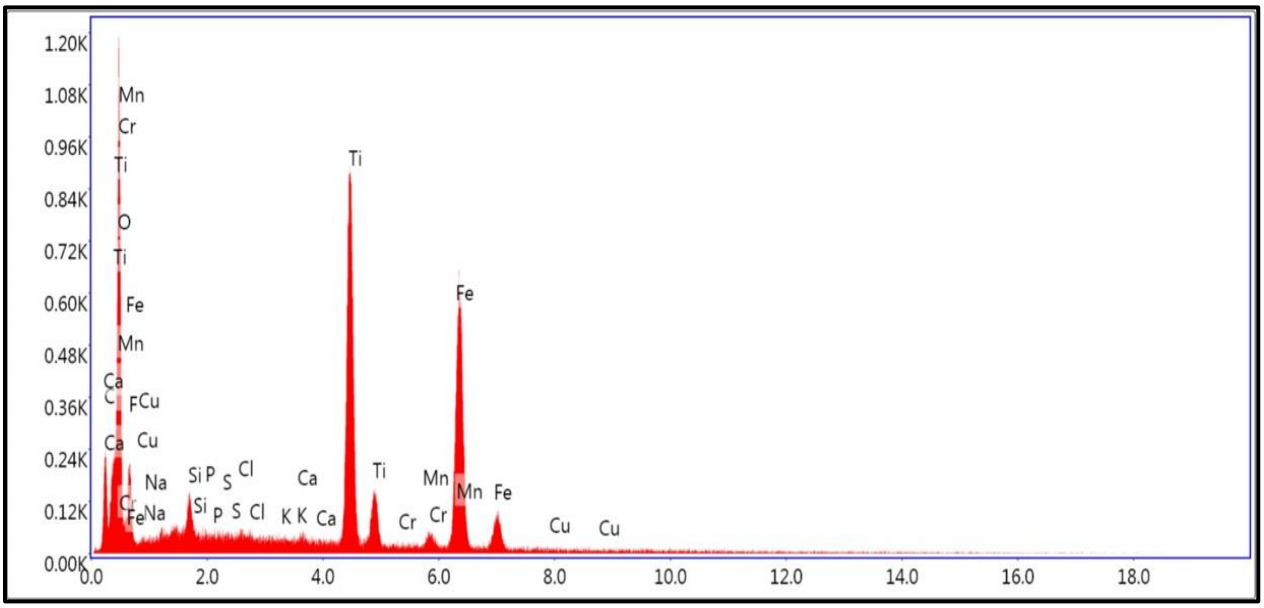

Figure 45 Shows the EDS spectra of Ulvospinel mineral, acquired from SEM.

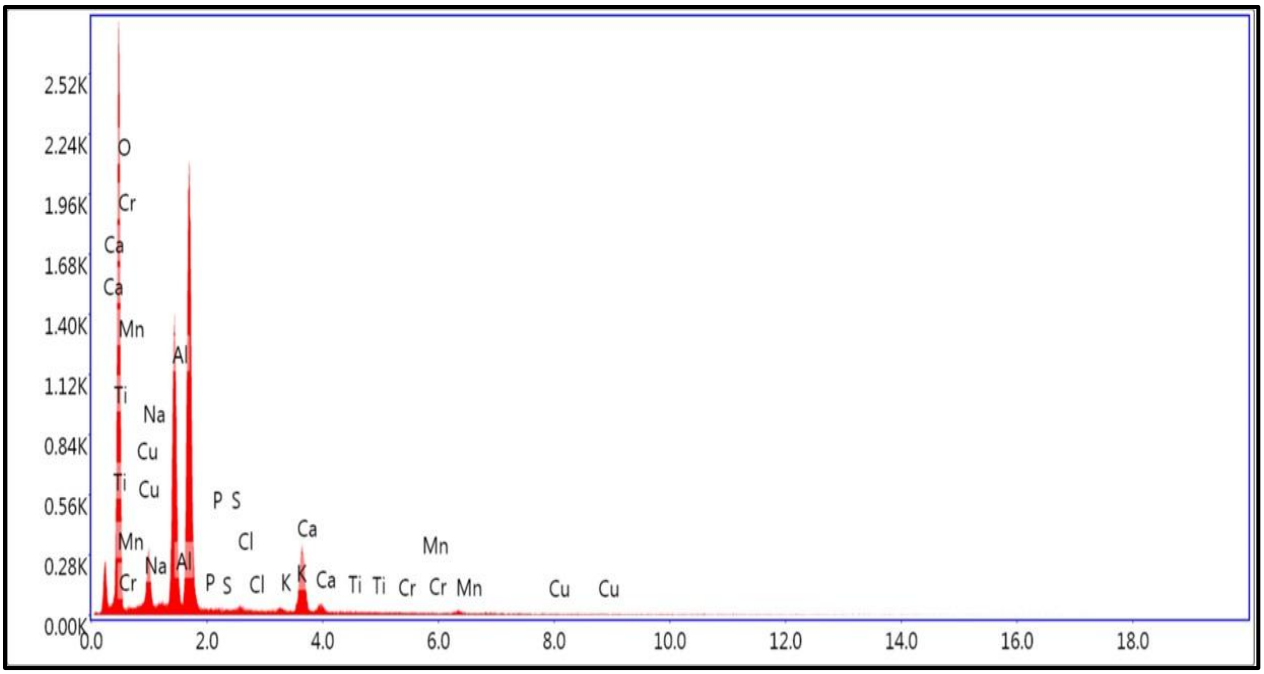

Figure 46 Shows the EDS spectra of Zeolite mineral, acquired from SEM.